UNIMORE
UNIVERSITÀ DEGLI STUDI DI
MODENA E REGGIO EMILIA

DIPARTIMENTO DI SCIENZE FISICHE, INFORMATICHE E MATEMATICHE

Corso di Laurea in Matematica

Mathematical Modelling of Social Homeostasis: Higher-Order Interactions, Temporal Networks and Adaptive Dynamic

Relatore:
Prof. Marco Villani

Candidato:
Marasti Mattia

Correlatore:
Prof. Iacopo Iacopini, Prof. Giovanni Petri

Anno Accademico 2025–2026

Contents

List of Figures

Abstract

Loneliness and social isolation have emerged as pressing public health concerns, yet their mathematical modelling remains underdeveloped. This thesis proposes a novel framework grounded in the theory of Social Homeostasis-the principle according to which individuals regulate their social behaviour around an optimal level of sociality, analogously to physiological homeostatic mechanisms.

The work develops along three main directions. First, we discuss Interpolating Higher-Order Temporal Networks (IHTNs), a class of temporal network models that interpolates between dyadic and group interactions. We analyse a specific model-the *r-SAD*-deriving analytical results for structural properties and for the epidemic threshold of an SIS process unfolding on the network. A key finding is the *Poor-Get-Richer* effect: group interactions disproportionately increase the connectivity of low-activity nodes, democratizing the degree distribution.

Second, we formalise a general framework for acute and chronic isolation, built around the concept of a Realization Adaptive Function (RAF) that governs the evolution of each agent's set point-their individually adaptive optimal sociality level. We prove several properties of the system, including conditions for the emergence of isolation.

Third, we combine both frameworks into a fully specified agent-based simulation. Numerical results reveal a phase transition controlled by the group interaction parameter: below a critical threshold, isolation vanishes in the long run; above it, a persistent fraction of isolated agents emerges.

Chapter 1

Introduction

The aim of this thesis is to propose a model for the dynamics of acute and chronic loneliness, grounded in the concept of social homeostasis. The model builds upon the latest developments in network science.

In recent years, the field of mathematical modeling of social phenomena has flourished. This is due to several factors: first, the use of computers, which enables the analysis and simulation of increasingly complex models; second, advances in network science, which, as a multidisciplinary paradigm, has provided tools for a deeper understanding of these phenomena; and finally, the vast amount of high-granularity data we can now collect, which has revealed patterns and regularities that have enriched mathematical modeling.

Building on this foundation, the work conducted in this thesis can be summarized as follows:

Chapter 2 provides a brief introduction to network theory, covering the fundamentals of graph theory, key network metrics, and generative models. It then illustrates how network topology influences dynamical processes, with a focus on the SIS model for infectious disease spread. The chapter also reviews more recent developments, including temporal networks (using the Activity-Driven model as a paradigm), higher-order networks (which go beyond dyadic interactions), and adaptive networks.

Chapter 3 introduces the theory of Interpolating Higher-Order Temporal Networks (IHTNs). These networks incorporate both dyadic and group interactions at a temporal level. The goal is twofold: to analyze the structural and dynamical processes on such networks, and to inject greater realism for simulating the model proposed in Chapter 5. Two types of IHTNs are presented-rSAD and mc-SAD-and their structural properties as well as SIS dynamics are studied.

Chapter 4 presents a general framework for modeling acute and chronic loneliness dynamics. This framework is built on a general structure and introduces the concept of a Realization Adaptive Function (RAF), which hard-codes the adaptation of an agent's behavior to the realization of a stochastic process. Several properties of the model are proven, and connections to stochastic process theory are established.

Chapter 5 presents the SH Model. Based on the framework from Chapter 4 and the IHTNs from Chapter 3, analytical approximations and numerical simulations are conducted to understand the dynamics of the phenomenon and the influence of

parameters.

Chapter 6 proposes various extensions of the model, including social reinforcement and memory mechanisms for the Activity-Driven model generalized through stochastic optimization tools, as well as psychological aspects not addressed in the core model.

The organization of the thesis is depicted in fig 1.1. This work provides a novel mathematical framework to quantify and simulate the interplay between social structure, individual adaptation, and the emergence of isolation, offering insights for both theoretical and applied social science.

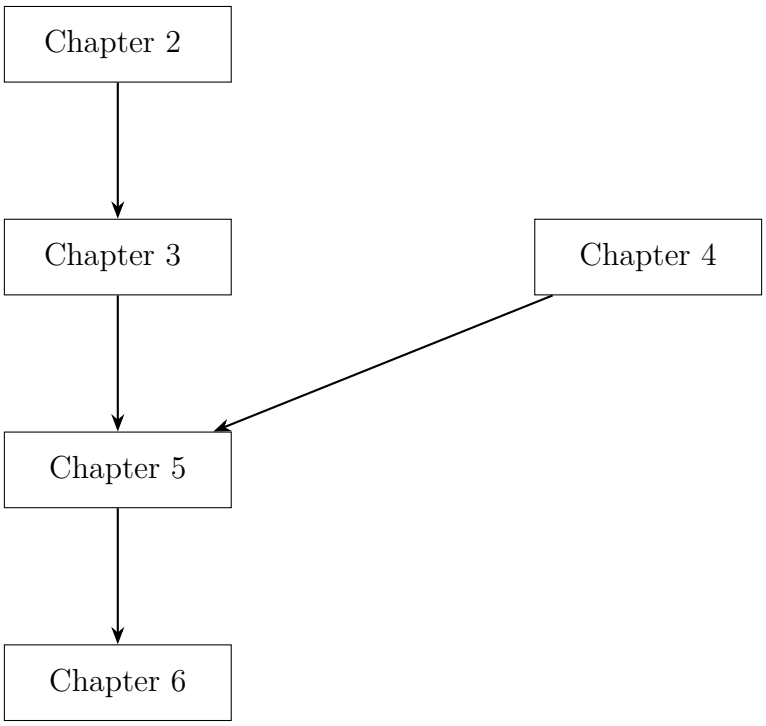

Figure 1.1: Flowchart of chapter dependencies

Chapter 2

A brief Inquiry Into Networks Theory

Network theory has proven to be a successful paradigm in science: its interdisciplinary nature has a wide range of applications, from pure mathematical properties to empirical studies of biological and social networks. In this chapter, we will give a brief introduction to fundamental concepts in the discipline. The discussion is far from original. In each section, we will provide references for the interested reader.

2.1 Networks: basic definitions

Definition 2.1.1. A graph $G = (V, L)$ is a pair where V is a non-empty set of elements called *vertices* and L is a subset of $V \times V$, called *links* or *edges*.

Roughly speaking, V is the set of the elements of the system that we are studying. L is the set of pairs of elements of V that encodes the relationships between them.

To give a concrete example, in 2.1 we plot a network of Florentine marriage alliances during Renaissance. The figure illustrates the elements of the system – namely, the most influential families of the Florentine Renaissance – and the connections between them, represented by links. This approach therefore makes it possible to capture the interactions between the different components of a system comprising multiple agents.

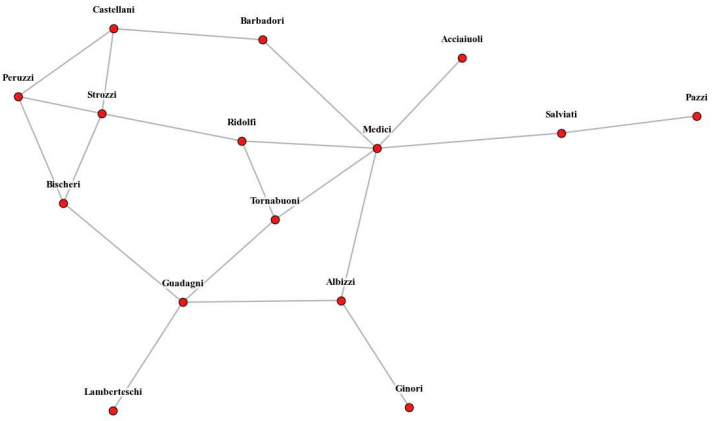

Figure 2.1: Network visualization of Florentine marriage alliances among prominent Renaissance families. Nodes represent families. Edges indicate marital connections. The force-directed layout (spring algorithm) reveals the social fabric of 15th-century Florence, with the Medici family occupying a strategically central position in the network. The visualization highlights the political importance of marriage alliances in Renaissance Florence's power dynamics, as analyzed in [23]

.

Another example is shown in figure 2.2. The network represents Facebook friendships between students who took part in [89].

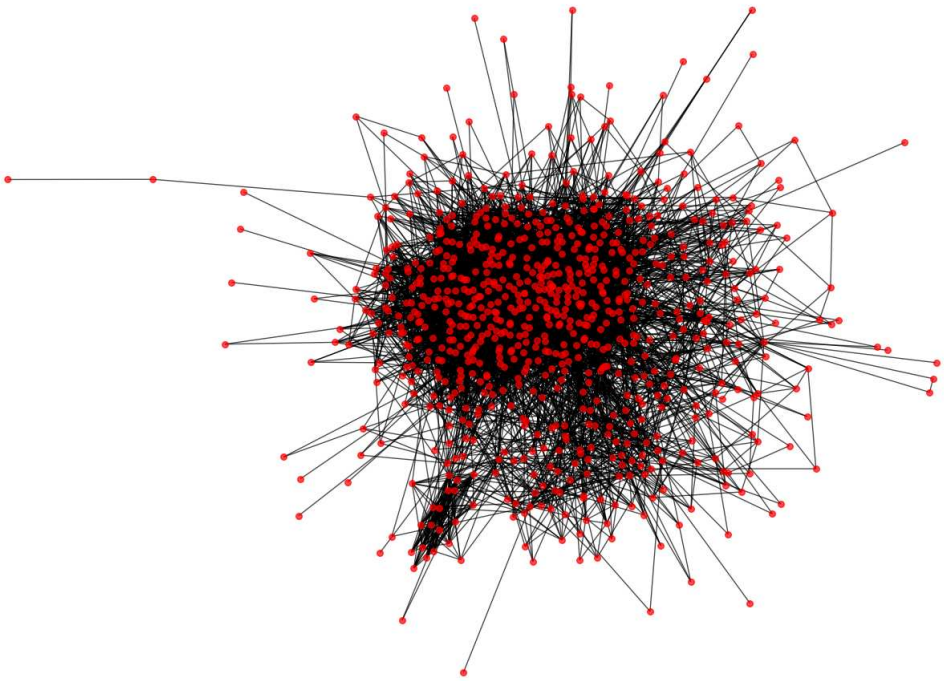

Figure 2.2: A representation of university students' Facebook friendship networks. The data comes from[89]

Definition 2.1.2. We say that two nodes i and j are adjacent if $(i, j) \in L$, which means if there is a link that connects them. The set of nodes which are adjacent to the node $i - th$ are the neighborhood $\mathcal{N}_i$.

Remark 1. *Throughout this thesis, we will always be considering undirected networks. Therefore, if i is connected to j, then j is also connected to i.*

If we are interested in studying the structure of the network, the plot we saw earlier is of limited use. We therefore need mathematical representations that allow us to extract information about the structure. The key tool in this case is the *Adjacency Matrix*.

Definition 2.1.3. Let $G = (V, L)$ be an undirected graph with N vertices. The adjacency matrix A of G is an $N \times N$ matrix defined as follows:

$$A_{ij} = \begin{cases} 1, & \text{if } i \text{ is connected to } j \\ 0, & \text{otherwise} \end{cases}$$

Roughly speaking it gives us a symmetric matrix, in the case of undirected networks, whose elements are one if the two nodes are adjacent and zero if there is no link between them.

Let us therefore consider the concept of a *path* in a network G.

Definition 2.1.4. A path between node i and j , namely $\mathcal{P}_{ij}$, is a sequence of n nodes and $n-1$ links such that each node is connected to the next node along the path by a link. The *length* of the path is the number of links that it contains.

This definition is the broadest one. Further ones impose constraints in order to obtain useful metrics for a network.

Definition 2.1.5. We say that a path between i and j is the *shortest path* or *geodesic path* d_{ij} if it is the path with the fewest number of links between nodes.

Remark 2. *It is important to remark that this definition is coherent with the definition of length for a path defined in 2.1.4. Of course the uniqueness of the shortest path is not guaranteed.*

From this definition, we can introduce:

Definition 2.1.6. We say diameter of a network d_{max} the maximal shortest path between any two nodes in V:

$$d_{max} = \max_{i,j \in V} d_{ij} \tag{2.1}$$

The adjacency matrix is useful in the calculation of the shortest path between two nodes i and j. In fact, following [9], we can consider N_{ij} as the number of paths between nodes i and j. The distance between them, d_{ij} can thus be computed by means of adjacency matrix by a simple argument. If $d_{ij} = 1$, then there is a link connecting i and j. This is equivalent to saying that $A_{ij} = 1$. If we consider a natural number d, then consider the subset of V:

$$\Sigma_{ij}^d = \{\{k_l\}_{l=0,\dots,d} : k_0 = i, k_d = j, \{k_l\} \text{ is a path}\} \tag{2.2}$$

This subset is just the set of d nodes that are a path from i to j. It is clear that $|\Sigma_{ij}^d| = N_{ij}^d$. Relying upon what we have seen for the case $d = 1$, it can be shown that a sequence of nodes form a path of length d if if for every nodes in Σ_{ij}^d all the product $A_{k_0 k_1} ... A_{k_{d-1} k_d}$ are equal to one. In fact, if there exist two node k_{l_h} and

$k_{l_{h+1}}$ such that $A_{k_{l_h} k_{l_{h+1}}} = 0$ then they are not part of the path, since they are not connected. It follows that the number of paths between node i and j with fixed length d can be computed as:

$$N_{ij}^{(d)} = \sum_{\Sigma_{ij}^d} A_{k_0 k_1} ... A_{k_{d-1} k_d} \tag{2.3}$$

where, by the definition of Σ_{ij}^d we are summing over the possible configuration of d nodes that satisfy the condition.

From this definition and basic matrix algebra it follows that:

$$N_{ij}^d = [A^d]_{ij} \tag{2.4}$$

So the number of paths can be calculated by means of the powers of the adjacency matrix. The distance d_{ij} is thus the first natural number such that the $N_{ij}^{(d)}$ is bigger than zero.

Despite the elegant formulation presented in this paragraph, in practice this is often infeasible. Instead, specific algorithms have been proposed to tackle the problem. See [9].

Now we will introduce one of the key metrics of Network Theory.

Definition 2.1.7. We define the degree of node i, denoted by k_i, as the cardinality of its neighborhood $\mathcal{N}_i$.

In the case of an undirected network, the number of adjacent nodes can be obtained considering, once again, the adjacency matrix. As A_{ij} is equal to 1 if they are connected, the degree satisfies:

$$k_i = \sum_j A_{ij} \tag{2.5}$$

If we repeat the same line of reasoning for all the nodes, we have the following formula for the number of links:

$$|L| = \frac{1}{2} \sum_{i,j} A_{ij} \tag{2.6}$$

where we have to take into account the symmetry of the matrix.

Combining eq. 2.5 and eq. 2.6, we get the average degree of the network in terms of the number of links:

$$\mathbb{E}[k] = \frac{1}{N} \sum_i k_i = \frac{2|L|}{N} \tag{2.7}$$

As we have just computed the expected degree of the network, it is useful to introduce the following:

Definition 2.1.8. We define the degree distribution p_k as the probability that a node chosen uniformly at random from the network has degree k.

The definition 2.1.8 holds even for networks in the thermodynamic limit ($N \longrightarrow \infty$). In the case of finite network with a fixed number of nodes N, it can be easily computed as:

$$p_k = \frac{N_k}{N} \tag{2.8}$$

where N_k is the number of nodes with degree k. The degree distribution is a concept of paramount importance in network theory. We will see how it has shaped the development of network theory over the years.

In the literature, there are other metrics that can be used to describe the structure of a network, both locally and globally. Interested readers are referred to articles and books such as [9], [29], [77], [11], [18].

Figure 2.3 shows another example of a network, Zachary's Karate Club [105], with the key metrics listed in the table.

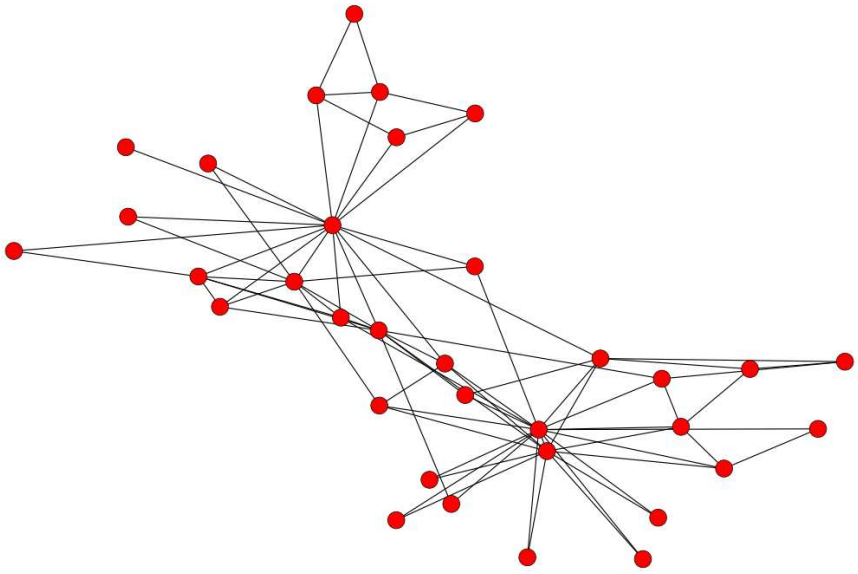

Figure 2.3: Zachary's karate club representation, see [35] for the significant role this network has played in the field.

Metric	Value
nr. of Nodes	34
nr. of Edges	78
Density	0.14
Avr Degree	4.59
Degree Standard Deviation	3.82
Max Degree	17
Min Degree	1
Degree Assortativity	-0.48
Avr Clustering Coefficient	0.57
Transitivity	0.26
nr. of Connected Components	1
Avr Shortest Path Length	2.41
Diameter	5
Radius	3
Avr Degree Centrality	0.14
Avr Betweenness Centrality	0.04
Avr Closeness Centrality	0.43
Avr Eigenvector Centrality	0.15

Table 2.1: Key Metrics of the Zachary's Karate Club Network

2.1.1 Generative Models

We will now focus on the two main generative models: the *Random Graph Model* and the *Albert-Barabasi Model*. These models have played a crucial role in the history of network theory, albeit for different reasons. From a historical perspective, it is worth mentioning the Small-World model, introduced in [103].

Random Graph Model

The *Random Graph Model* was introduced in [33]. In their original work, the two authors focused on the ensemble of graphs with a fixed number of nodes N and links M, commonly denoted as $G(N, M)$. Within this ensemble, each graph is assigned equal probability, meaning that all possible configurations with exactly M edges are equally likely [20].

This construction defines a model in which no structural preference is imposed beyond the global constraints on the number of nodes and edges. As a consequence, the model serves as a natural null model for the study of real-world networks, allowing one to assess whether observed structural properties deviate from randomness. This is of fundamental importance for motifs, i.e. subgraphs that occur frequently in real networks [96].

One of the key results of the Erdős–Rényi framework is the emergence of a phase transition in the connectivity structure of the network [32]. As the average degree $\mathbb{E}[k]$ increases, the system undergoes a transition from a regime characterized by many small disconnected components to one in which a Giant Connected Component appears, containing a finite fraction of the nodes. This transition occurs at $\mathbb{E}[k] = 1$, marking a critical threshold in the model.

Another equivalent way of defining a random network is the one introduced around the same time by Gilbert [34]: the $G(N,p)$. Whereas in the $G(N,L)$ we fix the number of links, in the $G(N,p)$ each node pair is connected with probability p. The procedure is then:

1. Consider N isolated nodes;
2. Consider a node pair of distinct nodes (i,j), generate a random number η between 0 and 1. If η is less than p, then connect the two nodes, otherwise leave them disconnected;
3. Repeat the same process above for all the pairs.

From this simple procedure it is possible to derive the degree distribution of the random network. In particular we want to compute:

$$p_k = \mathbb{P}(k(i) = k) \tag{2.9}$$

This probability involves three products. First of all, the probability that during the process the node i acquires k connections. Given that each connection is independent, this is given by p^k. Then, the probability that the remaining links are absent. Given that we are interested in the case $k(i) = k$ and the random network does not allow loops, this term is given by $(1-p)^{N-k-1}$ since each connection is independent and we are considering a Bernoulli Random Variable, so the probability that i and l are not connected is given by $1-p$. The third term accounts for the different possibilities of arranging $N-1$ potential links in k ways, which is equal to $\binom{N-1}{k}$. Hence, the probability that a node i has degree k is given by:

$$\mathbb{P}(k(i) = k) = \binom{N-1}{k} p^k (1-p)^{N-k-1} \tag{2.10}$$

Thus, the degree distribution in the Random Network Model follows the binomial distribution.

It is customary in network theory to approximate the binomial degree distribution with a Poisson distribution:

$$p_k = \exp(-\mathbb{E}[k]) \frac{\mathbb{E}[k]^k}{k!} \tag{2.11}$$

Indeed, when the average degree is much smaller than N, the Poisson distribution provides a good approximation to the binomial distribution, while offering greater analytical simplicity, as it depends on a single parameter.

However, real networks often deviate significantly from a Poisson degree distribution. In particular, empirical networks typically exhibit highly heterogeneous and skewed degree distributions, often characterized by heavy tails. By contrast, in the Random Graph Model, most nodes have degrees close to the average, and large fluctuations are exponentially suppressed.

Moreover, in the model, networks naturally exhibit short average path lengths, in qualitative agreement with many real-world systems.

However, the model fails to capture another fundamental property of empirical networks, namely the presence of a high clustering coefficient. In random graphs, the probability that two neighbors of a node are also connected is simply given by p, which is typically very small in sparse regimes. As a consequence, the clustering

coefficient remains low, in stark contrast with real networks, where strong local cohesiveness is commonly observed.

This limitation motivated the introduction of the small-world framework, most notably formalized in the Watts–Strogatz model [103], which interpolates between regular lattices and random graphs. Such models are able to simultaneously reproduce high clustering and short average path lengths, providing a more realistic description of many complex networks.

Power Law and Albert-Barabasi Model

As we have pointed out, real-world networks exhibit a more heterogeneous degree distribution that deviates significantly from that of the *Random Graph Model*. This has led to increased interest in distributions known as power laws [78]. A continuous *power law distribution* is the one described by a probability density function $p(x)$ which satisfies:

$$p(x)\,dx = \mathbb{P}(x \leq X < x + dx) = Cx^{-\gamma}\,dx \tag{2.12}$$

where C is a normalization factor, X is the observed data, $\gamma > 0$ is the exponent of the power law. In real world phenomena, moreover, there's a $x_{\min}$ at which the power law is obeyed. Even from a mathematical standpoint, if $x \longrightarrow 0$, there would be a singularity. We will state and prove some properties of the power laws distribution.

Proposition 2.1.9. *If $\alpha > 1$ the constant C is given by:*

$$C = (\alpha - 1)x_{min}^{\alpha-1} \tag{2.13}$$

Proof. From the definition of probability density we have:

$$\int_{x_{\min}}^{\infty} p(x)\ dx = 1 \tag{2.14}$$

Plugging the property 2.12 we get:

$$\int_{x_{\min}}^{\infty} p(x)\ dx = \int_{x_{\min}}^{\infty} Cx^{-\alpha}\ dx = \frac{C}{1-\alpha}[x^{1-\alpha}]_{x_{\min}}^{\infty} = 1 \tag{2.15}$$

Since $\alpha > 1$ we get that the term $x^{1-\alpha}$ tends to zero for $x \longrightarrow \infty$. Then 2.15 yield:

$$C = (\alpha - 1)x_{\min}^{\alpha-1} \tag{2.16}$$

□

From this result we get the expression for the power law density function:

$$p(x) = \frac{(\alpha - 1)}{x_{\min}} \left(\frac{x}{x_{\min}}\right)^{-\alpha} \tag{2.17}$$

Remark 3. *Note that the hypothesis $\alpha > 1$ assure that the l.h.s of 2.15 is convergent.*

Proposition 2.1.10. *Consider a power-law distribution as defined in 2.12. If $x_{min} > 0$, then the following results hold:*

1. *The expectation diverges if* $\alpha \leq 2$.

2. *The second moment diverges if* $\alpha \leq 3$.

Proof. The proof follows directly from the definition of moments.

1. For the expectation, we have:

$$\mathbb{E}[x] = \int_{x_{\min}}^{\infty} x\, p(x)\, dx = \int_{x_{\min}}^{\infty} C x^{1-\alpha}\, dx = \frac{C}{2-\alpha} \left[x^{2-\alpha}\right]_{x_{\min}}^{\infty} \tag{2.18}$$

   If $\alpha < 2$, the term $[x^{2-\alpha}]$ diverges. If $\alpha = 2$, the integral above can be written as:

$$C \int_{x_{\min}}^{\infty} \frac{1}{x}\, dx = C[\ln(x)]_{x_{\min}}^{\infty} \tag{2.19}$$

   Thus the first moment diverges.

2. For the second moment:

$$\mathbb{E}[x^2] = \int_{x_{\min}}^{\infty} x^2\, p(x)\, dx = \int_{x_{\min}}^{\infty} C x^{2-\alpha}\, dx = \frac{C}{3-\alpha} \left[x^{3-\alpha}\right]_{x_{\min}}^{\infty} \tag{2.20}$$

   If $\alpha < 3$, the term $[x^{3-\alpha}]$ diverges. A similar calculation as the one used above proves that for $\alpha = 3$ the integral is divergent. Thus the second moment also diverges.

□

In the literature, these distributions are often called *scale-free*. Indeed, the power-law functional form is the only one that satisfies the *scale invariance* condition:

$$p(bx) = g(b)\, p(x), \tag{2.21}$$

where $b > 0$ is an arbitrary scaling factor, $g(b)$ is a scaling function (depending solely on b), and scale invariance implies that the distribution's shape remains unchanged under rescaling of x. This uniqueness stems from the power-law solution $p(x) \propto x^{-\alpha}$, which yields $g(b) = b^{-\alpha}$. In fact, since the condition 2.21 must holds for every x we set $x = 1$, which yeld:

$$p(b) = g(b)p(1) \tag{2.22}$$

This implies:

$$g(b) = \frac{p(b)}{p(1)} \tag{2.23}$$

Then:

$$p(bx) = \frac{p(b)}{p(1)} p(x) \tag{2.24}$$

Since this must be true for all choice of b, we set $b = 1$ and differentiate both sides:

$$x\dot{p}(1x) = \frac{\dot{p(1)}}{p(1)} p(x) \tag{2.25}$$

where the dots denote the derivative of p with respect to its argument. Equation 2.25 is a linear ODE, whose general solution is:

$$ln(p(x)) = \frac{p(1)}{\dot{p}(1)} ln(x) + k \tag{2.26}$$

Now, setting again $x = 1$ we get:

$$p(x) = p(1)x^{-\alpha} \tag{2.27}$$

where $\alpha = \frac{-p(1)}{p(1)}$.

Thus, in order to fulfill the condition 2.21, the distribution must follow a power law.

Empirical evidence has highlighted the presence of power-law distributions in various phenomena [78]. For this reason, various generative models have been proposed to reproduce this characteristic. Following [18], they can be divided into two classes.

The first is that of static networks. Among these, the fitness model [24] is worth mentioning. Starting from a set of N nodes, a fitness η_i is assigned to each node, drawn from a distribution $F(\eta)$. For each pair of nodes (i, j), they are connected with probability $f(\eta_i, \eta_j)$ where f is a symmetric function. This method generates, for various choices of f, a power-law degree distribution, while for $f(\eta_i, \eta_j) = p$ the random network seen previously is recovered. In particular, the model shows a good-get-richer mechanism, in which nodes with larger fitness are more likely to become hubs.

Other approaches have been proposed in this regard; we refer to [18] for further details.

The second class of models belongs instead to those known as *evolving networks* [2, 9]. The paradigmatic example is certainly the Albert-Barabasi model [7], proposed by the two physicists in the late 1990s. The model is inspired by the study of the WWW and the Internet, which showed two phenomena. The first is that the number of nodes did not remain fixed over time. The second is that the most connected nodes were able to attract incoming nodes into the system more effectively. For this reason, the two mechanisms that led-as we will see at an analytical level-to a power-law degree distribution were:

1. **Growth**: At each step, a number m of nodes is added;
2. **Preferential Attachment**: The probability for a new node to connect to an existing node depends on the previous connections of that node, i.e., $\Pi(k_i) = \frac{k_i}{\sum_j k_j}$

However, to quote Sune Lenham [52]:

This mechanism has been 'discovered' at least twice before. Herbert Simon discovered a mechanism for generating power-laws as early as 1955. Simon's work was rediscovered by de Solla Price in 1976, who was the first to use these ideas in the context of networks (of scientific citations). Price also found an analytical solution to the model. In this sense, the Barabási-Albert model should arguably be called the Price-model.

Remark 4. *The emergence of power laws in certain phenomena is not a unique characteristic of networks. These had already been part of the debate between Mandelbrot and Simon [69, 93]. The interest in this type of distribution is certainly*

influenced by statistical mechanics, where they emerge in contexts of criticality and universality when a divergence of the correlation length occurs. Whereas in statistical mechanics, this happens through the variation of a control parameter, other theories have been explored, such as Self-Organized Criticality [6], which has been applied, for example, to evolution with the Bak-Sneppen model [5]. In this context, the emergence of power-law distributions stems from a reorganization of the system based on its internal rules, without any control parameter. A further line of research has been that of Highly Optimized Tolerance, where power laws emerge because the considered system is designed to be resilient to typical attacks but not to generalized failures [25].

Remark 5. *It is important to emphasize, especially in view of what follows, that evolving networks are treated as static networks. In other words, although they are generated through a growth process, their structure is typically analyzed as fixed. This is in contrast with temporal networks, where the time-varying nature of connections is explicitly taken into account.*

We recall here different approaches to the dynamical properties of the scale-free model. The first one is the *continum approach* [2], used in [7, 8].

The approach followed considers the time evolution of the degree k_i of node i. Given m as above, the evolution depends on the connection probability of new nodes, so the equation becomes:

$$\frac{\partial k_i}{\partial t} = m\Pi(k_i) = m\frac{k_i}{\sum_{j=1}^{N-1} k_j} \tag{2.28}$$

The quantity in the denominator is a sum over all nodes except the newly added ones, therefore:

$$\sum_{j=1}^{N-1} k_j = 2mt - m \tag{2.29}$$

And thus equation 2.28 becomes:

$$\frac{\partial k_i}{\partial t} = \frac{k_i}{2t} \tag{2.30}$$

The solution to this equation with the initial condition $k_i(t_i) = m$ is given by:

$$k_i(t) = m\left(\frac{t}{t_i}\right)^{\beta} \tag{2.31}$$

with $\beta = \frac{1}{2}$.
From 2.31 we can study the distribution:

$$\mathbb{P}[k_i(t) \leq k] = \mathbb{P}\left[t_i \geq \frac{m^{\frac{1}{\beta}}t}{k^{\frac{1}{\beta}}}\right] \tag{2.32}$$

Assuming that nodes are added at constant time intervals, we obtain:

$$\mathbb{P}(t_i) = \frac{1}{m_0 + t} \tag{2.33}$$

Substituting into 2.32:

$$\mathbb{P}\left[t_i \geq \frac{m^{\frac{1}{\beta}}t}{k^{\frac{1}{\beta}}}\right] = 1 - \frac{m^{\frac{1}{\beta}}t}{k^{\frac{1}{\beta}}(t+m_0)} \tag{2.34}$$

Finally, the density function can be calculated as:

$$\mathbb{P}(k) = \frac{\partial \mathbb{P}[k_i(t) \leq k]}{\partial k} = \frac{2m^{\frac{1}{\beta}}t}{k^{\frac{1}{\beta}+1}(t+m_0)} \tag{2.35}$$

And thus for $t \longrightarrow \infty$ we obtain:

$$\mathbb{P}(k) = 2m^{\frac{1}{\beta}}k^{-\gamma} \tag{2.36}$$

where we set $\gamma = \frac{1}{\beta} + 1$.
But $\beta = \frac{1}{2}$ and therefore $\gamma = 3$.

A second approach is based Rate Equations [104] and it is presented in [58].

2.2 Dynamical Processes on Networks

In addition to studying network properties, these can be used to study dynamic processes. In particular, we highlight two of them.

Firstly, dynamic systems. Without considering the network structure and its simpler terms, the dynamics of an element in the space of states X can be represented by an autonomous differential equation (or a system of ODEs) [97]:

$$\frac{dx}{dt} = F(x) \tag{2.37}$$

or by a difference equation:

$$x(t+1) = f(x(t)) \tag{2.38}$$

In the case of static networks, we recall the definition of *Dynamical Network*. We consider X_i as the state space of the nodes $v_i \in V$ of a given network G. The state of the network will therefore be an element of the product space of the states of each node, $\mathbf{x} = (\mathbf{x_1}, ..., \mathbf{x_N}) \in X = X_1 \times ..... \times X_N$. A *dynamical network* is thus described, analogously to the theory of continuous-time dynamical systems, by:

$$\frac{dx}{dt} = F(x, t, L) \tag{2.39}$$

where the vector field $F : X \times T \longrightarrow X$ is given, and the set L of links is provided as a parameter of the system.
A more structured and useful form for understanding is given by the following:

$$\frac{dx_i}{dt} = f_i(x, t) + \sum_{i \sim j} g_{ij}(x_i, x_j, t) \tag{2.40}$$

where $f_i : X_i \times T \longrightarrow X_i$ and $g_{ij} : X_i \times X_j \times T \longrightarrow X_i$.
The network can therefore be decomposed into a *local vector field* f_i and a *coupling function* g_{ij}, which describes the interaction that the i-th node has with

the set of its neighbors. Given that only the nodes connected with i contributes to the dynamic, equation 2.40 can be written by means of the Adjacency Matrix A:

$$\frac{dx_i}{dt} = f_i(x,t) + \sum_{i=1}^{N} A_{ij} g_{ij}(x_i, x_j, t) \tag{2.41}$$

Another approach is the one based on Markov Processes [38][53], also called the *microscopic approach* [11]. In particular, let us consider node i, and associate to each node the variable σ_i. To determine the microstate of the network, it is therefore necessary to know the vector $\sigma(t) = (\sigma_1(t), \dots, \sigma_N(t))$. The analysis thus involves studying a *master equation*, which describes the time evolution of the probability $\mathbb{P}(\sigma, t)$ of finding the system in a given configuration σ. Approximating in continuous time, the master equation takes the form:

$$\frac{\partial \mathbb{P}(\sigma,t)}{\partial t} = \sum_{\sigma'} \left[\mathbb{P}(\sigma',t)\, W(\sigma' \longrightarrow \sigma) - \mathbb{P}(\sigma,t)\, W(\sigma \longrightarrow \sigma')\right] \tag{2.42}$$

In this equation, σ' represents the various microstates of the system, σ is the state under consideration, and $W(\sigma \to \sigma')$ is the transition rate, i.e., the probability per unit time that the system transitions from σ to σ'.

SIS model on Networks

In this section, we focus on the *SIS* model, one of the main models used in the study of the spread of infectious diseases [56][44].

Consider a fixed population of N agents. In the model, each agent can belong to one of two mutually exclusive compartments: the infected compartment I and the susceptible compartment S. After recovering from the infection, each agent returns to the susceptible compartment S.

In the field, it is customary to distinguish between two types of processes [11]: spontaneous and binary. The former, such as recovery, occur without contact with other agents and are assumed to happen at a constant rate γ. This corresponds to an exponential process, where agents spend an average time γ^{-1} in the compartment I. In contrast, binary processes occur through interactions with other agents. It is customary to assume that these are governed by the *Law of Mass Action*, a chemical law stating that the reaction rate is proportional to the density of the reactants. Denoting by β the *infection rate*, the model can be written as:

$$\begin{cases} \frac{dS}{dt} = -\beta SI + \gamma I \\ \frac{dI}{dt} = \beta SI - \gamma I \end{cases} \tag{2.43}$$

where we set $N = 1$. This allow us to reduce the number of degrees of freedom of the system: $S = 1 - I$.

By plugging this identity in 2.43 we get the following differential equation:

$$\frac{dI}{dt} = \beta(1 - I) - \gamma I \tag{2.44}$$

It is possible to obtain an analytical expression for the solution, but we will work with a quantitative analysis. The equilibrium conditions reads:

$$\frac{dI}{dt} = 0 \Longrightarrow \beta(1-I)I - \gamma I = 0 \tag{2.45}$$

Then:

$$I[\beta(1-I) + \gamma] = 0 \tag{2.46}$$

The first equilibrium is the disease free equilibrium $I_{DF} = 0$. In order to obtain the second one, we set:

$$\beta(1-I) + \gamma = 0 \tag{2.47}$$

which implies $I_{end} = 1 - \frac{\gamma}{\beta}$, the so-called endemic equilibrium. There is a strong connection with statistical mechanics, in particular phase transition [81]. In fact, the *disease free* equilibrium is asymptotically stable when $\frac{\beta}{\gamma}$ is less than one, whereas the endemic equilibrium exist and is asymptotically stable when $\frac{\beta}{\gamma} \geq 1$. In Figure 2.4, the phase transition is depicted, which can be described by treating $\frac{\beta}{\gamma}$ as the control parameter and examining the equilibrium I_∞.

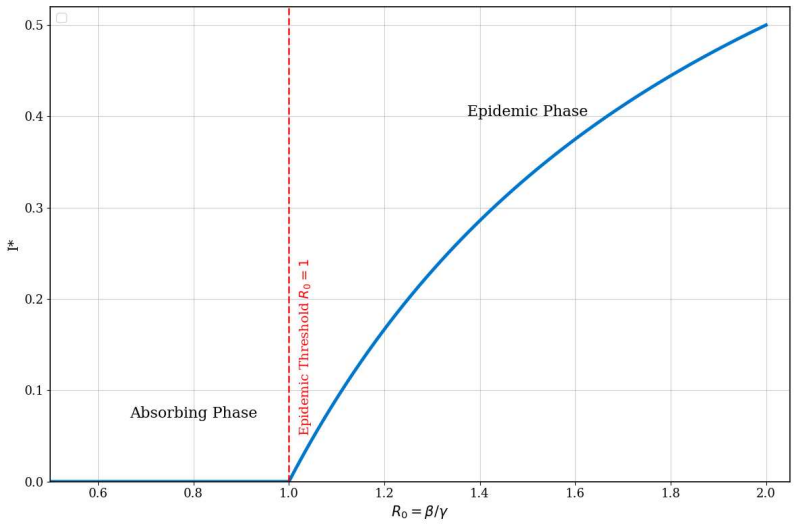

Figure 2.4: The phase transition in the SIS model in the HM hypothesis

We now extend the SIS model to take into account network features. As we emphasized in the previous section, an exact result is not practical due to the large dimension of the generator. For this specific reason in the literature several approaches can be found to obtain a Mean Field Approximation. We start by considering the Degree Based Approximation *(DBMFA)*. In this framework, it is assumed that all nodes with degree k are statistically equivalent. In this context, we study the density $\rho_k^I(t)$ of infected nodes of degree k at time t. The equation reads:

$$\frac{d\rho_k^I(t)}{dt} = -\rho_k^I(t) + \lambda k[1 - \rho_k^I(t)] \sum_{k'} \mathbb{P}(k'|k)\rho_{k'}^I(t) \tag{2.48}$$

Here, we have rescaled time by γ^{-1}, so we have $\lambda = \frac{\beta}{\gamma}$. In the equation 2.48 we have:

- The first term represents the recovery process;

- The second term consists of the probability that node k is susceptible, multiplied by the sum of the probabilities that an infected node k' is connected to node k, the infection probability λ, and the k links through which infection can occur.

A drastic simplification is obtained when the network is uncorrelated. In this case, we have:

$$\mathbb{P}(k'|k) = \frac{k'\mathbb{P}(k')}{\mathbb{E}[k]} \tag{2.49}$$

Substituting 2.49 into 2.48, we obtain:

$$\frac{d\rho^I k(t)}{dt} = -\rho^I k(t) + \lambda k[1 - \rho^I k(t)]\Theta \tag{2.50}$$

where:

$$\Theta = \sum k' \frac{k'\mathbb{P}(k')}{\mathbb{E}[k]} \rho^I_{k'}(t) \tag{2.51}$$

The relation 2.51 gives the probability of finding an infected node by following a random link. By imposing the stationary condition in 2.50, we obtain:

$$\rho^I_k = \frac{\lambda k \Theta(\lambda)}{1 + \lambda k \Theta(\lambda)} \tag{2.52}$$

since at equilibrium, Θ depends only on λ. Substituting 2.52 into the definition of Θ, we derive the equation:

$$\Theta(\lambda) = \frac{1}{\mathbb{E}[k]} \sum_k k\mathbb{P}(k) \frac{\lambda k \Theta(\lambda)}{1 + \lambda k \Theta(\lambda)} \tag{2.53}$$

which yield the following condition for the threshold:

$$\lambda > \lambda_c^{DMBF,unc} = \frac{\mathbb{E}[k]}{\mathbb{E}[k^2]} \tag{2.54}$$

If we take into account the structure and the properties of the network, an interesting result holds in the case of *scale free networks*, with a power law degree distribution. In the thermodynamic limit, if the exponent of the power law distribution satisfies the condition in the appendix, we have that the Second Moment of the Degree Distribution is divergent, viz the absence of the epidemic threshold [80].

The second method we present leverages the properties of *Bernoulli random variables*. We . Let $\{X_i(t)\}_{i=1}^N$ be a collection of Bernoulli random variables where, for each node i at time t:

$$X_i(t) = \begin{cases} 1 & \text{if node } i \text{ is infected at time } t, \\ 0 & \text{otherwise.} \end{cases} \tag{2.55}$$

Using standard properties of Bernoulli random variables, the expectation is

$$\mathbb{E}[X_i(t)] = \mathbb{P}(X_i(t) = 1) = \rho^I_i(t), \tag{2.56}$$

where $\rho^I_i(t)$ represents the probability that node i is infected at time t. Hence, the exact equations for the expectation of being infected for each node i of the SIS model are given by:

$$\frac{d\mathbb{E}[X_i(t)]}{dt} = \mathbb{E}\left[-\gamma X_i(t) + (1 - X_i(t))\beta \sum_{j=1}^{N} a_{ij} X_j(t) \right]. \tag{2.57}$$

For a static network, Eq. (2.57) reduces to:

$$\frac{d\rho_i^I(t)}{dt} = -\rho_i^I(t) + \lambda \sum_{j=1}^{N} a_{ij} \rho_j^I(t) - \lambda \sum_{j=1}^{N} a_{ij} \mathbb{E}[X_i(t) X_j(t)], \tag{2.58}$$

where time has been rescaled by $1/\gamma$ and $\lambda = \beta/\gamma$.

However, Eq. (2.58) is not yet closed, as it depends on the two-node expectations. In the *Individual-Based Mean-Field Approximation* (IBMF) [81] it is assumed that the states of adjacent nodes are independent:

$$\mathbb{E}[X_i(t) X_j(t)] \equiv \mathbb{E}[X_i(t)]\, \mathbb{E}[X_j(t)] = \rho_i^I(t) \rho_j^I(t), \tag{2.59}$$

which leads to the closed dynamical equations:

$$\frac{d\rho_i^I(t)}{dt} = -\rho_i^I(t) + \lambda \left[1 - \rho_i^I(t)\right] \sum_{j=1}^{N} a_{ij} \rho_j^I(t). \tag{2.60}$$

To predict the epidemic threshold, a linear stability analysis can be performed on Eq. (2.60). Linearizing around the disease-free equilibrium yields the Jacobian matrix with elements:

$$J_{ij} = -\delta_{ij} + \lambda a_{ij}. \tag{2.61}$$

An endemic state emerges when the largest eigenvalue of J becomes positive. This condition directly defines the epidemic threshold, linking the network topology to the critical value of λ at which a global outbreak can occur. This leads to:

$$\lambda_c = \frac{1}{\Lambda_{\max}(A)}, \tag{2.62}$$

where $\Lambda_{\max}(A)$ is the largest eigenvalue of the adjacency matrix A.

Cascade Model

In this brief paragraph, we provide an overview of the Watts model for complex contagion.

The Watts Cascade Model [102] offers a simple yet powerful framework to study complex contagion processes on networks. In this model, each node can occupy one of two states: inactive or active. A node adopts the active state if a sufficient fraction of its neighbors is already active, capturing the idea that some behaviors or innovations require reinforcement from multiple contacts to be adopted. More formally, each node i is assigned a threshold $\phi_i \in [0, 1]$, representing the minimum fraction of active neighbors required for activation, and the node becomes active when this fraction is exceeded. This approach allows the model to capture a wide range of social phenomena, from the diffusion of innovations to the spread of social norms and collective behaviors.

Watts investigated the conditions under which a social phenomenon could propagate to reach a substantial fraction of a network. Assuming a uniform threshold distribution and an Erdős-Rényi network, he showed that global cascades occur only within an intermediate connectivity regime. This result highlights the subtle interplay between local threshold dynamics and the global structure of the network.

In fact, when connectivity is low, the network is highly fragmented, and the behavior remains confined within disconnected components that cannot influence one another. Conversely, in highly connected networks, nodes exhibit greater initial resistance to activation: a highly connected node requires a substantial number of confirmations from its neighbors, who themselves require multiple sources of reinforcement before adopting the behavior. This recursive effect can significantly hinder cascade propagation, despite the abundance of connections.

Consequently, there exists a window in which cascades capable of spreading across a sizable portion of the network can emerge, defining two critical points: one at low connectivity, marking the lower bound of the cascade window, and one at high connectivity, marking the upper bound. At the lower critical point, the cascade size distribution follows a power-law, with cascades limited to small clusters. At the upper critical point, the behavior becomes more nuanced: most cascades still affect only a small number of nodes, yet in rare cases, a cascade can propagate extensively, potentially invading the entire network. These findings underscore the nontrivial relationship between network connectivity, local thresholds, and the global dynamics of complex contagion.

Extensions and generalizations of the Watts model have been proposed to account for heterogeneous thresholds, community structure, and weighted networks [28], providing a more comprehensive framework for understanding the emergence and spread of complex behaviors.

2.3 Temporal Network

So far, we have discussed static networks, in which interactions do not change over time. However, in real-world systems, the connections between entities are rarely fixed; they evolve dynamically as a function of time. This motivates the study of *Time-Varying Networks*, also referred to as *Temporal Networks*. We will not delve into the full complexity of this field. As highlighted in [47] [45], unlike static networks, providing a unified theoretical framework for temporal networks is considerably more challenging, particularly regarding generative models and analytical treatments. The landscape of temporal networks is highly heterogeneous: for example, a temporal network modeling the dynamics of a sexually transmitted disease differs substantially from one describing biological interactions among cells, both in terms of structure and the nature of contacts.

In particular, the specific model we consider falls within the category of *Contact Networks* [47]. In this framework, a network G_t is defined for each discrete time step t, capturing the instantaneous interactions among nodes. One can also consider the *aggregated network* over a time window, defined as $G = \bigcup_t G_t$, which retains information about which nodes have interacted at least once during the observed period. These networks can be described by a *time-dependent adjacency matrix*

$A_{ij}(t)$, where each element represents the presence or absence of a contact between nodes i and j at time t. An alternative representation is provided by the *Contact Matrix* $C(t)$, whose elements encode the number of contacts occurring between pairs of nodes within a single time step t.

A key aspect in the study of temporal networks is the consideration of *time scales* [29]. Specifically, the dynamics of the process of interest-such as the spread of information, epidemics, or social influence-interact with the time scale over which the network evolves. When the network evolves much faster than the dynamical process, an effective mean-field or aggregated approximation may be sufficient. Conversely, when the network changes on a comparable or slower time scale, the temporal ordering of contacts becomes crucial, and neglecting the time dimension can lead to inaccurate predictions of the system's behavior. This interplay between dynamical and structural time scales is essential for understanding spreading processes on temporal networks.

2.3.1 Activity Driven Model

A prominent example of a temporal network is the *Activity-Driven Network* model [82]. To motivate this framework, the authors analyzed several real-world datasets in order to quantify the level of engagement of individual agents. These datasets include: publications recorded in *Physical Review Letters*, direct message exchanges on *Twitter*, and the participation of actors and actresses in movies or television series as listed on *IMDB*.

In each dataset, an agent's *activity* is measured as the number of interactions performed over a fixed time interval. Specifically, this corresponds to the number of published papers, messages sent, or appearances in media productions. Based on these observations, each agent i is assigned an *activation potential* x_i, defined as the fraction of interactions carried out by agent i during a time window Δt relative to the total number of interactions in the system during the same interval. This quantity provides a measure of how actively an individual participates in the network at each moment.

The empirical distribution of activation potentials, denoted $F(x)$, characterizes the likelihood that a randomly selected agent exhibits a given level of activity x. These insights form the foundation for the formalization of the *Activity-Driven* model.

Consider a system with N nodes, each assigned an *activity rate* $a_i = \eta x_i$, representing the probability per unit time that node i becomes active and initiates interactions. The scaling factor η ensures that the average number of active nodes per unit time is $\eta \mathbb{E}[x]N$. The network evolves as follows:

1. At each discrete time step, the network G_t starts with N disconnected nodes.

2. Each node becomes active with probability $a_i \Delta t$. Upon activation, the node generates m links connecting to other randomly selected nodes (inactive nodes can still receive links from active nodes).

3. At time $t + \Delta t$, all edges in G_t are removed, so that the duration of each interaction is fixed and equal to $\tau_i = \Delta t$.

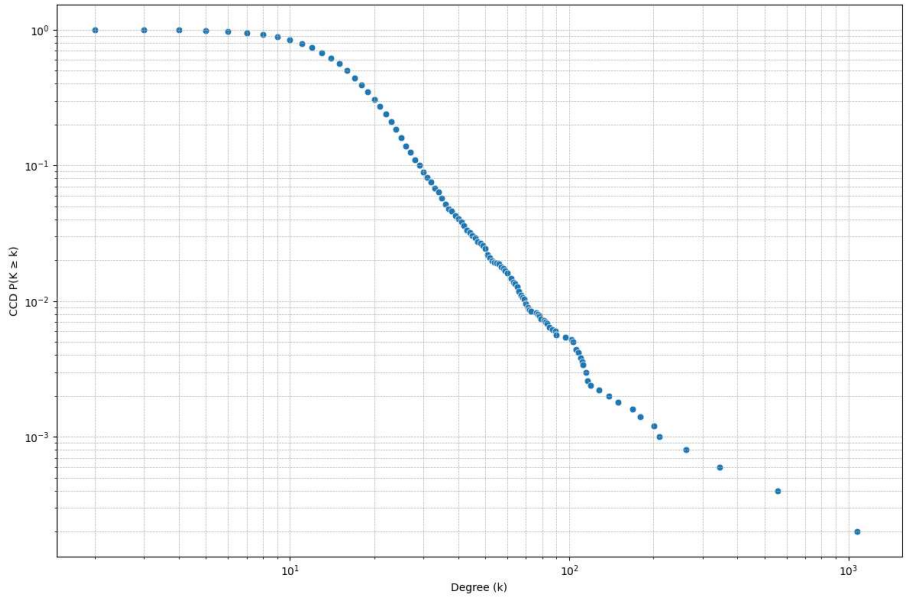

Figure 2.5: CCDF in Log-Log Scale for a single realization of an Activity-Driven Temporal Network. Parameters: $N = 5000$, $t = 1000$, $m = 4$. Activity is sampled from a power-law distribution with a cut-off near the origin (10^{-3}) to avoid singularities and exponent 2.7, compact support in $[10^{-3}, 1]$.

Assuming discrete time steps with $\Delta t = 1$, the instantaneous network at a given time t is formed by nodes representing agents that are active at that moment, together with nodes that receive connections from these active agents. Each active node generates m links, resulting in a total of $L_t = mN\eta\mathbb{E}[x]$ links per time step. Consequently, the average degree per node within a single time step is:

$$k_t = \frac{2L_t}{N} = 2m\eta\mathbb{E}[x]. \tag{2.63}$$

Structurally, the instantaneous network can be viewed as a collection of star-like configurations: the active nodes form the hubs with degree at least m, while other nodes have lower connectivity, being linked only to active nodes. In contrast, the integrated network, obtained by aggregating all instantaneous networks up to a final time T, tends to be significantly denser. For large T and N, the expected degree of node i in the aggregated network can be approximated as:

$$k_i(T) = N\left[1 - \exp\left(-\frac{Tm\eta x_i}{N}\right)\right]. \tag{2.64}$$

This expression highlights how the cumulative activity of each agent over time determines its overall connectivity in the integrated network.

The network structure has important implications for dynamical processes such as epidemic spreading. In particular, the *Invasion Threshold Problem* for the SIS model can be addressed on an activity-driven network using the *Activity-Based Mean-Field Approximation* (ABMF) [82]. Let I_a^t denote the number of infected nodes with activity a at time t. The discrete-time evolution is given by:

$$I_a^{t+\Delta t} - I_a^t = -\gamma\Delta t\, I_a^t + \beta m(N_a^t - I_a^t)a\Delta t \int da' \frac{I_{a'}^t}{N} + \beta m(N_a^t - I_a^t) \int da' \frac{I_{a'}^t a'\Delta t}{N}, \tag{2.65}$$

where the third term accounts for susceptible nodes of class a that are active and get infected by any other infected node, and the fourth term accounts for susceptible nodes that are inactive but receive a connection from an active infected node.

Defining the total fraction of infected nodes as $I(t) = \int \frac{I_a(t)}{N} da$ and the auxiliary quantity $\theta(t) = \int \frac{I_a(t)}{N} a\, da$, we linearize Eq. (2.65) and neglect terms of order $1/N$ to obtain the following system of ordinary differential equations:

$$\begin{cases} \frac{dI}{dt} = -\gamma I(t) + \beta m \mathbb{E}[a] I(t) + \beta m \theta(t), \\ \frac{d\theta}{dt} = \beta m \mathbb{E}[a^2] I(t) - \gamma \theta(t) + \beta m \mathbb{E}[a] \theta(t). \end{cases} \tag{2.66}$$

The epidemic threshold can be determined using the largest eigenvalue $\lambda_{\max}$ of the Jacobian associated with the linearized system (2.66). The critical point occurs at $\lambda_{\max} = 0$, yielding the epidemic threshold:

$$\frac{\beta}{\gamma} = \frac{1}{m\left(\mathbb{E}[a] + \sqrt{\mathbb{E}[a^2]}\right)}. \tag{2.67}$$

Empirical comparisons between the spread of a pathogen on the temporal activity-driven network and its integrated (aggregated) counterpart show that temporal fluctuations tend to slow down the spread, effectively increasing the *epidemic threshold*. The interplay between temporal structure and epidemic dynamics is therefore a key aspect in understanding contagion on activity-driven networks [81]. In this thesis, this approximation will be applied in Chapter 3.

2.4 HONs

2.4.1 Higher-Order Interactions and High-Order Networks

Over the last decade, one of the most active areas of research in network theory has been the study of *higher-order interactions* (HOIs). Up to this point, we have considered networks composed of pairwise interactions, where links connect nodes in dyads and the system's dynamics are fully captured by two-body interactions. However, in many real-world systems, interactions naturally occur in groups rather than pairs. Examples include chemical reactions, social gatherings, and economic transactions [17].

To formalize the notion of HOIs, it is necessary to define precisely what constitutes an interaction:

Definition 2.4.1. Consider a system of N elements $P = \{p_i\}_{i=0,\dots,N-1}$. An *interaction* is a set $I = (p_0, \dots, p_{k-1})$ consisting of k elements of the system. The *order* of an interaction is defined as $k - 1$.

Within this framework, a 0-interaction corresponds to a single node interacting with itself, a 1-interaction corresponds to a standard link between two nodes, and a k-interaction involves $k + 1$ nodes simultaneously.

Definition 2.4.2. An *interacting system* is a pair $(V, \mathcal{I})$, where V is the set of nodes and $\mathcal{I} = \{I_j\}_{j \in J}$ is the collection of interactions occurring on V.

Although such systems can be described using traditional network tools (e.g., bipartite graphs or cliques), these approaches often introduce limitations when representing group interactions. To capture HOIs more naturally, the network science

community has proposed explicit representations such as simplicial complexes and hypergraphs [12]. In broad terms, a Higher-Order Network is a network representation that explicitly captures interactions involving groups of nodes, rather than only pairwise connections.

In particular, there are two common approaches to represent higher-order interactions. The first is through *simplicial complexes*, which explicitly encode interactions as simplices of various dimensions, capturing not only nodes but also their group structure and all subgroups. The second approach is through *hypernetworks* (or *hypergraphs*), where interactions are represented as hyperedges connecting arbitrary numbers of nodes without necessarily including all subfaces. Both formalisms allow the study of dynamical processes beyond pairwise interactions, but they emphasize different structural aspects of the system.

We thus introduce simplices and simplicial complexes [16] [17] [12].

Definition 2.4.3. Let V be a finite node set. An *n-simplex* $\sigma = \{v_0, \dots, v_n\}$ is a subset of $n+1$ nodes in V. The *dimension* of σ is n, and any subset $\tau \subset \sigma$ is called a *subface* of σ.

Definition 2.4.4. A *simplicial complex* $X = \{\sigma_0, \dots, \sigma_n\}$ is a finite collection of simplices such that for every $\sigma_i \in X$, all its subfaces of any dimension also belong to X.

To develop a more intuitive understanding of simplicial complexes, following [83], it is useful to start from the notion of the *k-skeleton*. Given a simplicial complex X, its k-skeleton, denoted by X_k, contains all simplices of dimension up to k. For instance, the 1-skeleton includes only vertices and edges, thus recovering the underlying graph associated with the complex.

We now introduce the concept of *chains*. The set of n-chains, denoted by $C_n(X)$, is defined as the collection of formal linear combinations of n-simplices with integer coefficients:

$$C_n(X) = \{r_1\sigma_1 + r_2\sigma_2 + \cdots \mid r_i \in \mathbb{Z},\ \sigma_i \in X_n\}. \tag{2.68}$$

This construction provides an algebraic framework that allows one to study the topological properties of simplicial complexes.

A key ingredient in this framework is the *boundary operator* ∂_n, which maps n-chains to $(n-1)$-chains by associating to each simplex the sum of its faces. More precisely, for an n-simplex $[v_0, \dots, v_n]$, the boundary is given by

$$\partial_n[v_0, \dots, v_n] = \sum_{i=0}^{n} (-1)^i [v_0, \dots, \hat{v}_i, \dots, v_n], \tag{2.69}$$

where $\hat{v}_i$ denotes the omission of the vertex v_i. As an example, the boundary of a 2-simplex (a filled triangle) is given by the alternating sum of its three edges. An important property of the boundary operator is that applying it twice always yields zero, that is $\partial_n \partial_{n+1} = 0$.

These operators define a sequence of spaces and maps, known as a *chain complex*:

$$\cdots \to C_{n+1}(X) \xrightarrow{\partial_{n+1}} C_n(X) \xrightarrow{\partial_n} C_{n-1}(X) \to \cdots$$

From this structure, one can define the n-th *homology group* $H_n(X)$, which characterizes the n-dimensional topological features of the complex. It is defined as

$$H_n(X) = \ker \partial_n \,/\, \operatorname{im} \partial_{n+1}. \tag{2.70}$$

The dimension of $H_n(X)$, known as the n-th *Betti number* β_n, provides a count of the number of n-dimensional holes in the complex.

We can also define the notion of a *simplicial connected k-component*, namely a set of k-simplices in X satisfying the following properties:

1. Each simplex shares at least one $(k-1)$-face with another simplex in the same component;

2. Any two simplices A and B in the component are connected by a sequence of k-simplices $[A_0 = A, A_1, \dots, A_n = B]$ such that consecutive simplices share a $(k-1)$-face.

Finally, given a simplicial complex X, it is often useful to consider derived constructions:

1. The *1-skeleton* X_1, consisting of all vertices and edges, which recovers the underlying graph and is particularly relevant for processes such as the SIS model;

2. The *clique complex* $\mathrm{Cl}(X)$, obtained from X_1 by promoting each $(k+1)$-clique of the graph to a k-simplex. For example, a 4-clique corresponds to a 3-simplex in $\mathrm{Cl}(X)$.

Remark 6. *More generally, higher-order interactions can be represented using hypergraphs, which are defined by a node set V and a collection of hyperedges H, specifying which nodes participate in each interaction.*

Remark 7. *It is worth briefly highlighting the advantages and disadvantages of simplicial interactions. As mentioned, these are less general structures than hypernetworks. The condition regarding the topology therefore does not allow us to capture effects that might occur in a three-body interaction. Consider, for example, the expression of a phenotypic trait that depends on three genes which, when taken in pairs, have no function.*

However, the simplicial representation allows us to make use of the tools of Algebraic Topology [43].

For this reason, it is necessary to consider under what conditions a system can be represented by simplicial interactions-that is, where the approximation is legitimate-and when, on the other hand, hypernetworks are more natural.

As pointed out in [13], one of the most interesting dynamical features of higher-order network models is the emergence of first-order phase transitions, which are much less common in traditional pairwise interaction models. This highlights how group interactions can fundamentally alter the collective behavior of a system, leading to abrupt changes in the state of the network that would not be observed in standard dyadic networks (or at least, not so often).

2.4.2 Simplagion

Building upon our previous discussion of the SIS model on pairwise networks, it is possible to extend epidemic dynamics to simplicial complexes and hypergraphs. A

notable example is the *Simplagion* model [49], which describes complex contagion processes on simplicial complexes.

The main idea of Simplagion is that contagion may occur not only via pairwise interactions but also through group interactions. This aligns with empirical observations in social systems [39], where the adoption of behaviors or beliefs often requires simultaneous exposure to multiple peers.

The mean-field equation governing the dynamics up to simplices of dimension D can be written as:

$$\dot{\rho}(t) = -\gamma\rho(t) + \sum_{\omega=1}^{D} \beta_\omega \langle k_\omega \rangle \rho^\omega(t)(1-\rho(t)), \tag{2.71}$$

which for the simplest case including pairwise and 2-body interactions becomes

$$\dot{\rho}(t) = -\gamma\rho(t) + \beta\langle k\rangle\rho(t)(1-\rho(t)) + \beta^\Delta\langle k_\Delta\rangle\rho(t)^2(1-\rho(t)). \tag{2.72}$$

This system admits up to three stationary states. Defining $\lambda = \frac{\beta}{\gamma}$ and $\lambda^\Delta = \frac{\beta^\Delta}{\gamma}$, the fixed points are

$$\rho^*_{2\pm} = \frac{\lambda^\Delta - \lambda \pm \sqrt{(\lambda-\lambda^\Delta)^2 - 4\lambda^\Delta(1-\lambda)}}{2\lambda^\Delta}. \tag{2.73}$$

The phenomenology of the model can be summarized as follows:

- If $\lambda^\Delta \leq 1$, the transition is continuous, similar to the classical SIS model.
- If $\lambda^\Delta > 1$ and $\lambda > 2\sqrt{\lambda^\Delta} - \lambda^\Delta$, two regimes arise:
  1. For $\lambda > 1$, the system behaves like the standard SIS model.
  2. For $2\sqrt{\lambda^\Delta} - \lambda^\Delta < \lambda < 1$, both solutions $\rho^*_{2\pm}$ exist. In this case, the quasi-stable fixed point ρ^*_{2-} defines a threshold: if the fraction of infected nodes surpasses this value, the system undergoes a discontinuous (first-order) transition.

As the authors point out, the presence of a metastable state highlights the importance of a critical mass for the spread of complex contagion, in line with sociological research.

2.4.3 Simplicial Activity Driven *SAD*

The theory of Time Varying HONs is still in its infancy. In this section we will then focus on a specific model proposed by Petri and Barratt [83]. Building on the Activity Driven, they proposed the Simplicial Activity Driven *SAD*.
In particular, we will focus on the *Nodes Preserving Model*. Consider then a fixed set of nodes N. Each node has an activity a_i assigned. At each time step t, the node becomes active with probability a_i and forms a *m-simplex*. At time $t+1$ every link is removed and the process starts again. In their work, the authors analyzed the structure of the model and the dynamics of a SIS model analytically.

The first quantity of interest is the average degree. In order to evaluate it, consider the expected number of contacts made by a single node in T time steps.

It consists of two terms: the number of times the node became active and formed a *m-simplex*; the number of times the node participated in a *m-simplex* originated by another node. This gives us:

$$k_T(i) = mTa_i + \sum_{j \neq i} \frac{m^2 T a_j}{N-1} \tag{2.74}$$

For $N >> 1$, we can approximate:

$$k_T(i) = ma_i T + \sum_{j \neq i} \frac{m^2 T a_j}{N-1} \simeq mT(a_i + m\mathbb{E}[a]) \tag{2.75}$$

Now, For any node distinct from i, the probability not to have been involved in any of these interactions is given by: $(1 - (\frac{1}{N-1})^{k_T(i)})$.

Using this formula, they get the number of distinct nodes having interacted with i by inserting the number of contacts in eq. 2.75

$$\begin{aligned} k_T^{SAD}(i) &= (N-1)\left[1 - \left(1 - \frac{1}{N-1}\right)^{k_T(i)}\right] && (2.76) \\ &\simeq N\left[1 - e^{-\frac{T\dot{m}(a_i + \mathbb{E}[a]m)}{N}}\right] && (2.77) \end{aligned}$$

Then, they consider the simplicial structure of the model. In particular, they compute the average number $k_2(i,T)$ of 2-simplices to which a node i belongs in the SAD aggregated until T. Using a similar argument, they get:

$$k_2(i,T) = \binom{N-1}{2}\left(1 - e^{-\frac{(m)(m-1)}{(N-1)(N-2)}T(a_i + m\mathbb{E}[a])}\right). \tag{2.78}$$

As noted by the authors, this is equivalent to evaluate the number of distincts cliques of three nodes to which i has participated from time 0 to T.

$$\begin{aligned} \partial_t I_a = &-\gamma I_a + \beta m\, S_a\, a \int \frac{I_{a'}}{N}\, da' \\ &+ \beta m\, S_a \int a' \frac{I_{a'}}{N}\, da' \\ &+ \beta S_a \int a' m \frac{S_{a'}}{N}\, da' \int (m-1)\frac{I_{a''}}{N}\, da'' \end{aligned} \tag{2.79}$$

The last term in Eq. (2.79) represents the characteristic contribution of simplicial interactions. Unlike pairwise contagion, here a susceptible node may become infected not only by the node that initiated the interaction, but also due to the presence of another infected node within the same group interaction. This term therefore captures the higher-order mechanism of infection through group contacts.

Following the procedure outlined previously for linearization and threshold analysis, the epidemic threshold can be derived and is given by:

$$\lambda_c^{\text{SAD}} = \frac{\beta}{\gamma} > \frac{2}{\mathbb{E}[a](m+1)m) + m\sqrt{\mathbb{E}[a]^2(m+1)2 + 4(\mathbb{E}[a^2] - \mathbb{E}[a]^2\}}} \tag{2.80}$$

2.5 Adaptive Networks

Over the past few years, a substantial body of literature has developed around so-called *Adaptive Networks*. The defining feature of these models is the mutual interplay between the dynamical system under study and the underlying network topology on which it is embedded. In other words, not only does the network structure influence the evolution of the dynamical variables, but the dynamics themselves can feed back to reshape the network connectivity over time.

More formally, we can now introduce *Adaptive Dynamical Networks* (ADNs), in which the network structure is an integral part of the dynamical system. Starting from Eq. 2.39 and following [15] we extend the state space to $\mathcal{L} = \{0,1\}^M$ with $\mathbf{l} \in \mathcal{L}$. In general terms, the evolution of an adaptive dynamical network can then be written as:

$$\begin{cases} \frac{d\mathbf{x}}{dt} = f(x_1, \dots, x_N, l_1, \dots, l_M, t), \\ \frac{d\mathbf{l}}{dt} = h(x_1, \dots, x_N, l_1, \dots, l_M, t), \end{cases} \tag{2.81}$$

where $\mathbf{x} = (x_1, \dots, x_N)$ denotes the dynamical variables associated with the nodes, and $\mathbf{l} = (l_1, \dots, l_M)$ encodes the network structure.

In the literature, a more practical representation is often used. Consider, as usual, the adjacency matrix of the network with elements $a_{ij} \in \{0,1\}$. The dynamics can then be expressed as:

$$\begin{cases} \frac{dx_i}{dt} = f_i(x,t) + \sum_{j=1}^{N} a_{ij}(t) g(x_i, x_j, t), \\ a_{ij}(t) = H_{ij}^t[x(\cdot), A(\cdot), t], \end{cases} \tag{2.82}$$

where H_{ij}^t is an operator governing the appearance or disappearance of a link, i.e., determining when a_{ij} transitions from 0 to 1 (or vice versa). This formulation captures the coevolution of node dynamics and network topology, which is the defining feature of adaptive networks.

To make the discussion more concrete, we can consider the case of an *Adaptive SIS* model. As usual, we assume a *continuous-time SIS model* with infection rate β and recovery rate γ. We now describe the dynamics of the links. Mathematically, the network is encoded by a *time-dependent adjacency matrix* $A(t)$. The adaptive dynamics of the links consist of two processes:

1. If one of the nodes i or j is infected and the other is susceptible, the link between them can be removed with a *Poisson rate* ξ;

2. If two susceptible nodes i and j are not connected, a link can be created between them with a *Poisson rate* η.

For our purposes, it is worth mentioning recent work that incorporates adaptive dynamics into temporal networks. In [68], the activity of the nodes is made adaptive to study adaptation and mitigation strategies in the context of epidemic spreading.

Chapter 3

Interpolating HO Temporal Networks (*IHTNs*)

3.1 The rationale behind Interpolating HO Temporal Networks

In the previous chapter, we recalled the Network Theory developments. In particular,we drew attention to group dynamics and the temporal properties. We have seen a paradigmatic example of pairwise temporal network: the *Activity Driven* model [82]. Then we recalled the SAD model [83], where the interaction is always simplicial. In social contexts, however, both types of interaction are present. A person might decide to contact part of their social circle for a group hangout (simplicial interaction) or see the same people individually (pairwise interactions).

In this chapter, we build on these frameworks to study how the tendency of nodes to form group interactions shapes network structure and dynamics. We introduce a minimal extension of the AD and SAD models by adding a single parameter r, which interpolates between dyadic and group-based interactions in the case of node preserving. Although reality is more nuanced, this model on the one hand allows for analytical results to be obtained, and on the other hand makes it possible to isolate, ceteris paribus, the impact that the type of interaction has on structure and dynamics.

In particular, we studied how group interaction influences the network structure (contacts and 1-skeleton). Subsequently, we investigated the invasion threshold problem of an SIS model [81] unfolding on the network.

Our analysis reveals that increasing r has two major effects:

1. it *democratizes* connectivity by boosting the degree of low-activity nodes,

2. it lowers the epidemic threshold of an SIS process unfolding on the resulting network, consistent with the role of large gatherings as epidemic accelerators.

Next, a more complex model, $mc-SAD$, is proposed, which takes into account the variability of the target of pairwise interactions and the size of the simplex. This model increases realism, but at the cost of greater complexity.

These results highlight the fundamental role of higher-order interactions in shaping both structural and dynamical properties of temporal networks. As we shall see in the *SH Model*, it is crucial for understanding social dynamics, where both group

and pairwise interactions take place.

Independently, in [41] the authors proposed a framework that allows for the incorporation of both pairwise and group interactions. Their work focuses on the edge preserving AD (eAD) of [83]. Given this interpolating nature, we call them Interpolating High Order Temporal Networks *(IHTNs)*.

3.2 r-SAD: structure and dynamics

We now introduce the *rSAD* model, an interpolation between the Activity-Driven (AD) and Simplicial Activity-Driven (SAD) models. The model employs a simple interpolatory parameter r, a strategy that is also widely used in the most recent literature [3]. Heuristically, the model work as the follow: fix the number of interactions per unit of time m; for every time step the node is active, with probability r the interactions with the nodes will be in a simplex; with probability $(1-r)$ the interactions will be pairwise. This is a drastic simplification, but allows us to understand how the propensity to form group interactions influence the structure of the corresponding network and eventually the properties of the dynamical processes that can be studied on the underlying structure. We highlight that when $r = 0$, we fall back into the original Activity Driven, whereas when $r = 1$, this is just the simplicial activity driven. The situation is depicted in fig. 3.1

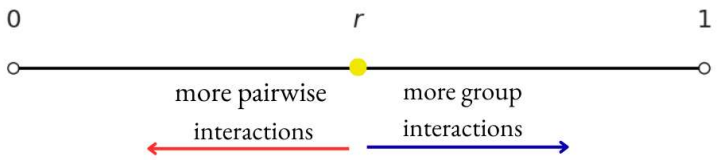

Figure 3.1: The figure illustrates the role of the parameter r, which allows interpolation between *AD* and *SAD*. This parameter also allows us to investigate the effect of group interactions in this class of models.

Definition 3.2.1. We say r-Simplicial Activity Driven (*r-SAD*) the following collection of graph $\{G_t\}$: given a set of N agents with activity $a_i \sim p(a)$ where p is a probability distribution with compact positive support $[\epsilon, 1]$, a parameter $r \in [0, 1]$, for each time step a node i activates with probability a_i and with probability r she forms a $m - simplex$ and with probability $1 - r$ she forms m dyadic interactions.

In more practical terms, for each step the model work as the follow:

1. For each agent i generate a random number $\eta_i(t)$;
2. If $\eta_i(t) < a_i$, then the node i is active;
3. If the agent is active, generate a second random number $\zeta_i(t)$;

4. If $\zeta_i(t) < r$ the node i forms a $m-simplex$ choosing the other nodes with uniform probability $\frac{1}{N-1}$ otherwise she forms m pairwise interactions;

5. Delete all the links created in the time stamp.

In line with the literature on temporal network we define:

Definition 3.2.2. We say integrated graph of the r-SAD the graph $G_t^{\text{r-SAD}}$ the one generated by the following adjacency matrix:

$$A_{G_t} = (a_{ij}(t)) = \begin{cases} 1 & \text{if} \quad C_{ij}(\tau) = 1 \text{for at least one } \tau = 0, \dots, t \\ 0 & \text{otherwise} \end{cases} \tag{3.1}$$

or more in line with the notation of Network Theory $G_t^{\text{r-SAD}} = \bigcup_0^t X_\tau$.

Contacts in the r-SAD

We start by calculating the number of expected contacts for a node i in a fixed window of time.

Consider a fixed time frame T, then the number of contacts accumulated by a generic node i can be broken down into three different components.
First of all, a node can be active with probability a_i and generate m contacts.
Then the node can be involved in both pairwise and group interactions. A node i can be selected by another node j to form a pairwise interaction among $N-1$ agents. Given that the number of agents contacted per unit of time is equal to m, the probability that a node j, once active, selects i to form a pairwise interaction is $\frac{m}{N-1}$. Given the interpolating nature of the r-SAD, we have that these interaction occurs with probability $(1-r)$.
Moreover, a node i can be selected by another node j to form a group interaction of size m. In this case, the number of partners is no longer just the active node j, but all the nodes involved in the group interaction. The two possibilities for an active node are depicted in fig. 3.2.

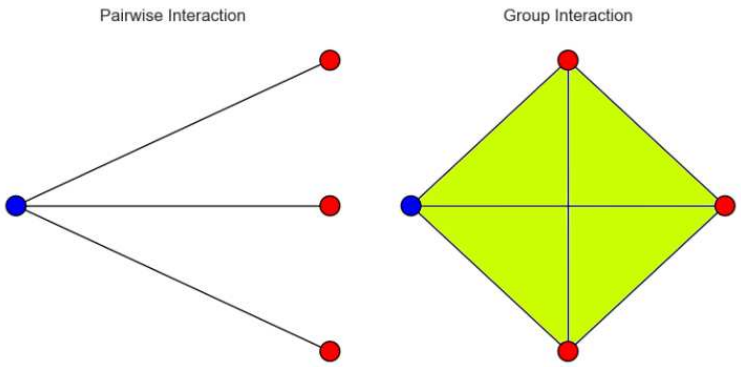

Figure 3.2: The figure shows the two interactions for an active node when $m = 4$. On the left, the interaction is of the dyadic kind, while on the right, it is of the group kind.

Theorem 3.2.3. *In the r-SAD model, the expected number of contacts of a node i with activity a_i is given by:*

$$\mathbb{E}_T[C](i) = ma_iT + \sum_{j \in V \setminus \{i\}} \frac{m^2 T a_j}{N-1} r + \sum_{j \in V \setminus \{i\}} \frac{mTa_j}{N-1}(1-r). \tag{3.2}$$

Proof. Let C_i^t be the random variable representing the number of contacts made by agent i at time step t. It can be written as

$$C_i^t = C_{i\text{-}in}^t + C_{i\text{-}out}^t, \tag{3.3}$$

where $C_{i\text{-}out}^t$ denotes the contacts initiated by i (if active), and $C_{i\text{-}in}^t$ the contacts received from other active nodes at time t.

The variable $C_{i\text{-}out}^t$ is defined as

$$C_{i\text{-}out}^t = m \cdot B_i^t, \qquad B_i^t \sim \text{Bernoulli}(a_i), \tag{3.4}$$

so that

$$C_{i\text{-}out}^t = \begin{cases} m & \text{with probability } a_i, \\ 0 & \text{with probability } 1 - a_i. \end{cases} \tag{3.5}$$

When node i is active, the number of contacts it generates is always m, regardless of whether interactions are pairwise or simplicial.

This is not the case for $C_{i\text{-}in}^t$. Since pairwise and group interactions cannot occur simultaneously, we decompose $C_{i\text{-}in}^t$ into two contributions:

$$C_{i\text{-}in}^t = C_{i,j,p\text{-}in}^t + C_{i,j,\Delta\text{-}in}^t, \tag{3.6}$$

where

$$C_{i,j,p\text{-}in}^t = \begin{cases} 1 & \text{with probability } \frac{ma_j}{N-1}(1-r), \\ 0 & \text{otherwise,} \end{cases} \tag{3.7}$$

and

$$C_{i,j,\Delta\text{-}in}^t = \begin{cases} m & \text{with probability } \frac{ma_j}{N-1}r, \\ 0 & \text{otherwise.} \end{cases} \tag{3.8}$$

For a single step t, we then have

$$\mathbb{E}[C_i^t] = \mathbb{E}[C_{i\text{-}out}^t] + \sum_{j \in V \setminus \{i\}} \mathbb{E}[C_{i,j,p\text{-}in}^t] + \sum_{j \in V \setminus \{i\}} \mathbb{E}[C_{i,j,\Delta\text{-}in}^t]. \tag{3.9}$$

Using the expectations of the single random variables we obtain

$$\mathbb{E}[C_i^t] = a_i m + \sum_{j \in V \setminus \{i\}} \frac{a_j m}{N-1}(1-r) + \sum_{j \in V \setminus \{i\}} \frac{a_j m^2}{N-1} r. \tag{3.10}$$

Summing over T time steps gives

$$\mathbb{E}[C_i^t] = \mathbb{E}\left[\sum_{t=0}^{T} C_i^t\right] = \sum_{t=0}^{T} \mathbb{E}[C_i^t], \tag{3.11}$$

which yields the desired result. □

We give two other properties of the $r - SAD$ model.

Proposition 3.2.4. *For any $T > 0$ the expectation of the number of contacts received by a node in T steps is a monotonic function of r if $m > 1$*

Proof. It follows from a direct computation. In fact if we derive for r the expected value of 3.2.3:

$$\frac{d\mathbb{E}_T[C_i]}{dr} = \frac{d\mathbb{E}_T[C_{i-in}]}{dr} = \frac{d}{dr}\Big(\sum_{j\in V\setminus\{i\}} \frac{m^2 T a_j}{N-1} r + \sum_{j\in V\setminus\{i\})} \frac{mTa_j}{N-1}(1-r)\Big) \tag{3.12}$$

we get:

$$\frac{d\mathbb{E}_T[C_{i-in}]}{dr} = \sum_{j\in V\setminus\{i\}} \frac{m^2 T a_j}{N-1} - \sum_{j\in V\setminus\{i\}} \frac{mTa_j}{N-1} \tag{3.13}$$

Note that, in the derivative, the terms originating from node activation do not appear. In fact, having fixed m, the parameter r has no influence on them.

Setting: $k = \sum_{j\in V\setminus\{i\}} \frac{mTa_j}{N-1}$ and plugging it in 3.13:

$$\frac{d\mathbb{E}_T[C_{i-in}]}{dr} = (m-1)k \tag{3.14}$$

Now $k > 0$, in fact it is a sum of positive quantities. Then we get, if $m > 1$:

$$(m-1)k > 0 \tag{3.15}$$

□

Proposition 3.2.5. *The expected number of contacts received by a node is bigger than the expected number of contacts created if:*

$$\frac{a_i}{\sum_{j\in V\setminus\{i\}} a_j} < \frac{(m-1)r+1}{N-1} \tag{3.16}$$

Proof. We consider:

$$\mathbb{E}[C_{i-out}] - \mathbb{E}[C_{i-in}] < 0 \tag{3.17}$$

From previous calculations:

$$ma_i T - \sum_{j\in V\setminus\{i\}} \frac{m^2 T a_j}{N-1} r - \sum_{j\in V\setminus\{i\}} \frac{mTa_j}{N-1}(1-r) < 0 \tag{3.18}$$

We can simplify this relation by dividing both sides by mT. It yields:

$$a_i < \sum_{j\in V\setminus\{i\}} \frac{ma_j r + a_j(1-r)}{N-1} \tag{3.19}$$

Since m, r and $N-1$ are not involved in the summation, we get:

$$a_i < \frac{(m-1)r+1}{N-1} \sum_{j\in V\setminus\{i\}} a_j \tag{3.20}$$

and then:

$$\frac{a_i}{\sum_{j\in V\setminus\{i\}} a_j} < \frac{(m-1)r+1}{N-1} \tag{3.21}$$

□

First of all these two results provide a framework for understanding the effect of group interactions on contacts. As the parameter r increases, the number of contacts increases, but this increase stems from received contacts. As shown by the second result, this can cause a node to shift from a net giver to a net receiver, depending on its activity level. Therefore, the two results highlight the impact that group interaction has on nodes with low activity.

This result allows us to define a new index for activity driven temporal networks to quantify the importance of nodes in the process. In fact we can distinguish between *Net Receiver* and *Net Giver*, based on whether the inequality holds or not. Given the activity distribution, we define:

$$\frac{a_i}{\sum_{j\in V\setminus\{i\}} a_j} - g_i = \frac{(m-1)r+1}{N-1} \tag{3.22}$$

where g_i measures the distance of the node's weight in the distribution from the critical value as r varies. We say that g_i is the activity centrality. In particular, we have that if $g_i > 0$, then the node is a *Net Giver*, otherwise a *Net Receiver*.

Now from theorem.3.2.3 we can derive an approximation for the expected degree in the Integrated Graph $G_T = \bigcup_{t=0}^{T} G_t$.

Following [83], we can approximate the number of contacts derived in 3.2.3 in the case of $N >> 1$. In fact, applying the *Law of Large Numbers*[38] since the activities are *IID* and satisfies the conditions of the theorem, we get:

$$\mathbb{E}_t[C(i)] = ma_iT + \sum_{j\in V\setminus\{i\}} \frac{m^2Ta_j}{N-1}r + \sum_{j\in V\setminus\{i\}} \frac{mTa_j}{N-1}(1-r) \cong mT[a_i+((m-1)r+1)\mathbb{E}[a]] \tag{3.23}$$

The simulation, shown in figure 3.3 yields striking agreements with the theoretical prediction of 3.23.

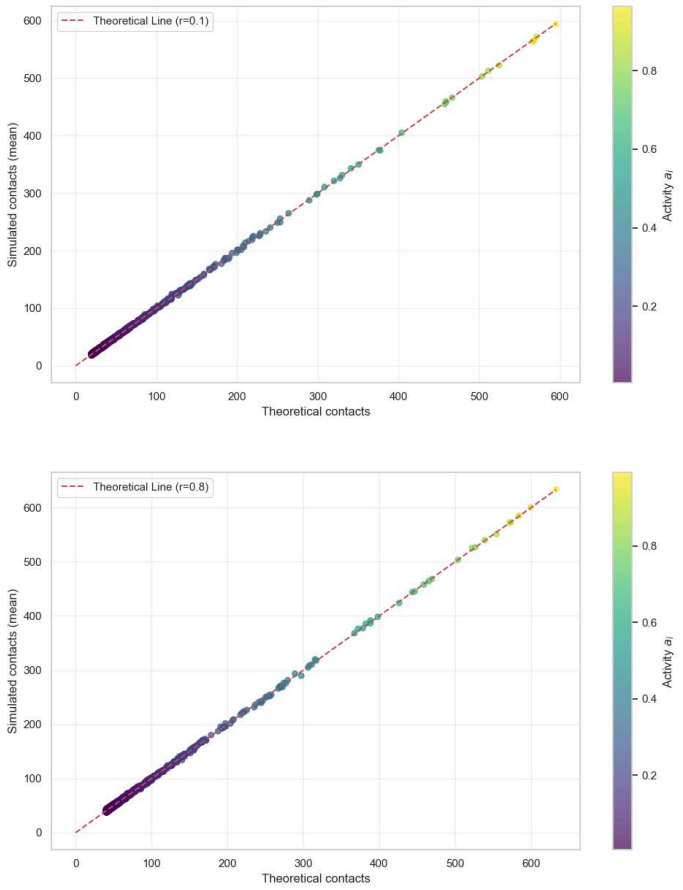

Figure 3.3: Number of Contacts: Simulated vs Theoretical. Simulations for different values of r obtained with $m = 3$, $N = 5000$, T =1000, activity from a power law with threshold $\varepsilon = 0.005$ and $\gamma = 2.4$. Results averaged over 30 simulations.

In order to evaluate the average degree $k_T^{r-SAD}(i)$ in the integrated network G after T steps, we use the same approximation used in the *Supplementary Information* of [82], which draw an analogy with an urn model with replacement. This approximation is valid in the case $N >> m$. Therefore the probability that a single node j have never been in contact with i at time T is given by:

$$p^T_{i \nleftrightarrow j)} = (1 - \frac{1}{N-1})^{\mathbb{E}_T[C(i)]} \tag{3.24}$$

It follows immediately that:

$$p^T_{i \leftrightarrow j)} = 1 - [(1 - \frac{1}{N-1})^{\mathbb{E}_T[C(i)]}] \tag{3.25}$$

From this quantity we can compute the average degree of the $i-th$ node. In fact, multiplying for the number of nodes we get:

$$k_T^{r-SAD}(i) = (N-1)[1 - (1 - \frac{1}{N-1})]^{\mathbb{E}_T[C(i)]} \cong N[1 - e^{\frac{-mT[a_i + ((m-1)r+1)\mathbb{E}[a]}{N}}] \tag{3.26}$$

where we use the Neper approximation. The approximation is valid when $N \gg 1$ and $\frac{T}{N}$ is small.

We highlight that, for $r = 1$, the expression 3.26 become:

$$k_T^{1-SAD}(i) \cong N[1 - e^{\frac{-mT[a_i + m\mathbb{E}[a]}{N}}] \tag{3.27}$$

which is equivalent to the one found in [83].

From this quantity we get an important feature of the effect of group interactions.

Theorem 3.2.6 (Poor Get Richer Effect)**.** *Consider $r_2 > r_1$ and define the function:*

$$f(a) = k^{r_2}(a) - k^{r_1}(a) \tag{3.28}$$

where k is defined in 3.26. Then $f(a)$ is a monotonically decreasing function of a

Proof. Inserting the approximation for k we get:

$$f(a) = e^{-\frac{mT\left[a+((m+1)r_1+1)\mathbb{E}[a]\right]}{N}} - e^{-\frac{mT\left[a+((m+1)r_2+1)\mathbb{E}[a]\right]}{N}} \tag{3.29}$$

Set $B = \frac{mT}{N}$ and $g(r) = [(m+1)r + 1]\mathbb{E}[a]$. Then:

$$f(a) = e^{-Ba}e^{-Bg(r_1)} - e^{-Ba}e^{-Bg(r_2)} = e^{-Ba}\left[e^{-Bg(r_1)} - e^{-Bg(r_2)}\right] \tag{3.30}$$

Notice that $g(r)$ is monotonically increasing in r and $B > 0$, which implies:

$$\gamma = e^{-Bg(r_1)} - e^{-Bg(r_2)} > 0 \quad \text{since } r_1 < r_2 \tag{3.31}$$

Therefore:

$$f(a) = \gamma e^{-Ba} \tag{3.32}$$

which is clearly a monotonically decreasing function of a. □

Remark 8. *The calculations show that, on average, the gain in degree distribution as r varies increases more for nodes with lower activity. This democratising effect is confirmed by numerical simulations.*

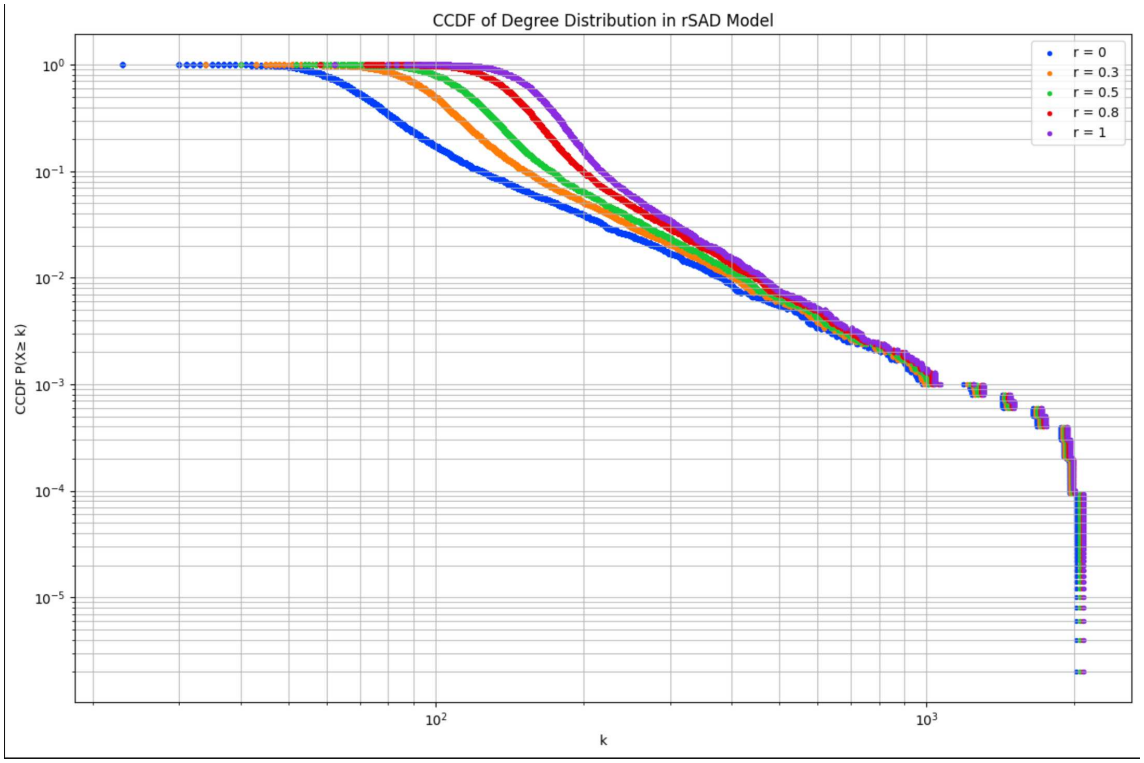

Figure 3.4: Simulation for different values of r obtained with $m = 3$, $N = 5000$, T =1000, activity from a power law with threshold $\varepsilon = 0.005$ and $\gamma = 2.4$. Results averaged over 100 simulations.

Calculations for the r-SAD 2-skeleton

Then we focus on the 2-skeleton.

We start by considering the average number of group interaction in the aggregated network:

Theorem 3.2.7. *In the r-SAD model defined in 3.2.1, the expected number of group interactions of a node i with activity a_i is given by:*

$$\mathbb{E}_T[\chi_i] = a_i r T + \sum_{j \in V \setminus \{i\}} \frac{m T a_j}{N-1} r \tag{3.33}$$

Proof. As we have done in th. 3.2.3, we consider the random variable χ_i^t. This represents the number of group interactions at time t involving node i. We can decompose the active and passive contribution, allowing us to write:

$$\chi_i^t = \chi_{i-in}^t + \chi_{i-out}^t \tag{3.34}$$

In particular we have:

$$\chi_{i-out}^t = \begin{cases} 1 & \text{with probability } a_i r \\ 0 & \text{with probability } 1 - a_i r \end{cases} \tag{3.35}$$

This accounts for the number of group interactions originated by node i in a time step t.

$$\chi_{i,j-in}^t = \begin{cases} 1 & \text{with probability } \frac{a_j r m}{N-1} \\ 0 & \text{with probability } 1 - \frac{a_j r m}{N-1} \end{cases} \tag{3.36}$$

Then for a single time step we have:

$$\mathbb{E}[\chi^t] = \mathbb{E}[\chi_{i-out}^t + \sum_{j \in V \setminus \{i\}} \chi_{i,j-in}^t] = \mathbb{E}[\chi_{i-out}^t] + \sum_{j \in V \setminus \{i\}\}} \mathbb{E}[\chi_{i,j-in}^t] \tag{3.37}$$

Since they are I.I.D. the expectation over T steps is given by:

$$\mathbb{E}[\sum_{t=0}^{T} \chi^t] = \sum_{t=0}^{T} \mathbb{E}[\chi^t] \tag{3.38}$$

Inserting the values of the expectations, we get:

$$\mathbb{E}_T[\chi_i] = a_i r T + \sum_{j \in V \setminus \{i\}} \frac{m T a_j}{N-1} r \tag{3.39}$$

□

From this formula, we can get an approximation for the 2-skeletons following [83]. We consider $l \neq k \neq i$ nodes. For each simplex $\chi_T(i)$, assuming that the node choose with uniform probability $\frac{m}{N-1}$ and that each choice is independent, the probability $p_{[i,j,l]}$ that they are part of it can be approximated by:

$$p_{[i,j,l]} = \frac{m(m-1)}{(N-1)(N-2)}$$

And therefore probability that the pair of nodes (l, k) is not involved in any of these simplices is given by:

$$p_\Delta = (1 - \frac{m(m-1)}{(N-1)(N-2)})^{\chi_T(i)} \tag{3.40}$$

The number of pairs excluding the point i $\mu[(l, j)]$ is simply given by the arrangement of $N-1$ elements by couple, which leads to:

$$\mu[(l,j)] = \binom{N-1}{2} = \frac{(N-1)!}{2(N-3)!} = \frac{(N-1)(N-2)(N-3)!}{2(N-3)!} = \frac{(N-1)(N-2)}{2} \tag{3.41}$$

Taking stock we get that the average number of 2-simplex $k_2^T(i)$is given by:

$$k_2^T(i) = \frac{(N-1)(N-2)}{2}(1 - \frac{m(m-1)}{(N-1)(N-2)})^{\chi_T(i)} \tag{3.42}$$

which can be approximated as:

$$k_2^T(i) = \frac{(N-1)(N-2)}{2}\left(1 - \exp\left[\frac{m(m-1)rT(a_i + m\mathbb{E}[a])}{(N-1)(N-2)}\right]\right) \tag{3.43}$$

Once again, in the case $r = 1$ we get the formula derived in [83]. And, of course, when $r = 0$ the average number of 2-simplex is 0, since there are no group interactions.

SIS on r-SAD

Next, we study the dynamics of an SIS model-a cornerstone in the field of *Infectious Disease Modelling* [21, 22, 55, 64]-on the *r-SAD*. We focus on the *threshold phenomenon*, i.e., the existence of a critical point above which an epidemic outbreak becomes likely. This allows for a mathematical simplification, as the early-stage dynamics can be studied through a linearized version of the model.

In literature, several approaches have been proposed to understand different aspects of disease spreading on temporal networks (see, for example, Chapter 11 of [29]).

Here, we adopt the so-called *Activity-Based Mean Field Approximation (ABMF)*, introduced in [82] and used in [83][68]. The key idea behind the *ABMF* is to track the density of infected agents as a function of their activity level. In a continuous-time setting, we obtain the following equation for the number of infected agents with activity a, denoted by I_a:

$$\begin{aligned}\partial_t I_a = &-\gamma I_a + \beta m\, S_a\, a \int \frac{I_{a'}}{N}\, da' \\ &+ \beta m\, S_a \int a' \frac{I_{a'}}{N}\, da' \\ &+ \beta S_a \int a' r m \frac{S_{a'}}{N}\, da' \int (m-1)\frac{I_{a''}}{N}\, da''\end{aligned} \tag{3.44}$$

Here, the first term on the right-hand side accounts for spontaneous recovery. The second and third terms describe infection events occurring through "pairwise" interactions: the second term accounts for cases in which a susceptible node becomes infected by forming a connection with an infected one, while the third term accounts

for the reverse situation, where the infected node initiates the contact. The fourth term accounts for higher-order (simplicial) transmission events, where a susceptible node becomes infected through a group interaction involving another susceptible and an infected node.
Next we define the quantity:

$$\theta(t) = \int I_a a da \tag{3.45}$$

Integrating the equation 3.44 over the activity a:

$$\begin{aligned}\int \partial_t I_a \, da &= -\gamma \int I_a \, da + \beta m \int a S_a \, da \int \frac{I_{a'}}{N} \, da' \\ &\quad + \beta m \int S_a \, da \int a' \frac{I_{a'}}{N} \, da' + \beta \int S_a \, da \int r a' m \frac{S_{a'}}{N} \, da' \int (m-1) \frac{I_{a''}}{N} \, da'' \\ &= -\gamma I^t + \beta m \mathbb{E}[a] I^t + \beta m \theta^t + \beta r \mathbb{E}[a] m(m-1) I^t\end{aligned} \tag{3.46}$$

In order to get a closed form for θ we multiply 3.44 by a the equation 3.44 and then integrating we get:

$$\partial_t \theta = -\gamma \theta^t + \beta m \mathbb{E}[a^2] I^t + \beta m \mathbb{E}[a] e \theta^t + \beta r m (m-1) \mathbb{E}[a]^2 I^t \tag{3.47}$$

Taking stock, the system around the equilibrium can be studied as:

$$\begin{cases} \partial_t I = -\gamma I^t + \beta m \mathbb{E}[a] I^t + \beta m \theta^t + \beta r \mathbb{E}[a] m(m-1) I^t \\ \partial_t \theta = -\gamma \theta^t + \beta m \mathbb{E}[a^2] I^t + \beta m \mathbb{E}[a] \theta^t + \beta r m (m-1) \mathbb{E}[a]^2 I^t \end{cases} \tag{3.48}$$

The problem of invasion threshold can be addressed considering the dominant eigenvalue of the Jacobian matrix. In particular, from the theory of dynamical system [19, 97], an endemic state exist if the dominant eigenvalue of the Jacobian matrix is positive, which implies that the disease free equilibrium is unstable.

Theorem 3.2.8. *Consider the system defined by:*

$$\begin{cases} \partial_t I = -\gamma I^t + \beta m \mathbb{E}[a] I^t + \beta m \theta^t + \beta r \mathbb{E}[a] m(m-1) I^t \\ \partial_t \theta = -\gamma \theta^t + \beta m \mathbb{E}[a^2] I^t + \beta m \mathbb{E}[a] \theta^t + \beta r m (m-1) \mathbb{E}[a]^2 I^t \end{cases} \tag{3.49}$$

The Disease Free Equilibrium is unstable if:

$$\lambda_c^{rSAD} = \frac{\beta}{\gamma} > \frac{2}{\mathbb{E}[a] m [r(m-1)+2] + m\sqrt{\mathbb{E}[a][r^2(m+1)(m-1) + r(4m-4)] + 4\mathbb{E}[a^2]\}}} \tag{3.50}$$

Therefore, it is monotonically decreasing with r.

Proof. We start by evaluating the Jacobian Matrix associated to the 3.49:

$$J = \begin{bmatrix} -\gamma + \beta m \mathbb{E}[a] + \beta r m (m-1) \mathbb{E}[a] & \beta m \\ \beta m \mathbb{E}[a^2] + \beta r m (m-1) \mathbb{E}[a]^2 & -\gamma + \beta m \mathbb{E}[a] \end{bmatrix} \tag{3.51}$$

As we are interested in the stability of the Disease Free Equilibrium we evaluate the eigenvalues of the matrix 3.51:

$$Det[J - \Lambda \mathbb{1}_2] = 0 \tag{3.52}$$

The eigenvalues of this matrix are given by:

$$\Lambda_{\pm} = \frac{1}{2}\{\beta\mathbb{E}[a]m(r(m-1)+2) - 2\gamma \pm \beta m\sqrt{\mathbb{E}[a](r^2m^2 - 2r^2m + 4rm + r^2 - 4r) + 4\mathbb{E}[a^2]}\} \tag{3.53}$$

Choosing the positive root, we get:

$$\lambda_c^{\text{rSAD}} = \frac{\beta}{\gamma} > \frac{2}{\mathbb{E}[a]m[r(m-1)+2] + m\sqrt{\mathbb{E}[a][r^2(m+1)(m-1) + r(4m-4)] + 4\mathbb{E}[a^2]}\}} \tag{3.54}$$

from eq. 3.54 we note that, if $m > 1$, which means unless the degenerate case, the critical value is monotonically decreasing with r. □

Moreover, the threshold is equivalent to the one in [83]. Recall that, as stated above, in the *rSAD* we use m as the size of the simplex whereas in the *SAD* the size is $s-1$. Once we plug this into 3.54 and set $r = 1$ we get:

$$\lambda_c^{\text{1-SAD}} = \frac{\beta}{\gamma} > \frac{2}{\mathbb{E}[a]s(s-1) + (s-1)\sqrt{\mathbb{E}[a]^2s^2 + 4(\mathbb{E}[a^2] - \mathbb{E}[a]^2\}} \tag{3.55}$$

Once again, numerical simulation highlights the role of the parameter r on the critical value. This is in agreement with the importance of superspreader events [1, 44, 65] in an epidemic.

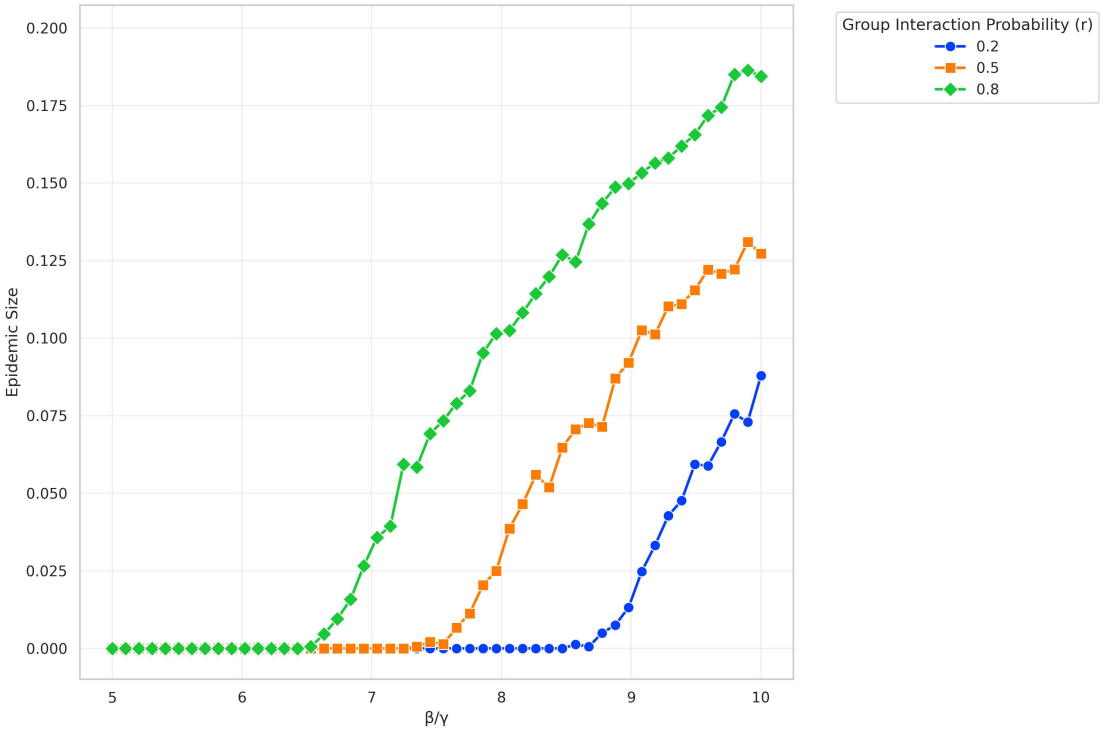

Figure 3.5: SIS model on rSAD for different values of r, obtained with $m = 3$, $N = 1000$, activity from a power law with threshold $\varepsilon = 0.005$ and $\alpha = 2.7$. Results averaged over 100 simulations.

3.3 A generalized model: *mc-SAD*

In the previous section, we proposed and analyzed a simple model interpolating between dyadic and group interactions within the activity driven framework. At each time step, a single active node would form a group interaction with probability r and a dyadic interaction with the complementary probability. However, the number of contacted nodes per interaction remained fixed, regardless of whether it was a group or dyadic interaction. This does not allow for the study of the impact of the target set's size.

A possible generalization that accounts for heterogeneity in the target size is the following. Consider a natural number m greater than 1. This represents the maximum limit of nodes in the target set. Then, consider the $2m$-dimensional vector $\mathbf{c} = (c_{1d}, \dots, c_{md}, c_{1s}, \dots, c_{ms})$ such that $\sum c_{ij} = 1$. This vector represents the probabilities that, once active, a node forms a dyadic or a group interaction involving $j = 1, \dots, m$ other nodes with uniform probability. To avoid the degenerate case, we set $c_{1s} = 0$.

This model, the *m**c**-SAD*, accounts for heterogeneity in the interaction size, at the cost, however, of a considerable number of parameters. These can be reduced in different ways, for example by assuming a decay for the size starting from an initial probability for the two types of interaction or by defining a probability distribution as in [83]. L

3.4 Discussion and Limitations

In this work, we introduced the r-SAD model, a minimal extension of the Simplicial Activity-Driven, that interpolates between dyadic and simplicial interactions. By combining analytical results with simulations, we demonstrated that increasing the probability of group interactions (r) profoundly alters network structure and dynamics.

Structurally, group interactions *democratize* connectivity: low-activity nodes gain disproportionately more links, reducing heterogeneity in degree distributions and mitigating the isolation of peripheral agents. Dynamically, the presence of group interactions lowers the invasion threshold of an SIS process, showing that large gatherings can accelerate epidemic outbreaks. Both results are consistent with the intuition that higher-order interactions amplify connectivity in ways that pairwise models cannot capture.

Beyond epidemiology, our findings are relevant for broader social and organizational systems. Group interactions can promote integration and reduce segregation, ensuring that even less active individuals remain connected to the system. At the same time, they introduce vulnerabilities by facilitating the rapid spread of contagion. This dual role underscores the importance of explicitly incorporating higher-order mechanisms into temporal network models.

Several directions remain open. The model could be enriched by introducing heterogeneity in r, as has been done in the case eAD [41]. Extensions of the AD framework such as memory[61, 99, 106], attractiveness [85], or burstiness [67, 75, 100] can also be incorporated into the rSAD. Finally, our model currently enforces an *either-or* choice between dyadic and group interactions at each activation. A more general framework that allows both types of interactions simultaneously would fur-

ther enhance realism, paving the way for a new class of Interpolating Higher-Order Temporal Networks (IHTNs).

Chapter 4

The SH Model: A Minimal Model for Chronic and Acute Isolation

In recent years, themes such as the "loneliness epidemic" or the "anti-social century" have received widespread attention. Data indicate that the number of close social connections has sharply declined in the past 30 years, at least in the USA. Moreover, loneliness has detrimental effects on individuals' physical and mental health[48] [59, 98, 101].

In this chapter, we leverage the theory of Social Homeostasis to propose a model of isolation and loneliness. Social Homeostasis Theory is a framework proposed in 2019 in [73] and further elaborated in [63], in which each agent is characterized by a set point representing its optimal level of sociality. This set point adapts to the social conditions of the environment in which the individual is embedded, in order to maintain a state of social homeostasis. At the same time, states of acute isolation or acute overcrowding increase the agent's compensatory effort to correct significant deviations from the optimal level of sociality.

The formulation of the model is deliberately chosen to be minimal, in order to capture the key mechanism of set point adaptation and how this, in turn, affects the dynamics of (Acute) Isolation and Chronic Isolation. To simplify the analysis, a zero-effort modeling approach is adopted. While this assumption abstracts from several aspects of Social Homeostasis Theory, the results nonetheless reveal clear effects of set point adaptation in shaping the individual's state.

Starting from this chapter, we will use the term *Isolation* as a synonym for *Acute Isolation*. Conversely, we will specify when we are referring to *Chronic Isolation*.

Thus, the model belongs to the class of mechanistic models on networks in social science [46], such as Axelrod's [4], Social Impact Theory-inspired models [79], Schelling's [90], and, even more profoundly, the Cascade Model for complex contagion introduced by Watts [102].

4.1 A Framework for Acute-Chronic Isolation

The model consists of three main elements.

First, it is necessary to consider a Temporal Network. In this chapter, it is assumed to be a *Contact Network*. Its realization can be represented by a time-dependent matrix $C(t) = c_{ij}(t)$, where:

$$c_{ij}(t) = \begin{cases} u_{i\to j}(t) & \text{if } i \text{ and } j \text{ are in contact at time } t \\ 0 & \text{otherwise} \end{cases} \tag{4.1}$$

where $u_{i\to j}(t)$ represents the benefit of the interaction that agent i receives from contacts with j at time t.

In the simplest case, the elements of (4.1) are given by:

$$c_{ij}(t) = \begin{cases} 1 & \text{if } i \text{ and } j \text{ are in contact at time } t \\ 0 & \text{otherwise} \end{cases} \tag{4.2}$$

where it is assumed that the benefit of contact at time t is unitary, $u_{i\to j} = 1$, so that the matrix is symmetric, $c_{ij} = c_{ji}$. This form will be employed in Chapter V.

Since the Contact Network is itself a stochastic process, it can be conveniently represented by a continuous random vector

$$\mathbf{C}(t) = (C_1(t), \dots, C_N(t)), \tag{4.3}$$

with joint probability density

$$\mathbf{C}(t) \sim f(\mathbf{c}) = f(c_1, \dots, c_N). \tag{4.4}$$

We assume that the contact network forms a sequence of independent and identically distributed (IID) r.v. in time, i.e.,

$$C(t_1), C(t_2), \dots \text{ are independent and each } C(t) \sim f(\mathbf{c}). \tag{4.5}$$

Remark 9. *The assumption that $\{C(t)\}_{t\in\mathbb{N}}$ forms an IID sequence is a strong one. While this assumption abstracts away temporal correlations in the contact sequence, it simplifies the analysis.*

For the model, we make two assumptions about the support of the distribution. First, the marginal distribution $f(c_i)$, where C_i represents the random variable of contacts weighted by their benefit for agent i, has compact support $[0, b]$:

$$\int_0^b f(c_i)\, dc_i = 1. \tag{4.6}$$

The lower bound implies that interactions cannot have negative benefit,

$$u_{i\to j} \geq 0, \tag{4.7}$$

and the upper bound establishes that at a given instant an agent can obtain only a finite benefit from their contacts.

Moreover, we assume

$$f(c_i) > 0 \quad \text{almost surely (a.s.)}, \tag{4.8}$$

unless otherwise stated.

Second, we are interested in the dynamic process that defines the "optimal" level of sociability. It is important to emphasize that, unlike other types of models, the concept of optimality must be understood in a broad sense. The agent is not optimizing this function in the strict sense of the term. The adjustment mechanism is in fact based on hard-coded rules rather than on a true optimization process.

Definition 4.1.1. The optimal sociability or *set point* of agent i-th at time t is the value $\phi_i(t)$.

Definition 4.1.2. A *Realization Adaptive Function* is a function $F : \mathbb{R}^+ \times [0, b] \longrightarrow \mathbb{R}$ such that:

1. $F(\phi, x) > 0$ if $\phi + \delta < x$;
2. $F(\phi, x) < 0$ if $\phi - \delta > x$;
3. $F(\phi, x) = 0$ if $x \in [\phi - \delta, \phi + \delta]$
4. $|F(\phi, x)| \geq |F(\phi, y)|$ if $|\phi - x| \geq |\phi - y|$

Here $\delta \geq 0$ and the interval $[\phi - \delta, \phi + \delta]$ defines the no-update band, $\mathbb{B}(\phi) = [\phi - \delta, \phi + \delta]$.

Starting from the definition of *RAF* given in 4.1.2, we can define the dynamics of the individual set point:

$$\phi_i(t + 1) = [\phi_i(t) + \sigma F(c_i(t), \phi_i(t))]^+ \tag{4.9}$$

where $\sigma \in [0, 1]$ is a parameter that allows us to distinguish the time scales, imposing a limited correction over time, in accordance with the view that the *adaptation* process is slower than that of contacts. Note that in the case in which $\sigma = 0$, the version of the model without update is obtained. This dynamics allows the agent to adapt its optimal level of sociability based on the realization of the random variable of contacts. In particular, note that, according to the definition of *RAF*, if the realization falls outside the homeostasis band $B(\phi)$, the *set point* decreases if this discrepancy is downward, and increases otherwise. To ensure that the level of sociability remains greater than zero, the positive part of the update has been taken.

Let us now introduce the concept of *Embedded Compartments*.

In order to model these states, we rely on compartmental theory [104], a framework widely applied in fields like pharmacokinetics [26] and Infectious Disease Dynamics [55] [44] [22]. So we define three different *Embedded Compartments*: Isolated (I), Social Homeostasis (SH), and Overcrowded (OV). It is important to emphasize that because SH theory is a subjective theory of isolation, the compartments depend not only on the dynamic process on the network but also on a *target* value. To avoid confusion, we refer to these as *Embedded Compartments (EC)*.

Definition 4.1.3. Let $T \in \mathbb{R}^+$ be fixed such that $T > 0$:

- The i-th agent is said to be in *Isolation (IS)* at time $t + 1$ if:

$$c_i(t) < \phi_i(t) - T \tag{4.10}$$

- The i-th agent is said to be in *Overcrowding (OV)* at time $t + 1$ if:

$$c_i(t) > \phi_i(t) + T \tag{4.11}$$

- The i-th agent is said to be in *Social Homeostasis (SH)* at time $t + 1$ if:

$$c_i(t) \in [\phi_i(t) - T, \phi_i(t) + T] \tag{4.12}$$

The definition given reflects what has been emphasized by psychological research on the topic: loneliness is not an absolute state, but rather a significant deviation, quantified by T, from a certain optimal level of sociability, in this case the set point ϕ.

Remark 10. *The threshold T can be generalized, allowing for heterogeneity, regarding the individual agent, time and the set point.*

From the definition 4.1.3, we can straightforwardly write:

$$\mathbb{P}(EC_i(t+1) = IS) = \begin{cases} 1 & if c_i(t) < \phi_i(t) - T \\ 0 & otherwise \end{cases} \tag{4.13}$$

where EC_i is the random variable associated to the *Embedded Compartment*. Therefore, it can be seen as *Monotonic Threshold Dynamics* [84] thus drawing an analogy with *Complex Contagion* [102]. The same line of reasoning can be used for the *Overcrowded EC*. The situation is different, however for *SH*:

$$\mathbb{P}(EC_i(t+1) = SH) = \begin{cases} 1 & if c_i(t) \in [\phi_i(t) - T, \phi_i(t) + T] \\ 0 & otherwise \end{cases} \tag{4.14}$$

In this case, as we are dealing with an interval, the response is no longer monotonic.

Remark 11. *As we have stated, it should be seen as an analogy, since we are dealing with probabilities and not transition probability. In fact, the transition from one EC to another is driven not by the EC at the previous state, but by the contact network realization and the value of the set point.*

Mathematically, each Embedded Compartment $EC_i(t+1)$ should be interpreted as both a *state variable* and a *random variable*. It is a state variable because it represents the agent's social condition at time $t+1$ (IS, SH, or OV), and it is random because it depends on the stochastic realization of the contact network $c_i(t)$.

To take stocks, we have outlined the structure of the model. We defined the contact network, which serves as the basis for the model. Secondly, we defined the two main mechanisms of social homeostasis. Firstly, the set-point dynamic, which acts as an adjustment of optimal sociality in relation to the realisation of the contact network. Secondly, we considered the Embedded Compartments, which allow us to classify the state of the i-th agent, given the set point and the realisation of the contact network.

4.1.1 Properties of the Framework

From the general framework we have introduced in this section we can derive a set of related properties.

It is important to emphasise that this section is not devoted to a systematic analysis of the model, which will be left to future work. On the contrary, the results will serve as a guide for our analysis of the phenomenon under consideration.

Theorem 4.1.4 (Isolation Path)**.** *Consider an agent i who is in isolation for $t+1, \dots, t+\Delta t+1$, then if $T > \delta$ and $\sigma \neq 0$, for $\tau = t, \dots t+\Delta t$:*

1. $\phi_i(\tau) > T$;
2. $\phi(\tau)$ *is a strictly decreasing sequence in the time interval* $\{t+1, \dots, t+1+\Delta t\}$;
3. $\phi(\tau+1) - \phi(\tau) \geq \sigma F(\phi(\tau), \phi(\tau) - T)$.

Proof. 1. For contradiction.
Suppose that agent i is in isolation at $\bar{t}+1$. Therefore, condition 4.10 implies that:

$$c_i(\bar{t}) < \phi_i(\bar{t})) - T \tag{4.15}$$

If $\phi(\bar{t}) < T$, then we get:

$$\phi_i(\bar{t}) - T < 0$$

Using again 4.10 yields:

$$c_i(\bar{t}) < \phi_i(\bar{t}) - T < 0$$

Since we have assumed that the random variable associated to the contact network has positive support, the agent can not be in Isolation at time $\bar{t}+1$, which contradict the hypothesis.
If $\phi(\bar{t}) = T$, the condition 4.10 gives:

$$c_i(\bar{t}) < \phi(\bar{t}) - T \tag{4.16}$$

But the l.h.s of 4.16 is equal to zero and we get, once again, $c_i(\bar{t}) < 0$. Then $\phi(\bar{t}) > T$.

2. Suppose that agent i is in isolation for two consecutives $\bar{t}$ and $\bar{t}+1$. Therefore, once again, condition 4.10 yields:

$$c_i(\bar{t}) < \phi_i(\bar{t}) - T$$

From the discussion above, we can write 4.9 without the positive part:

$$\phi_i(\bar{t}+1) = \phi_i(\bar{t}) + \sigma F(\phi(\bar{t}), c_i(\bar{t}))$$

Using the fact that:

$$\phi_i(\bar{t}) - c_i(\bar{t}) > T > \delta$$

Therefore, from the condition of the *RAF* 4.1.2, we have:

$$F(\phi_i(\bar{t}), c_i(\bar{t})) = \beta < 0$$

which implies, since $\sigma \neq 0$:

$$\phi_i(\bar{t}+1) = \phi_i(\bar{t}) + \sigma F(\phi(\bar{t}), c_i(\bar{t})) = \phi_i(\bar{t}) + \sigma\beta < \phi_i(\bar{t}) \tag{4.17}$$

3. Without loss of generality, we set $\sigma = 1$.
From the discussion above, we are interested in $\phi_i(\bar{t}+1) - \phi_i(\bar{t})$. Using 4.9, we get:

$$\phi_i(\bar{t}+1) - \phi_i(\bar{t}) = \sigma F(\phi(\bar{t}), c_i(\bar{t}))$$

Using condition 4.10, we can rewrite the problem of finding the minimum as a one dimensional constrained optimization problem:

$$\min_x F(\phi_i(\bar{t}), x) \quad \text{s.t.} \quad x \leq \phi_i(\bar{t}) - T \tag{4.18}$$

where we have inserted the equality to obtain the optimization over a closed set. The solution of this problem can be easily obtained, even if we include the point $x = \phi_i(\bar{t}) - T$ using the conditions of 4.1.2, in particular the monotonicity 4 which yields the thesis.

□

Theorem 4.1.5. *Let $\phi^*(t) = \{\phi_i^*\}_{i=1}^N$ an equilibrium for the dynamics 4.9, namely:*

$$\phi_i(t+1) = [\phi_i(t) + \sigma F(\phi_i(t), c_i(t))]^+ = \phi_i^*, \qquad \forall i, \forall t \tag{4.19}$$

then:

1. *If $\delta < T$, at the equilibrium all agents are in Social Homeostasis;*
2. *The equilibrium exist if and only if:*

$$\int_{\min\{0, \phi_i^* - \delta\}}^{\phi_i^* + \delta} f_t(c_i) = 1, \qquad \forall i, \forall t \tag{4.20}$$

Proof. 1. We prove the statement by showing that both condition 4.10 and 4.11 are not satisfied. By contradiction, suppose that for $\bar{t}+1$ there exists an agent i who is in Isolation *EC*.
Therefore, we have:

$$c_i(\bar{t}) < \phi_i(\bar{t})) - T \tag{4.21}$$

And therefore:

$$\phi_i(\bar{t})) - c_i(\bar{t}) > T > \delta \tag{4.22}$$

where in the last inequality we have used the hypothesis.
From the discussion in the previous theorem, we can write down:

$$\phi_i(\bar{t}+1) - \phi_i(\bar{t}) = \sigma F(\phi(\bar{t}), c_i(\bar{t}))$$

But using 4.22, it follows that:

$$\sigma F(\phi(\bar{t}), c_i(\bar{t})) < 0 \tag{4.23}$$

Therefore:

$$\phi_i(\bar{t}+1) - \phi_i(\bar{t}) \neq 0 \tag{4.24}$$

therefore the set point is not at the equilibrium.

A similar argument can be used to prove it for condition 4.11.

2. For the sake of simplicity we assume that $\bar{\phi}_i > 0$. If $\bar{\phi}_i$ is an equilibrium as defined above, it follows that:

$$\phi_i(t+1) - \phi_i(t) = \bar{\phi}_i - \bar{\phi}_i = 0 \tag{4.25}$$

Recalling the definition 4.9:

$$F(\phi_i(t), c_i(t)) = 0$$

And from the conditions of the *RAF* 4.1.2, this is guaranteed when:

$$c_i(t) \in \mathbb{B}(\phi_i(t))$$

Therefore, if $\bar{\phi}_i$ is an equilibrium, the condition is equivalent to:

$$\int_{\bar{\phi}_i - \delta\}}^{\bar{\phi}_i + \delta} f_t(c_i) = 1, \qquad \forall t \tag{4.26}$$

The other implication follows from the fact that if 4.20 holds, then every realization of the contact network falls into $\mathbb{B}(\bar{\phi})$. Therefore if $\phi_i(0) = \bar{\phi}_i$, it is an equilibrium $\forall i$.

□

The two theorems we have proved provide an interpretive key for the phenomenon under consideration. In particular, the first theorem guarantees that for an agent to be in Isolation, its set point at the step prior to the *EC* update must be greater than the threshold T. Below this threshold, since the contact network has been assumed to have positive support, it is not possible for an agent to enter Isolation. Conversely, we have seen in the second theorem that at equilibrium, all agents are in Social Homeostasis. This occurs when the realization of the contact network is extremely regular, i.e., within the homeostasis band.

We can therefore conclude that Isolation is a dynamic phenomenon that corresponds precisely to what scientific research confirms on the matter, namely a significant deviation from the optimal level of sociality. But, for this very reason, under the assumptions of the model, this condition is never met below a certain optimal sociality level. This motivates the following definition.

Definition 4.1.6. We say that an agent is experiencing Chronic Isolation at time t if $\phi_i(t) \leq T$.

Definition 4.1.7. We define the intensity of Chronic Isolation for an agent i at time t in a population with threshold T as the following quantity:

$$\mathcal{I}_T(i,t) = \frac{|\phi_i(t) - T|}{T} \tag{4.27}$$

Definition 4.1.8. Given an equilibrium $\bar{\phi}$ of the dynamic defined in 4.9 and in th. 4.1.5, we say that $\bar{\phi}$ is a *Ill-Equilibrium* if all agents are in *Chronic Isolation*

Corollary 1 (Ill-Equilibrium Condition)**.** *Given an equilibrium $\bar{\phi}$ as defined in th. 4.1.5, this is an Ill-Equilibrium iff:*

$$\sup_i(\bar{\phi}_i) \leq T \tag{4.28}$$

Proof. The result follows directly from the definition 4.1.6 and 4.1.8.

Suppose that $\bar{\phi}$ is a *Ill-Equilibrium*, then 4.28 is satisfied. On the other hand, if 4.28 is satisfied:

$$\bar{\phi}_j \leq \sup_i(\bar{\phi}_i) \leq T \tag{4.29}$$

then every agent is in chronic isolation from the uniform bound on the set points, which is the definition of *Ill-Equilibrium* □

Theorem 4.1.9. *We have the following:*

1. *Consider the function:*

$$h(\phi) = \mathbb{P}(E^{t+1} = OV \mid \phi_i(t) = \phi) \tag{4.30}$$

Then $h(\cdot)$ is a monotonic decreasing function in $[0, T)$;

2. *Consider the function:*

$$g(\phi) = \mathbb{P}(E^{t+1} = IS \mid \phi_i(t) = \phi) \tag{4.31}$$

then $g(\cdot)$ is a monotonic increasing function for $\phi > T$.

Proof. 1. Using 4.11 we can write the probability in 4.30 as:

$$\mathbb{P}(E^{t+1} = OV \mid \phi_i(t) = \phi) = \mathbb{P}(c > \phi + T) \tag{4.32}$$

The r.h.s of eq. 4.32 is equal to:

$$\mathbb{P}(c > \phi + T) = \int_{\phi+T}^{b} f(c)dc \tag{4.33}$$

Consider then two set points ψ and φ such that: $\psi < \varphi$. In order to prove the statement, we evaluate:

$$h(\varphi) - h(\psi) = \int_{\varphi+T}^{b} f(c)dc - \int_{\psi+T}^{b} f(c)dc \tag{4.34}$$

Since $\psi < \varphi$, we get that: $\psi + T < \varphi + T$. Therefore:

$$\begin{aligned} h(\varphi) - h(\psi) &= \int_{\varphi+T}^{b} f(c)dc - \int_{\psi+T}^{b} f(c)dc \\ &= \int_{\varphi+T}^{b} f(c)dc - \int_{\psi+T}^{\varphi+T} f(c)dc - \int_{\varphi+T}^{b} f(c)dc \\ &= -\int_{\psi+T}^{\varphi+T} f(c)dc \end{aligned}$$

Since $\int_{\psi+T}^{\varphi+T} f(c)dc > 0$, it follows that: $h(\varphi) - h(\psi) < 0$.

2. Following the same line of reasoning, we get:

$$\mathbb{P}(E^{t+1} = IS \mid \phi_i(t) = \phi) = \mathbb{P}(c < \phi - T) = \int_{0}^{\phi-T} f(c)dc \tag{4.35}$$

Consider then two set points ψ and φ such that: $\psi < \varphi$. From th. 2.1.4 we get that $\varphi > \psi > T$, which in turn implies: $\varphi - T > \psi - T > 0$.

Now, we evaluate:

$$\begin{aligned} g(\varphi) - g(\psi) &= \int_{0}^{\varphi-T} f(c)dc - \int_{0}^{\psi-T} f(c)dc \\ &= \int_{0}^{\psi-T} f(c)dc + \int_{\psi-T}^{\varphi-T} f(c)dc - \int_{0}^{\psi-T} f(c)dc \\ &= \int_{\psi-T}^{\varphi-T} f(c)dc \end{aligned}$$

Since $\int_{\psi-T}^{\varphi-T} f(c)dc > 0$, we have that $g(\cdot)$ is monotonically increasing.

□

Remark 12. *Theorem 4.1.9 should be interpreted as a static result: it characterizes the probability of entering each Embedded Compartment at a single time step, conditional on the current set point. It does not directly imply a dynamical trap. However, combined with the set point dynamics 4.9, it suggests that agents in Chronic Isolation - characterized by low set points - face a higher probability of Overcrowding- especially given the reduction in effort, which is not takes into account in this minimal framework- which may hinder the recovery of the set point above the threshold T. A rigorous dynamical characterization of this phenomenon remains an open direction.*

4.2 A Birth-and-Death Process for Set Point Dynamics

In this section we consider a simple example of the *RAF*. This choice can be viewed as an approximation of a more general *RAF* whose value is neglectable around the set point, whilst it saturates rapidly outside this range. Thus, it can also be seen as a birth-and-death process, in which the transitions are driven by the realization of the contact network.

Furthermore, the model is limited to the analysis of a single *set point*. It can therefore be interpreted as a *psychological* model. A generalisation that explicitly accounts for correlations with other agents regarding the contact network and considers macroscopic variables represents a future direction.

We define the following piecewise constant *RAF*:

$$F(\phi, c) = \begin{cases} +1 & \text{if } c \in]\phi+1, b], \\ 0 & \text{if } c \in [\phi-1, \phi+1], \\ -1 & \text{if } c \in [0, \phi-1[. \end{cases} \tag{4.36}$$

The band of no update is symmetric and defined as

$$\mathbb{B}(\phi) := [\phi-1, \phi+1], \tag{4.37}$$

and has Lebesgue measure equal to 2.

From eq.4.36 we get that it can be mapped into a simple *Markov Chain*. In fact, assuming that the contact network has density distribution given by $C \sim f(c)$, the probability that $c \in]\phi+1, b]$ is simply given by $\int_{\phi+1}^{b} f(c)dc$. On the other hand, the probability that $c \in [0, \phi-1[$ is $\int_{0}^{\phi-1} f(c)dc$. Finally the probability that the realization falls into the no update ball is $\int_{\phi-1}^{\phi+1} f(c)dc$.

If we assume that the initial distribution $\mu_0(\phi)$ is equal to zero outside $\mathbb{N}_0$ we have the the Markov Chain $\{\phi_n\}_{n\in\mathbb{N}}$ with state space S-see the next theorem- and transmission probabilities given by:

$$\mathbb{P}(\phi \mid \phi') = \begin{cases} \int_{\phi'+1}^{b} f(c)\,dc & \text{if } \phi = \phi' + 1, \\ \int_{\phi'-1}^{\phi'+1} f(c)\,dc & \text{if } \phi = \phi', \\ \int_{0}^{\phi'-1} f(c)\,dc & \text{if } \phi = \phi' - 1, \\ 0 & \text{otherwise.} \end{cases} \tag{4.38}$$

The Markov chain $\{\phi_t\}_{t\in\mathbb{N}}$ satisfies the following discrete-time master equation:

$$\begin{aligned} \mathbb{P}(\phi, t+1) - \mathbb{P}(\phi, t) =& \mathbb{P}(\phi - 1, t) \int_{\phi}^{b} f(c)\,dc \\ &+ \mathbb{P}(\phi + 1, t) \int_{0}^{\phi} f(c)\,dc \\ &- \mathbb{P}(\phi, t)[1 - \int_{\phi-1}^{\phi+1} f(c)\,dc] \end{aligned} \tag{4.39}$$

The first term represents the gain contribution due to transitions from state $\phi-1$ to ϕ, weighted by the corresponding transition probability defined in Eq. (4.38). The second term analogously accounts for the gain contribution from state $\phi + 1$. The last term represents the loss contribution, corresponding to the probability that the system leaves state ϕ at time t, which is obtained as the complement of the probability of remaining within the band of no update.

Theorem 4.2.1. *Consider the markov chain $\{\phi_t\}_{t\in\mathbb{N}}$, if $b \notin \mathbb{N}$, $f > 0$ a.s in $[0, b]$, then we have:*

1. *If μ_0 have null component outside $S = \{0, 1, \dots, \lfloor b \rfloor\}$, the state space is finite and it coincides with S;*

2. *Suppose that $\phi_{n-m} \neq 0$ for at least one $m \in \{1, \dots, n\}$. Then*

$$P\left(\phi_n = 0 | \exists\, m \in \{1, \dots, n\} : \phi_{n-m} \neq 0\right) = 0. \tag{4.40}$$

   In other words, once the chain has left state 0, it cannot return to it, or, more rigorously, the state $\phi = 0$ does not communicate with any state

3. *Assume $\mu_0(\{0\}) = 0$, so that $\phi_0 \in S' = \{1, \dots, \lfloor b \rfloor\}$. Then the chain $\{\phi_t\}_{t\in\mathbb{N}}$ restricted to S'' admits a unique stationary distribution π, given by:*

$$\pi(\phi) = \frac{1}{Z} \prod_{k=1}^{\phi-1} \frac{\int_{k+1}^{b} f(c)\,dc}{\int_{0}^{k} f(c)\,dc}, \qquad \phi \in S'' \tag{4.41}$$

   where the normalization constant is:

$$Z = \sum_{\phi=1}^{\lfloor b \rfloor} \prod_{k=1}^{\phi-1} \frac{\int_{k+1}^{b} f(c)\,dc}{\int_{0}^{k} f(c)\,dc} \tag{4.42}$$

4.

5. *Let $\phi_0 \in S' = \{1, \dots, \lfloor b \rfloor\}$ and let $n \in \mathbb{N}$ be such that $n < \phi_0$. Let D_n denote the event that the chain decreases at every step for n consecutive steps starting from ϕ_0, i.e.*

$$D_n := \{\phi_1 = \phi_0 - 1, \phi_2 = \phi_0 - 2, ..., \phi_n = \phi_0 - n\}. \tag{4.43}$$

Then $\mathbb{P}(D_n)$ is strictly decreasing in n.

Proof. 1. The chain moves at most of ± 1. Therefore we just need to check the upper and lower bound, namely $\phi = 0$ and $\phi = \lfloor b \rfloor$.

The *upper bound* is given by $\phi = \lfloor b \rfloor$. In fact, the state is admissible for the chain. In fact:

$$\mathbb{P}(\lfloor b \rfloor \mid \lfloor b \rfloor - 1) = \int_{\lfloor b \rfloor}^{b} f(c)dc$$

that we have assumed bigger than zero. Using the transition probabilities defined in 4.38, we easily get:

$$\mathbb{P}(\lfloor b \rfloor + 1 \mid \lfloor b \rfloor) = \int_{\lfloor b \rfloor + 1}^{b} f(c)dc$$

But, since we have assumed that the distribution of contacts have positive compact support $[0, b]$ and clearly $\lfloor b \rfloor + 1 > b$ the integral is equal to zero. Therefore set points above $\lfloor b \rfloor$ are an unadmissible region for the chain. The lower bound is similar given that the transition from 0 to -1 is given by:

$$\mathbb{P}(-1 \mid 0) = \int_{0}^{-1} f(c)dc$$

The same argument employed above can be used to establish that the integral is equal to zero;

2. It suffices to show that state 0 is inaccessible from any state $\phi \geq 1$, i.e. that

$$P(\phi_{t+1} = 0 \mid \phi_t = \phi) = 0 \quad \forall\, \phi \geq 1, \forall\, t. \tag{4.44}$$

Since the chain moves by at most ± 1 at each step, the only state from which 0 could be reached in one step is $\phi = 1$. The corresponding transition probability is

$$\mathbb{P}(0 \mid 1) = \int_{0}^{1-1} f(c)\, dc = \int_{0}^{0} f(c)\, dc = 0, \tag{4.45}$$

since the integration domain $[0, 0]$ has Lebesgue measure zero. For all $\phi \geq 2$, reaching 0 in one step would require a jump of size ≥ 2, which is impossible by construction.

Therefore, for every $\phi \geq 1$:

$$P(\phi_{t+1} = 0 \mid \phi_t = \phi) = 0. \tag{4.46}$$

By the Markov property, conditioning on the last time the chain was in a state $\neq 0$, all subsequent steps have zero probability of reaching 0. Formally, by induction on $k = 1, \dots, n$:

$$P(\phi_{t+k} = 0 \mid \phi_t = \phi \geq 1) = 0 \quad \forall\, k \geq 1, \tag{4.47}$$

which gives the result;

3. We start by proving the irriducibility of the chain on S''. For every $\phi \in \{1, \dots, \lfloor b \rfloor - 1\}$, the transition probabilities satisfy:

$$P(\phi + 1 \mid \phi) = \int_{\phi+1}^{b} f(c)\, dc > 0 \tag{4.48}$$

since $\phi + 1 \leq \lfloor b \rfloor < b$ (which follows from $b \notin \mathbb{N}$) and from the hypothesis on f stated above.

Analogously, for every $\phi \in \{2, \dots, \lfloor b \rfloor\}$:

$$P(\phi - 1 \mid \phi) = \int_{0}^{\phi-1} f(c)\, dc > 0 \tag{4.49}$$

since $\phi - 1 \geq 1 > 0$.

Therefore every state communicates with its neighbors and by transitivity the chain is *irreducible* on S'.

For every $\phi \in S'$:

$$P(\phi \mid \phi) = \int_{\phi-1}^{\phi+1} f(c)\, dc > 0 \tag{4.50}$$

since the interval $[\phi - 1, \phi + 1] \subseteq [0, b]$ has positive Lebesgue measure and $f > 0$ a.e. on $[0, b]$.

The existence of a self-loop, which depend on the no update ball- implies that every state has period 1, hence the chain is aperiodic.

Together with irreducibility on the finite state space S', aperiodicity guarantees that the chain is *ergodic*, i.e. it converges to the unique stationary distribution π

$$\lim_{t\to\infty} P(\phi_t = \phi \mid \phi_0) = \pi(\phi), \qquad \forall\, \phi \in S'', \forall\, \phi_0 \in S'' \tag{4.51}$$

Although state $0 \notin S'$, we verify consistency. In fact, imposing the *detailed balanced condition* we get:

$$\pi(0)\mathbb{P}(1 \mid 0) = \pi(1)\mathbb{P}(0 \mid 1) \tag{4.52}$$

From the discussion above, it follows that:

$$\mathbb{P}(0 \mid 1) = 0 \tag{4.53}$$

Considering the l.h.s of eq. 4.52, we have:

$$\mathbb{P}(1 \mid 0) = \int_{1}^{b} f(c) dc > 0 \tag{4.54}$$

Therefore, combining 4.52, 4.53, 4.54, we get:

$$\pi(0) = 0. \tag{4.55}$$

The structure of the transition matrix (jumps of at most ± 1) guarantees that detailed balance is sufficient to characterize π. In fact, since the chain is a finite irreducible Markov chain, any distribution satisfying detailed balance coincides with the unique stationary distribution.
For every adjacent pair $(\phi, \phi+1)$ with $\phi \in S''$, we impose the *Detailed Balace Condition* [40]:

$$\pi(\phi)\, P(\phi+1 \mid \phi) = \pi(\phi+1)\, P(\phi \mid \phi+1) \tag{4.56}$$

Substituting the transition probabilities from 4.38:

$$\pi(\phi) \int_{\phi+1}^{b} f(c)\, dc = \pi(\phi+1) \int_{0}^{\phi} f(c)\, dc \tag{4.57}$$

Solving the recurrence:

$$\pi(\phi+1) = \pi(\phi) \cdot \frac{\int_{\phi+1}^{b} f(c)\, dc}{\int_{0}^{\phi} f(c)\, dc} \tag{4.58}$$

Iterating from $\phi = 1$:

$$\pi(\phi) = \pi(1) \prod_{k=1}^{\phi-1} \frac{\int_{k+1}^{b} f(c)\, dc}{\int_{0}^{k} f(c)\, dc} \tag{4.59}$$

The constant $\pi(1)$ is determined by the normalization condition $\sum_{\phi=1}^{\lfloor b \rfloor} \pi(\phi) = 1$:

$$\pi(1) = \frac{1}{Z}, \qquad Z = \sum_{\phi=1}^{\lfloor b \rfloor} \prod_{k=1}^{\phi-1} \frac{\int_{k+1}^{b} f(c)\, dc}{\int_{0}^{k} f(c)\, dc} \tag{4.60}$$

The sum Z is finite and strictly positive, since it is a finite sum of strictly positive terms. Therefore $\pi(1)$ is well-defined, and the stationary distribution is uniquely determined;

4. By the Markov property and the definition of the transition probabilities 4.38:

$$\mathbb{P}(D_n) = \prod_{k=0}^{n-1} \int_{0}^{\phi_0 - k - 1} f(c)\, dc. \tag{4.61}$$

Passing from n to $n+1$:

$$\mathbb{P}(D_{n+1}) = \mathbb{P}(D_n) \cdot \int_{0}^{\phi_0 - n - 1} f(c)\, dc. \tag{4.62}$$

It remains to show that the additional factor is strictly less than 1. Since $n < \phi_0$ and $\phi_0 \le \lfloor b \rfloor$, we have:

$$0 \le \phi_0 - n - 1 \le \lfloor b \rfloor - 1 < \lfloor b \rfloor < b \tag{4.63}$$

where the last inequality follows from $b \notin \mathbb{N}$. Therefore:

$$\int_0^{\phi_0-n-1} f(c)\,dc = 1 - \int_{\phi_0-n-1}^{b} f(c)\,dc < 1 \tag{4.64}$$

where the strict inequality holds because $f > 0$ almost everywhere on $[0, b]$ and $\phi_0 - n - 1 < b$, so the subtracted integral is strictly positive. Hence $\mathbb{P}(D_{n+1}) < \mathbb{P}(D_n)$ for all admissible n.

□

Remark 13. *The most immediately interpretable result concerns the probability of decreasing trajectories, which we have shown to be a necessary condition for isolation. The theorem tells us that periods of prolonged isolation are rare. By virtue of theorem 4.1.4, this depends on the adaptive factor induced by the RAF 4.1.2. This highlights once again the fundamental difference between acute isolation and chronic isolation -which, in the model, depends on the choice of threshold T.*

4.3 Discussion and Limitations

In this chapter, we proposed a minimal framework to model the concept of Social Homeostasis. We introduced a *contact network* encoded by a probability distribution, together with a dynamical adaptation of the optimal level of sociality-the set point-through the introduction of the concept of *RAF*. We then defined the *Embedded Compartments*, which allow us to characterize the state of an agent based on the deviation of the realized contact network from the set point.

Starting from this minimal model, we derived several properties. First, we proved a theorem concerning the trajectories of the set point associated with a state of Isolation. The analysis revealed that this state can emerge, due to the assumptions on the contact network, only above a certain threshold value of the set point, corresponding to the threshold T that defines the transition between states. Moreover, we showed that the trajectories of the set point for an agent in Isolation are associated with a significant decrease in the set point. However, this is not sufficient to uniquely characterize trajectories corresponding to Isolation without further assumptions on the behavior of the RAF.

We then established an equilibrium theorem for the set points. Since Social Homeostasis, and more generally the psychological literature on Isolation, identifies such states as significant deviations from an optimal level of sociality, the existence of an equilibrium implies that all agents are in a condition of Social Homeostasis. However, this equilibrium condition is strictly linked to the behavior of the *contact network*: it corresponds to a certain regularity in the pattern of contacts, weighted by their benefit.

This allowed us to distinguish between the phenomena of *Isolation* and *Chronic Isolation*. By the Equilibrium Theorem, Isolation is a dynamical condition that can arise only above a certain threshold T, as previously discussed. In contrast, the concept of *Chronic Isolation* is identified as a state characterized by a deficiency in social expectations mediated by the set point. This clearly separates the two phenomena. We also introduced the notion of *Ill-Equilibrium*. Even though agents' set

points are at equilibrium, in this case none of them exceeds the threshold required to enter *Isolation*, resulting in a situation of systematic lack of sociality.

We further proved a local susceptibility theorem for two *Embedded Compartments*, namely Overcrowding and Isolation. In particular, the result concerning *Overcrowding* provides an interesting insight into social dynamics. It shows that the probability of entering *Overcrowding*, when in a condition of *Chronic Isolation*, is higher for agents with a lower set point. This can be interpreted-with appropriate caution-as a form of trap induced by a persistent lack of sociality.

Finally, we analyzed a specific form of *RAF*, namely the *piecewise constant* case, mapping it into an adaptive stochastic process through a Markov chain. The resulting model can thus be described as a *birth-and-death process* dependent on the realization of the contact network. We derived the *master equation* governing the temporal evolution of the probability distribution of the set point and proved a result connecting our model to fundamental properties of Markov chain theory. Moreover, we showed that in this case the probability of decreasing trajectories tends to decline with the number of steps of the chain.

The model lends itself to further analytical and modeling developments. In particular, a key direction would be to derive an equation for the evolution of aggregate quantities, such as the average set point, thus moving from a psychological to a sociological description. Moreover, several modeling choices introduced here could be generalized and further investigated to allow for a more nuanced understanding of the phenomenon.

Finally, it is worth emphasizing that, due to the analytical difficulties that would have arisen otherwise, we adopted strong assumptions both on the distribution associated with the contact network and on the increase of effort-which is not explicitly included in the model. Further analytical and modeling studies on this aspect represent a promising direction for future research.

Chapter 5

The SH Model on rSAD

In this chapter we use the framework developed in the previous chapter within the context of the rSAD model, introduced in Chapter 3. This allows us to investigate the effects of group interactions on the dynamics of isolation and chronic isolation that we have described. For this reason, it fits into the broader framework of models on HO-Networks, while adding a temporal dynamics to them.

5.1 Description of the Model

Following the structure adopted in Chapter 4, we now present in detail the various components of the model.

First, the contact network. As mentioned, we build upon the rSAD model developed earlier. Despite its simplicity, the model allows us to control, through a single parameter, the probability of group interactions-i.e., simplices-and dyadic interactions. We fix a number of agents N. For simplicity, we do not consider node aging effects or replacement mechanisms. Each agent is assigned an activity $a_i \in [\varepsilon, 1]$, drawn from a distribution $p(a)$. In line with Activity Driven models [82][83], we assume a *Power Law* distribution:

$$p(x) = Cx^{-\gamma} \tag{5.1}$$

where C is a positive constant. Specifically, we use inverse transform sampling to sample from a Power Law distribution in $[0.1, 1]$. The choice of the *cut-off* ε deserves some discussion. While the model follows the activity-driven tradition, where activity is Power Law distributed, this assumption has not been calibrated on real data. Simulations showed that lower values lead to extremely sparse networks. Therefore, we opted for a higher value. A more detailed discussion will be provided in the next chapter.

As for the exponent, we set $\gamma = 2.7$.

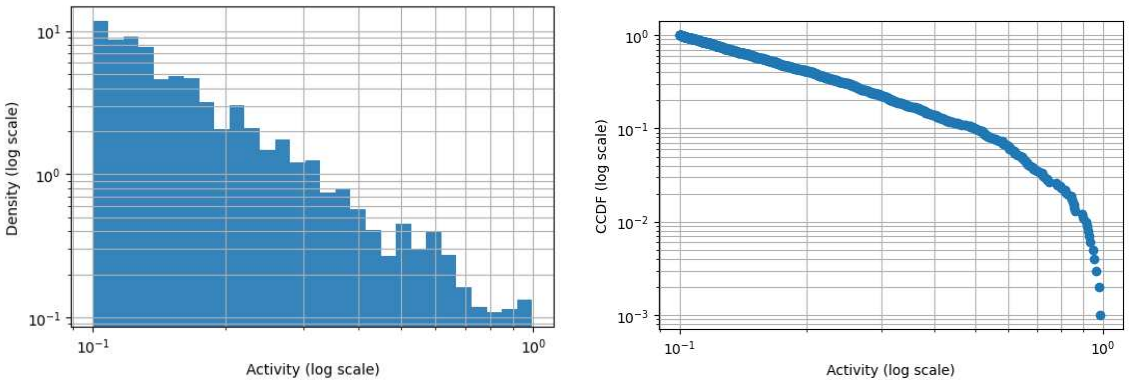

(a) Histogram (log-log) (b) Complementary CDF

Figure 5.1: Comparison between log-log histogram and CCDF of activity

Unlike the rSAD model in Chapter 3, in this context it is necessary to account for the increase in agents' effort. This connects the model to recent activity-driven works that incorporate adaptive dynamics. For simplicity, we model this as a percentage variation:

$$a_i^{IS} = a_i(1 + eff), \quad a_i^{OV} = a_i(1 - eff) \tag{5.2}$$

where $eff \in [0, 1]$. Several simulations were performed on this parameter. The results, not reported here, indicate a limited effect. Of course, it is possible to distinguish the two parameters with respect to *EC*. Finally, note that in the case of a^{IS}, for highly active agents the value may exceed 1. While theoretically one should impose an upper bound, in practice this simply implies that the agent is always active during the simulation.

From a notation perspective, we denote by $a_i(t)$ the activity of agent i at time t, reflecting the *EC* in which the agent is.

At each time step, with probability a_i-depending on her *EC*-agent i becomes active. Once active, with probability r she forms an m-simplex (i.e., a group interaction), whereas with probability $1 - r$ she forms m pairwise interactions. If the node is not active, it can still receive links from active nodes. Note that the group interaction involves m agents plus the active node, so the simplex has size $m + 1$.

Once this process is completed,

To keep track of the interactions, it is useful to define a time-dependent contact matrix $C(t)$ whose elements are:

$$c_{ij}(t) = \begin{cases} 0 & \text{if } i \text{ and } j \text{ are not connected at time } t, \\ |I_{ij}^t| & \text{if } i \text{ and } j \text{ are connected at time } t. \end{cases} \tag{5.3}$$

where $|I_{ij}^t|$ counts the number of contacts between nodes i and j at time t. It follows that the number of contacts made by agent i at time t is given by:

$$C_i^t = \sum_{j=1}^{N} c_{ij} = \sum_{j=1}^{N} |I_{ij}| \tag{5.4}$$

Since the diagonal is zero, the sum can be taken over all agents.

In the study of dynamical processes on temporal networks, a useful generalization consists in considering contacts accumulated over a wider time window[54], denoted here by μ. We define the accumulated contact matrix $C^{\mu}(t)$ as:

$$c^{\mu}(t)_{ij} = \sum_{\tau=t-(\mu-1)}^{t} c_{ij}(\tau) \tag{5.5}$$

For clarity, $\mu = 1$ means that agents consider only contacts in the current time step, while $\mu > 1$ includes past contacts. In the simulations, we consider $\mu = 1$, hence no accumulation, and $\mu = 2$, including the previous step.

It is worth highlighting the differences with Chapter 4. There, we assumed that the benefit distribution followed a function f on $\mathbb{R}$. Here, for simplicity, we assume that each interaction yields a unit benefit. This can later be generalized to include group dynamics or interaction intensity.

Moreover, although an active node selects m distinct partners, it may still receive additional contacts from other active nodes. Therefore, the contact matrix accounts for the total number of interactions, not just their presence.

This concludes the description of the *Contact Network*.

We now turn to the set point dynamics. As the *RAF* function, we choose $-\tanh$, which enforces a zero-measure no-update region:

$$\phi_i(t+1) = [\phi_i(t) - \sigma \tanh(\phi_i(t) - \sum_{\tau=t-(\mu-1)}^{t} c_{ij}(\tau))]^{+} \tag{5.6}$$

This choice is common in the modeling of complex systems, particularly in *opinion dynamics* [14]. In *deep learning* , the function also appears as an activation mechanism [31]. However, unlike those settings, here the set point adjustment does not depend on signals from other agents, but rather on the discrepancy between past desired sociality and realized interactions.

An analogy can be drawn with *gradient descent* [88], although here the adjustment is *hard-coded*, consistent with biological evidence suggesting that evolutionary processes are not optimal (for a discussion see [74]). In this sense, while optimization methods resemble classical game theory, our mechanism is closer to evolutionary game theory,[92] where strategies are fixed. The analogy is explained in [51].

As regards the initial conditions for the *set points*, deterministic conditions were chosen, specifically:

$$\phi_i(0) = exp(a_i)k \tag{5.7}$$

This choice, though arbitrary, is based on two factors. The first is the assumption that a higher activity leads to a higher initial set point. Secondly, the factor $k > 0$ allows the initial set point to be increased or decreased in a straightforward manner.

Note that, since the activity lies between ε and 1, the choice of a monotonically increasing function with respect to it could have been arbitrary, without causing

significant changes. Obviously, different initial conditions are possible and may be explored in future work.

Now we define the *EC*. To introduce heterogeneity, we define the threshold as:

$$T_i = (1 + \mu) \ln(1 + T a_i(t)) \tag{5.8}$$

where $T > 0$ is a sensitivity parameter. The baseline $+1$ ensures higher thresholds for low-activity nodes.

The logarithmic form reflects diminishing marginal returns, consistent with microeconomic theory [72] and studies on human perception. This ensures that more active nodes have higher thresholds, but with sublinear growth. Additionally, adaptivity through $a_i(t)$ implies higher thresholds in *Isolation*.

One assumption, in the case of a heterogeneous threshold, is that the value of this threshold for agents with high activity must be greater than m. This implies a dependence on the *Contact Network* even for the most active nodes. This assumption can be interpreted as the need for validation by more extroverted agents, bearing in mind the dual nature of the threshold derived from the theorem demonstrated in the previous chapter.

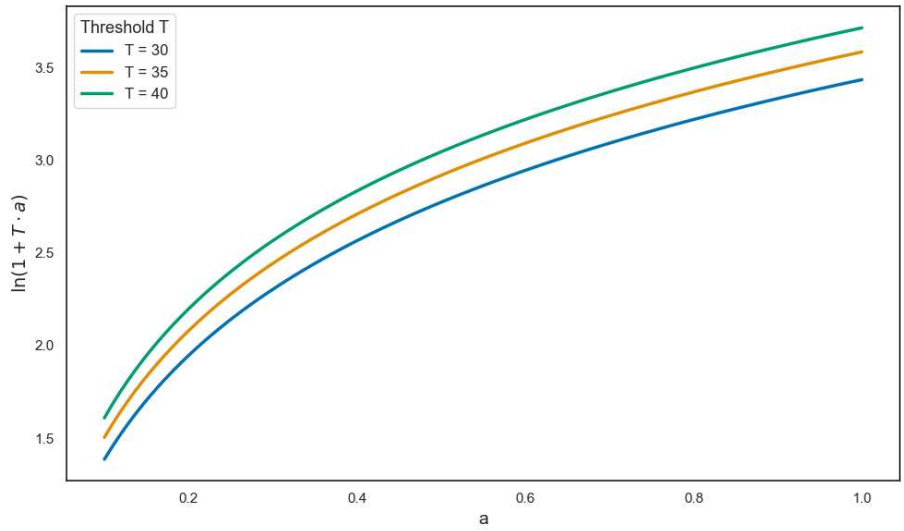

Figure 5.2: Threshold for different values of the T parameter.

We now define the *Embedded Compartments*:

Definition 5.1.1. We say that:

1. Agent i is in *Social Homeostasis (SH)* at time $t + 1$ if:

$$\sum_{\tau=t-(\mu-1)}^{t} \sum_{j} c_{ij}(\tau) \in [\phi_i(t) - T_i, \phi_i(t) + T_i]$$

2. Agent i is in *Isolation (IS)* if:

$$\sum_{\tau=t-(\mu-1)}^{t} \sum_{j} c_{ij}(\tau) < \phi_i(t) - T_i$$

3. Agent i is in *Overcrowding (OV)* if:

$$\sum_{\tau=t-(\mu-1)}^{t} \sum_{j} c_{ij}(\tau) > \phi_i(t) + T_i$$

In the simulations, we consider several quantities. First, the average set point:

$$\bar{\phi}(t) = \frac{1}{N} \sum_{i=1}^{N} \phi_i(t) \tag{5.9}$$

This captures the average sociality level and can be interpreted as a proxy for emergent social behavior.

Second, the fraction of agents in each EC:

$$\begin{cases} IS(t) = \frac{\sum_i [EC_i(t)=IS]}{N} \\ SH(t) = \frac{\sum_i [EC_i(t)=SH]}{N} \\ OV(t) = \frac{\sum_i [EC_i(t)=OV]}{N} \end{cases} \tag{5.10}$$

We are particularly interested in IS_∞, the fraction of isolated agents at equilibrium.

Finally, we track the fraction of agents in *chronic isolation*:

$$ChIS(t) = \frac{\sum_i \mathbf{1}_{\{\phi_i(t) \leq T_i\}}}{N} \tag{5.11}$$

Table 5.1: *Parameters of the Model*

Activity	a
Cut-off Power Law	ε
Chronic prm	σ
Size of Simplex	m
Probability of Group Interaction	r
Increase/Reduction in Activity	eff
Sensitivity prm	T
Accumulation of Interactions	μ

For the sake of interpretability, a single step of the model is depicted in the image 5.3.

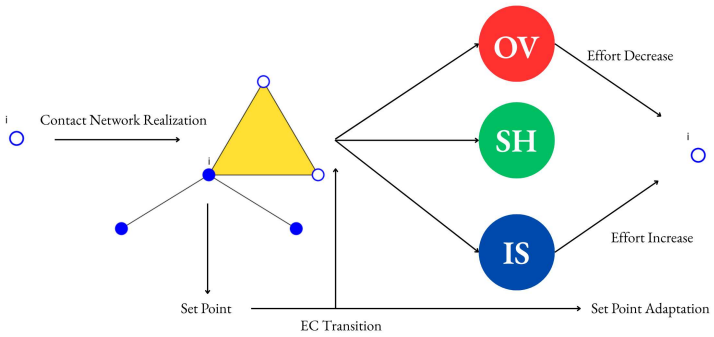

Figure 5.3: Realization of the Process. The individual node is active and forms a simplex interaction. It also receives two contacts from other nodes in the network. Subsequently, the update on the embedded compartments and the set point update takes place. Depending on the compartment, the activity increases or decreases.

5.2 Analytical approximation and numerical results

In this section we provide an analytical approximation for the dynamics of set points in the long run.

We start from the dynamics of the set points. We assume eff $= 0$, that the set point at time $t+1$ is always greater than zero so that we can neglect the positive part. Moreover, assume that $\sigma \neq 0$, thus considering the adaptive case. This leads us to write:

$$\phi_i(t+1) = \phi_i(t) - \sigma \tanh[\phi_i(t) - \sum_{\tau=t-(\mu-1)}^{t} \sum_j c_{ij}(\tau)] \tag{5.12}$$

.

At this point we can make a mean-field type approximation by replacing the sum over the realization of contacts with the average over the temporal window:

$$\sum_{\tau=t-(\mu-1)}^{t} \sum_j c_{ij}(\tau) = \mathbb{E}_\mu[C_i] \tag{5.13}$$

We note that, as specified in the first chapter, the temporal window in our model reaches at most 2. This strongly limits the approximation-as is well known from the theory of convergence of random variables and from large deviation theory.

Substituting into equation 5.12, we obtain:

$$\phi_i(t+1) = \phi_i(t) - \sigma \tanh[\phi_i(t) - \mathbb{E}_\mu[C_i]] \tag{5.14}$$

Imposing the stationary condition, we obtain:

$$\phi_i^* = \phi^* i - \sigma \tanh[\phi_i^* - \mathbb{E}\mu[C_i]] \tag{5.15}$$

Having assumed $\sigma \neq 0$, the stationary condition corresponds to the zero of the equation, therefore:

$$\tanh[\phi_i^* - \mathbb{E}_\mu[C_i]] = 0 \tag{5.16}$$

Fortunately, from the properties of tanh, the solution is trivial:

$$\phi_i^* - \mathbb{E}_\mu[C_i] = 0 \Longrightarrow \phi_i^* = \mathbb{E}_\mu[C_i] \tag{5.17}$$

At this point we can explicitly write the r.h.s. of equation 5.17, according to what was shown in Chapter 3:

$$\mathbb{E}_\mu[C_i] = ma_i\mu + \sum_{j \nsim i} \frac{m^2 a_j \mu}{N-1} r + \sum_{j \nsim i} \frac{m a_j \mu}{N-1}(1-r) \tag{5.18}$$

At this point, for $N \gg 1$, we can approximate 5.18 as:

$$\mathbb{E}\mu[C_i] = ma_i\mu + \sum j \nsim i \frac{m^2 a_j \mu}{N-1} r + \sum_{j \nsim i} \frac{m a_j \mu}{N-1}(1-r) \approx m\mu[a_i + \mathbb{E}[a]((m-1)r+1)] \tag{5.19}$$

And therefore:

$$\phi^* = m\mu[a_i + \mathbb{E}[a]((m-1)r+1)] \tag{5.20}$$

We compared the approximation with the simulation results for different values of r and μ.

When $\mu = 1$, it can be seen that the approximation for $r = 0.2$ shows quantitative agreement for nodes with intermediate *activity*. From a qualitative point of view, however, an *S-shaped* relationship emerges compared to the linear one of the approximation. The situation is different for $r = 0.8$. In this case, the approximation shows greater qualitative agreement with the distribution of set points, although for high values of activity the linear relationship tends to become weaker. The situation is depicted in fig. 5.4.

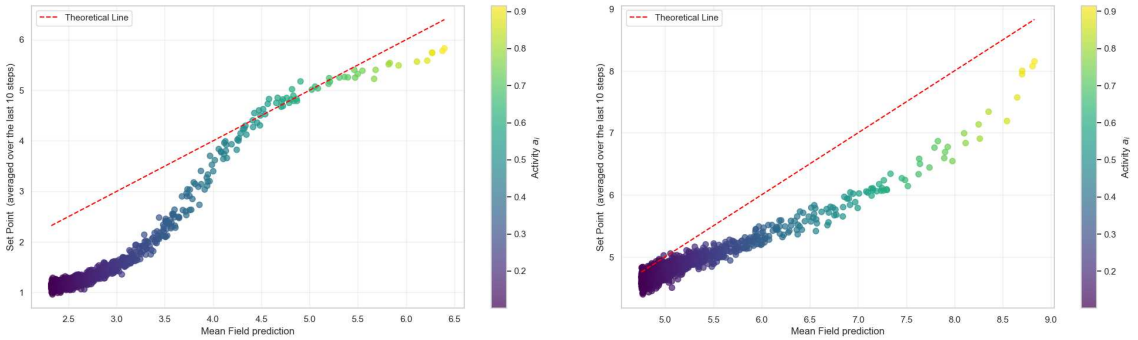

(a) (b)

Figure 5.4: Results averaged over 30 simulations, $\mu = 1$: (a) $r = 0.2$, (b) $r = 0.8$.

What emerges is precisely the effect of group interactions 3.2.3. As the value of r increases, the distribution of contacts-which in turn influences that of the set points-tends towards greater democratisation, thereby raising the set points of agents with lower activity. The S-shaped curve observed when the probability of group interaction is low is broken when the parameter r is increased, resulting in a more linear relationship.

Unlike the case where $\mu = 1$, when $\mu = 2$, the approximation shows both qualitative and quantitative agreement for $r = 0.2$. However, when $r = 0.8$, the qualitative agreement persists, but the approximation tends to systematically overestimate the values of the set points. The situation is depicted in 5.5

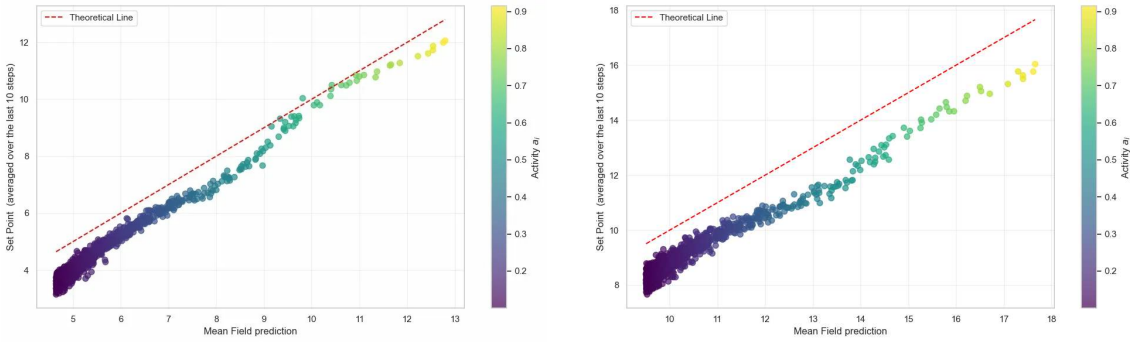

(a) (b)

Figure 5.5: Results averaged over 30 simulations, $\mu = 2$: (a) $r = 0.2$, (b) $r = 0.8$.

The greater accuracy in the case where $\mu = 2$ is not surprising. In fact, the contacts are more stable than in the previous case-although it should be emphasised that the time windows are small. This increase in accumulation in itself leads to an increase in the number of contacts used to evaluate the set point. This therefore makes the approximation more accurate than the previous one, for both values of r.

We now move on to the discussion of the results of the numerical simulations for the entire model.

In figure 5.6 and 5.7 we observe the fraction of agents in the EC for $\mu = 1$, that is, when only the current step is taken into account, and the evolution of the individual set points together and the macroscopic average $\bar{\phi}(t)$. The two simulations were performed with $r = 0.8$ and $r = 0.2$.

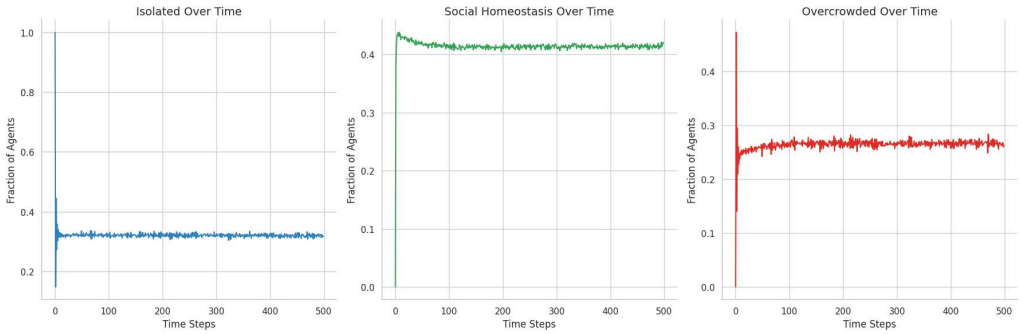

(a)

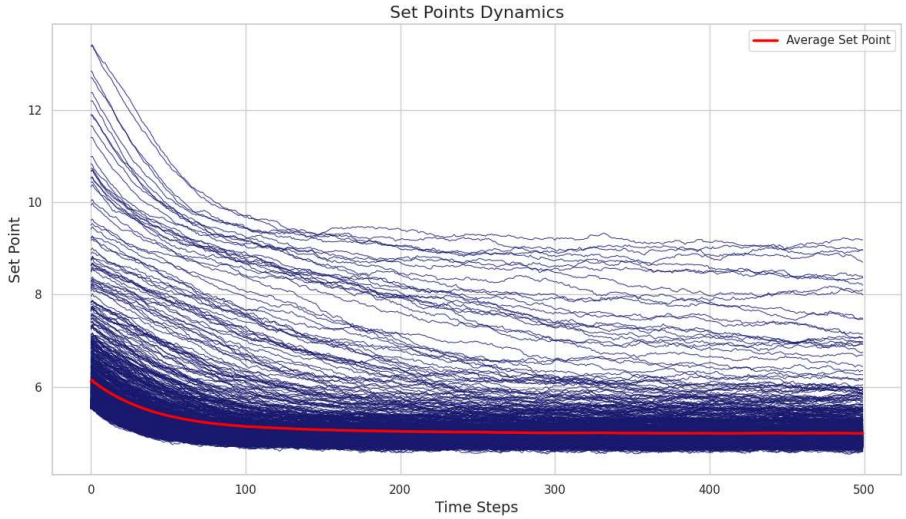

(b)

Figure 5.6: (a) Agent density for EC over time for $\mu = 1$. Simulation parameters: $Eff = 0.8$, steps=500, $\sigma = 0.1$, $T = 30$, $k = 5$, $r = 0.9$. Results averaged over 30 simulations; (b) Individual Set Points and Average Set Point associated with the simulation above.

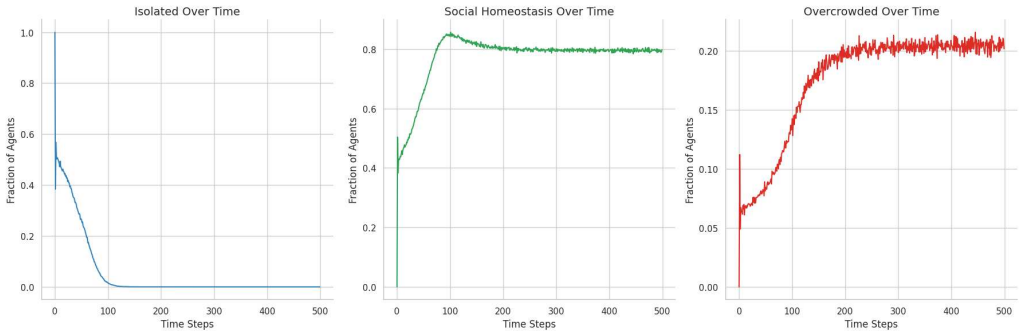

(a)

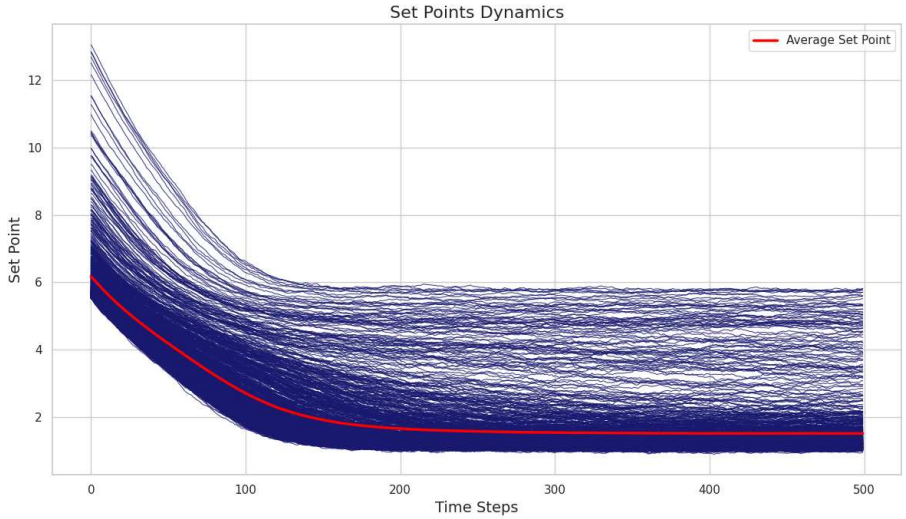

(b)

Figure 5.7: (a) Agent density for EC over time for $\mu = 1$. Simulation parameters: $Eff = 0.8$, steps=500, $\sigma = 0.1$, $T = 30$, $k = 5$, $r = 0.2$. Results averaged over 30 simulations; (b) Individual Set Points and Average Set Point associated with the simulation above.

The case $mu = 2$ is shown in fig.5.8.

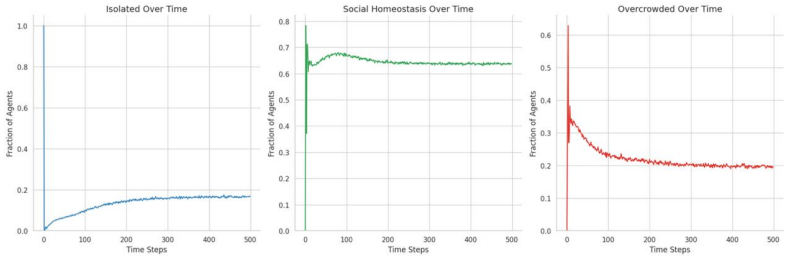

(a)

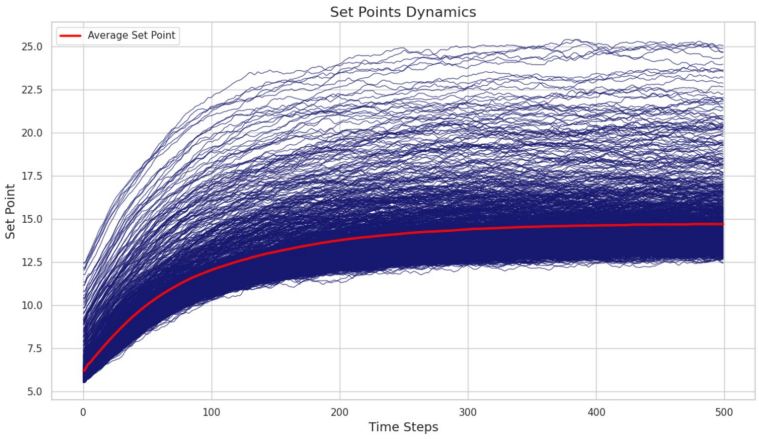

(b)

Figure 5.8: (a) Agent density for EC over time for $\mu = 2$. Simulation parameters: $Eff = 0.8$, steps=500, $\sigma = 0.1$, $T = 30$, $k = 5$, $r = 0.8$. Results averaged over 30 simulations; (b) Individual Set Points and Average Set Point associated with the simulation above.

In both cases we observe the convergence of $\bar{\phi}(t)$ toward a stationary state, while the set points, after a decreasing phase, continue with stochastic oscillations due to the realization of the *contact network*. Other numerical simulations have shown that the growth or decrease depends on the value k that defines the initial conditions of the set points. However, for any value, there is eventually a convergence of $\bar{\phi}(t)$. An interesting case is when $k = 0$, that is, when all agents have no social expectation. Even in this case, we observe a growth of the set points up to a relative stabilization. Therefore, without social expectations, the contact network and the set point dynamics drive agents toward levels of sociality greater than zero. The situation is depicted in fig. 5.9.

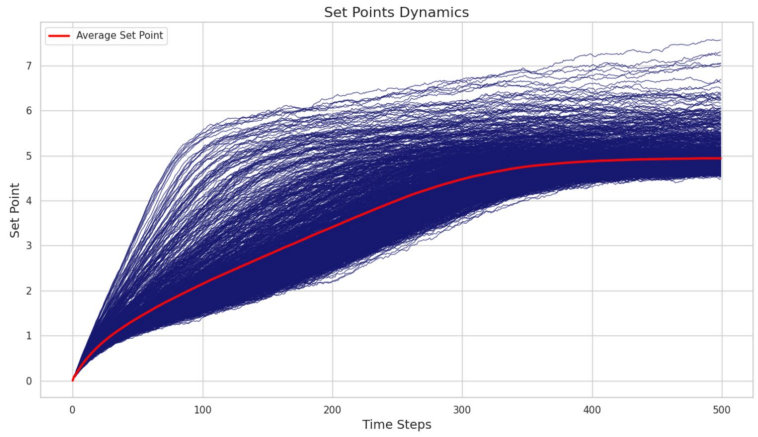

Figure 5.9: Simulation with set points $\phi_i(0) = 0$ for every i

Turning to the stability of the steady state, the figure 5.10 shows the results of the simulations for various initial conditions – i.e. as the value of k varies – for two different values of r. As can be seen, regardless of the initial conditions, the macroscopic average of the set points $\bar{\phi}$ converges to the same value in both scenarios. In turn, this value depends on the group interaction parameter. Indeed, as highlighted in Chapter 3, an increase in the probability of group interactions-that is, in the parameter r-in turn increases the average number of contacts. And this is reflected in the value of the macroscopic set point $\bar{\phi}$.

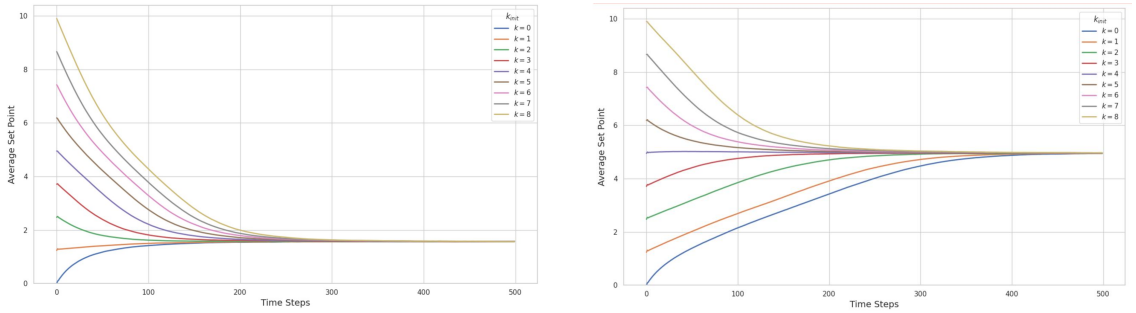

(a) (b)

Figure 5.10: Results averaged over 30 simulations, $\mu = 1$: (a) $r = 0.2$, (b) $r = 0.8$.

An interesting relationship can be found using the fact that the macroscopic average of the set points $\bar{\phi}(t)$ tends toward a stationary state. In fact, consider:

$$\bar{\phi}(t+1) = \frac{1}{N}\sum_{i=1}^{N}\phi_i(t+1) \tag{5.21}$$

Since from the simulation we see that $\phi_i(\tau) > 0$ for a certain τ, we write down the r.h.s. of eq. 5.21 using 4.9:

$$\bar{\phi}(t+1) = \frac{1}{N}\sum_{i=1}^{N}[\phi_i(t) + \sigma F(\phi_i(t), c_i(t))] \tag{5.22}$$

Now, the first term $\frac{1}{N}\sum_{i=1}^{N}\phi_i(t)$, since the macroscopic average set point tend toward the equilibrium, is equal to the r.h.s. of eq. 5.21, namely:

$$\bar{\phi}(t+1) - \frac{1}{N}\sum_{i=1}^{N}\phi_i(t) = \bar{\phi}^* - \bar{\phi}^* = 0 \tag{5.23}$$

Hence, we have:

$$\frac{1}{N}\sum_{i=1}^{N}\sigma F(\phi_i(t), c_i(t)) = 0 \tag{5.24}$$

Since $\sigma \neq 0$, we are interested in:

$$\sum_{i=1}^{N} F(\phi_i(t), c_i(t)) = 0 \tag{5.25}$$

We can decompose eq. 5.25 into two different contributions. Consider $I(t)^+$ the set of agents that, at time t, satisfy:

$$F(\phi_i(t), c_i(t)) > 0 \tag{5.26}$$

and $I(t)^-$ the set of agents that, at time t, satisfy:

$$F(\phi_i(t), c_i(t)) < 0 \tag{5.27}$$

Then eq. 5.25 reads:

$$\sum_{i \in I(t)^+} |F(\phi_i(t), c_i(t))| - \sum_{j \in I(t)^-} |F(\phi_j(t), c_j(t))| = 0 \tag{5.28}$$

The condition expressed in eq. 5.28, that holds for any *RAF* such that the no-update band has $\mu(\mathbb{B}(\phi)) = 0$ admits an interesting interpretation in the spirit of Statistical Mechanics [87]. At the macroscopic equilibrium of the average set point, the system does not reach a configuration where every agent is simultaneously satisfied.
Rather, the equilibrium is dynamic: agents whose realized contacts fall below their set point coexist with agents whose contacts exceed it, and the equilibrium condition requires that these two populations balance each other in terms of the magnitude of their adjustments.

This can be expressed as a form of *social frustration*: the system cannot simultaneously fulfill the social needs of all agents, and the macroscopic stationarity emerges precisely from this persistent tension between competing individual drives. In this sense, the equilibrium is not a state of collective satisfaction but a state of *balanced dissatisfaction* -analogous to the dynamic equilibrium in *Non-Equilibrium Statistical Mechanics* [66], where macroscopic stationarity arises from balanced fluxes rather than from the absence of fluctuations at the microscopic level.

It is worth noting that this condition relies on the assumption that the no-update band has zero measure. In this case, almost no agent is locally at equilibrium, and the stationarity of the macroscopic average cannot arise from inactivity at the microscopic level. Rather, it emerges from a non-trivial balance between positive and negative adjustments, reflecting a genuinely out-of-equilibrium steady state.

However this condition holds also for $\delta > 0$, i.e. when the no-update band 4.1.2has non-zero Lebesgue measure. In this case, the balance condition reads:

$$\sum_{i \in I_\delta^+(t)} |F(\phi_i(t), c_i(t))| - \sum_{j \in I_\delta^-(t)} |F(\phi_j(t), c_j(t))| = 0 \tag{5.29}$$

where $I_\delta^+(t) = \{i : F(\phi_i(t), c_i(t)) > 0\}$ and $I_\delta^-(t) = \{i : F(\phi_i(t), c_i(t)) < 0\}$ and the *RAF* has no-update band $\mu(\mathbb{B}(\phi)) = 2\delta$
The structure of the dynamic equilibrium thus depends critically on the size of I_δ^+ and I_δ^-. For small but positive δ, the sets remain large and the balance condition continues to hold in the spirit of a dynamic equilibrium, with persistent microscopic activity sustaining macroscopic stationarity.

As δ increases, however, fewer agents contribute to the balance, and the system transitions toward a regime of *approximate collective satisfaction*, where macroscopic stationarity emerges not from balanced fluxes but from the inactivity of most agents. In this sense, δ plays the role of a *social inertia* parameter: for large δ, the system

approaches a static equilibrium rather than a dynamic one.

It is worth stressing that this collective satisfaction is not a genuine state of fulfillment: the microscopic fluctuations of the contact network persist regardless of δ and the inactivity of agents reflects a higher tolerance threshold rather than an actual alignment between set points and realized contacts.

The situation is different for the fraction of agents in the *EC* corresponding to *IS*. In the case $r = 0.2$, assuming all agents are in IS at the beginning of the simulation, we observe a decrease that eventually leads to the disappearance of *isolation* in the long run, hence $IS_\infty = 0$.

The situation changes radically in the case $r = 0.8$. In this case, following a decreasing trajectory, we then observe a stabilization with $IS_\infty \neq 0$.

Therefore, for different values of the group interaction parameter r, we observe a qualitative change in IS_∞. As an analogy with statistical mechanics, we can identify r as the control parameter and IS_∞ as the macroscopic order parameter. In figure 5.11, we also evaluated the value of IS_∞ as a function of r for various values. What emerges is the existence of a critical parameter $r^* \approx 0.4$. Below this value, IS_∞ is zero, with the disappearance of *isolation* in the long run. Above this value, instead, we observe an increase of IS_∞.

As for the case $\mu = 2$, we observe a similar situation, although the critical value is significantly smaller. In both cases, *activity driven* without group interactions leads to the disappearance of *isolation*.

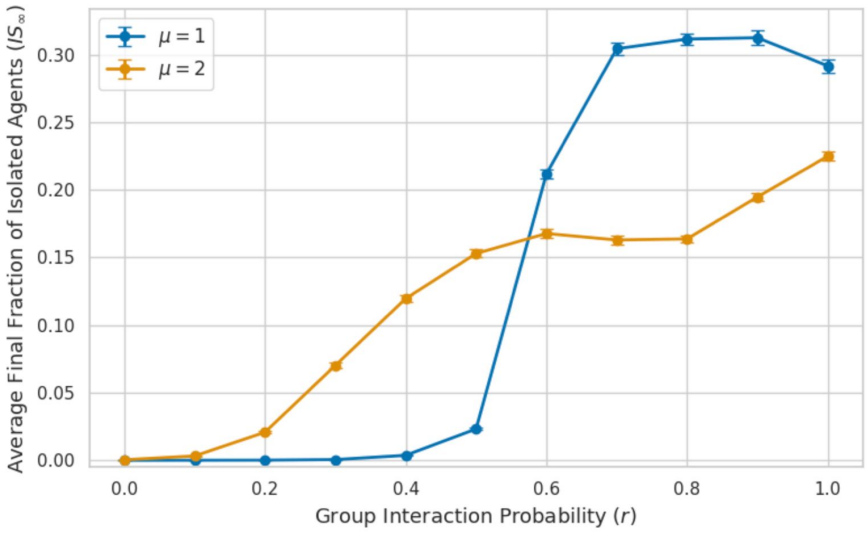

Figure 5.11: Simulation parameters: $Eff = 0.8$, steps=500, $\sigma = 0.1$, $T = 30$, $k = 5$. Results averaged over 30 simulations

The discussion so far seems to reveal an apparent contradiction. As the probability of group interaction increases, the number of agents in *isolation* also increases. Therefore, due to the contact properties in the *rSAD*, an increase in contacts leads to more isolation. However, this contradiction is only apparent. In fact, it is necessary to take into account-at this stage only speculatively-chronic isolation. In particular, as shown in Chapter 4, a condition for an agent to enter *isolation* is that the set point at the time of update must be greater than the threshold. A possible

explanation, considering these two aspects, is therefore the following.

When r is low, the number of contacts, once the set point ϕ_i has stabilized, does not allow surpassing the threshold T_i that would make *isolation* perceived. Referring to the set point dynamics in the simulations, the agent remains in *isolation* until, for a certain $\bar{t}$, the trajectory crosses the threshold T_i from above, bringing the agent into *Social Homeostasis*,but at the same time into the condition of *Chronic Isolation*.

On the contrary, for values of $r > r^*$, the number of contacts allow that agents to remain with a set point such that $\phi_i(t) > T_i$, with transitions still possible and experiencing *Chronic Isolation* when the realization of the *contact network* pushes it below the threshold.

Precisely by virtue of this possible explanation, which combines the results of the *rSAD* and the *SH model*, we considered the fraction of agents in *chronic isolation* for various values of r, in particular those above and below the threshold. The situation is depicted in fig. 5.12 and 5.13.

What emerges is that for values $r = 0.2$ we even observe a situation similar to the one previously described with *Ill-Equilibrium*. All agents are in *SH* but with $ChIS(t)$, that is, the fraction of agents in *chronic isolation*, which rapidly tends to 1. Increasing the value of r above the threshold, we instead observe a situation $ChIS(t) < 1$ in both cases.

This allows us to further clarify the phase transition described earlier. IS_∞ remains positive precisely because not all agents end up in *Chronic Isolation*, highlighting that IS_∞ and $ChIS_\infty$ capture two fundamentally distinct phenomena.

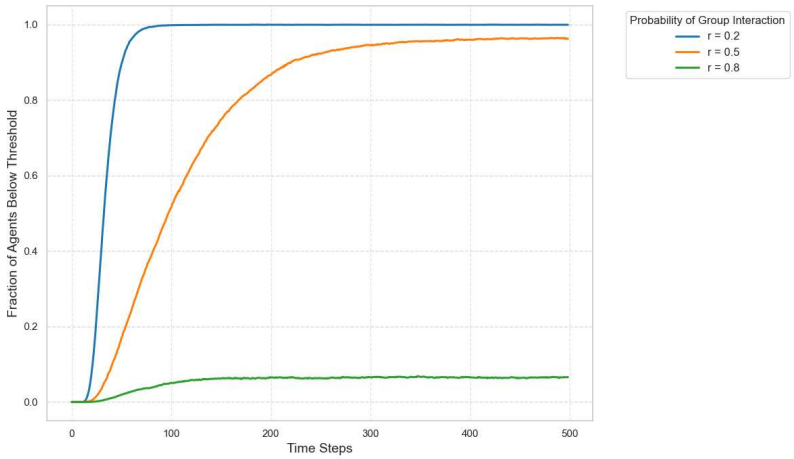

Figure 5.12: Agent in Chronic Isolation over time for $\mu = 1$ for different values of r. Simulation parameters: $Eff = 0.8$, steps=500, $\sigma = 0.2$, $T = 30$, $k = 5$, Results averaged over 30 simulations.

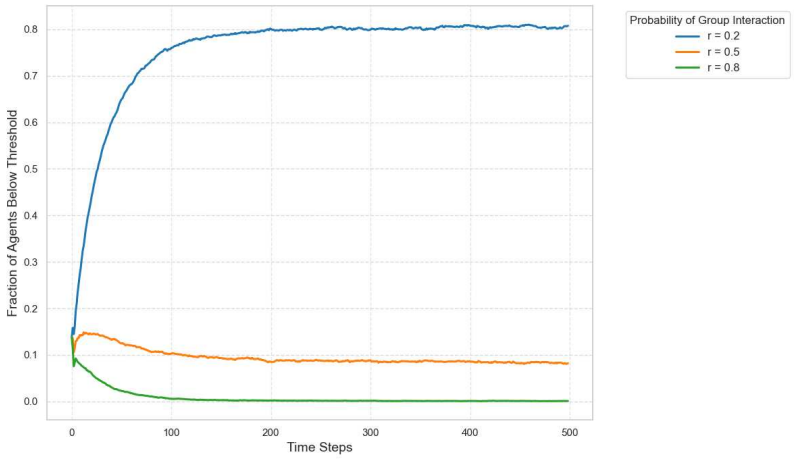

Figure 5.13: Agent in Chronic Isolation over time for $\mu = 2$ for different values of r. Simulation parameters: $Eff = 0.8$, steps=500, $\sigma = 0.2$, $T = 30$, $k = 5$, Results averaged over 30 simulations

To gain deeper insight into the nature of the phase transition induced by the group interaction parameter r, we analyze both the visitation frequency of EC and that of chronic isolation, defined as the number of time steps in which the i-th agent has a set point $\phi_i(t)$ below the threshold.

Figure 5.14 reports, for $r = 0.2$ and $r = 0.8$, the visitation frequency of IS. These values are deliberately chosen to represent the two regimes separated by the critical value r^*. In both cases, an inverse relationship between *activity* and the visitation frequency in *Isolation* is observed. The Spearman correlation coefficient is computed in both simulations.

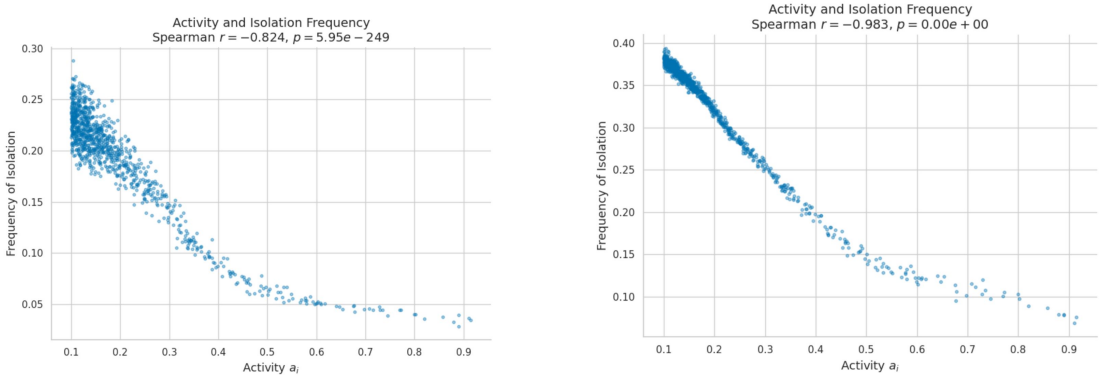

(a) (b)

Figure 5.14: Results averaged over 15 simulations, $\mu = 1$: (a) $r = 0.5$, (b) $r = 0.8$.

A more nuanced pattern emerges when analyzing the visitation frequency of $ChIS$, as shown in figure 5.15. In the *Isolation Free* regime, the relationship is weakly positive, indicating that agents with higher *activity* are more likely to cross the threshold defining $ChIS$, i.e., T_i. However, as confirmed by the figure 5.12, the system lies in an *Ill-Equilibrium* regime, where all agents exhibit high visitation frequencies. By contrast, for $r = 0.5$ and $r = 0.8$, a more structured pattern arises.

The *Spearman* coefficient remains positive, indicating a positive correlation between activity and visitation frequency to *ChIS*. However, since the *Spearman* coefficient captures monotonic relationships, it does not fully describe the observed behavior. Inspection of the scatterplot reveals a non-monotonic, approximately quadratic relationship. Nodes with low *activity* display low visitation frequencies to *ChIS*, which increase with activity up to a maximum at intermediate values, and subsequently decrease for higher activity levels, without reaching the low levels observed for minimally active nodes.

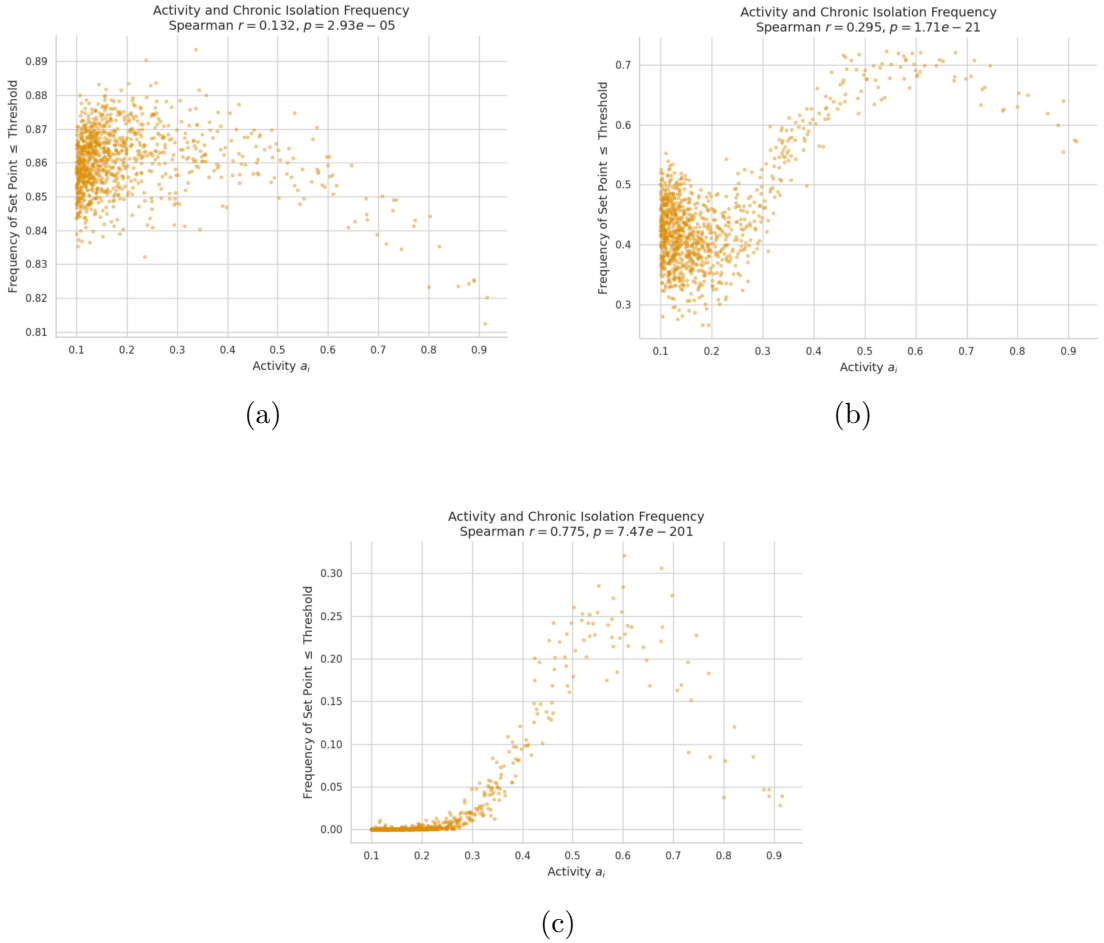

Figure 5.15: Results averaged over 15 simulations, $\mu = 1$: (a) $r = 0.2$, (b) $r = 0.5$, (c) $r = 0.8$.

This phenomenology is particularly relevant when interpreted in light of the *rSAD* and *SH* results. An increase in the group interaction parameter r disproportionately benefits low-activity nodes in relative terms. The additional received contacts enable these agents to achieve a set point exceeding the threshold T_i, thus entering *Isolation*. Conversely, for higher activity values, the marginal benefit of increasing r progressively diminishes. At the same time, higher-activity agents are characterized by larger *Threshold* values T_i.

This mechanism can be further clarified through a simple scaling argument. Let the asymptotic set point scale linearly with activity-as we have seen in 5.4- $\phi_i \sim a_i$, while the threshold grows sublinearly, $T_i \sim f(a_i)$ with $f(a_i)$ concave (e.g.

logarithmic). Then, the relevant quantity controlling the transition is the ratio:

$$\frac{\phi_i}{T_i} \sim \frac{a_i}{f(a_i)} \tag{5.30}$$

Since $f(a_i)$ grows slower than linearly, this ratio is increasing in a_i. However, the effect of increasing r is not uniform across activity classes. While the ratio ϕ_i/T_i is larger for high-activity nodes, these agents already rely predominantly on self-generated contacts. By contrast, low-activity nodes are characterized by small thresholds and low intrinsic contact generation, making their position relative to the threshold more sensitive to fluctuations in received contacts. As r increases, even a modest gain in incoming interactions can push them above T_i, enabling the transition out of *Chronic Isolation*.

Although this mechanism requires further analytical and computational investigation, the observed behavior can be interpreted as follows. Low-activity nodes benefit from increased group interactions, but remain structurally dependent on received contacts. As r exceeds the critical value r^*, they are able to surpass the threshold required to enter *IS*. However, this same dependence increases their susceptibility to *isolation*. High-*activity* nodes, for which the benefit of increasing r is smaller, rely instead on their intrinsic propensity to generate contacts, allowing them to remain above the threshold T_i in most realizations. This explains the decreasing trend observed at high activity levels. By contrast, the maximum observed at intermediate activity values results from the combined effect of *activity*, *threshold* T_i, and parameter r. In this regime, nodes exhibit a structural fragility arising from their simultaneous dependence on both received and generated contacts. The former depend on r, while their relative importance with respect to generated contacts depends on node activity.

From an analytical perspective, we have:

$$\frac{\mathbb{E}[C_{i-in}]}{\mathbb{E}[C_{i-out}]} \approx \frac{\mathbb{E}[a](1+r)}{a_i} \tag{5.31}$$

Differentiating with respect to activity yields:

$$\frac{\partial}{\partial a_i}\frac{\mathbb{E}[a](1+r)}{a_i} = -\frac{\mathbb{E}[a](1+r)}{a_i^2} < 0 \tag{5.32}$$

Thus, this ratio is, on average, monotonically decreasing in activity. This implies that links generated through activity alone are insufficient to sustain the set point dynamics for intermediate-activity nodes, in contrast to highly active nodes. This is further compounded by the higher threshold T_i relative to low-*activity* nodes. At the same time, group interactions mediated by r do not fully compensate for this deficit, as their benefits are, on average, skewed toward nodes with lower activity, while intermediate nodes still face relatively high thresholds.

This framework provides a more comprehensive interpretation of the phase transition driven by r. As r increases, and group interactions become more frequent, low-activity nodes are able to surpass the threshold T_i required to enter IS. According to the *rSAD* results, this is driven by the increase in received contacts associated with group interactions. However, this mechanism also amplifies fluctuations in their contact patterns, as these nodes depend on stochastic selection within

the contact network. As a result, they become more exposed to *isolation*, leading to the persistence of a finite fraction of agents in IS in the long run.

Conversely, high-activity nodes can rely on their intrinsic activity to remain above threshold despite higher T_i values. Intermediate-*activity* nodes, however, exhibit a structural fragility: the benefits of group interactions-arising primarily from received contacts-decrease with activity, while their activity level is insufficient to compensate for this loss. Moreover, their threshold T_i is higher than that of low-activity nodes, making it more difficult to remain above it.

In summary, the phase transition is driven by the increase in incoming contacts for low-activity nodes, which are also characterized by lower thresholds. However, these benefits-typically originating from more active nodes-do not feed back symmetrically due to the nature of group interactions, where highly active nodes maintain a relatively stable number of contacts. While this asymmetry is offset for high-*activity* nodes, it remains unresolved for intermediate-activity nodes, giving rise to the observed non-monotonic behavior.

The observed phenomenon can be studied within the *Mean Field Approximation*, taking into account the threshold condition:

$$\frac{\phi_i(t \mid r)}{T_i} = 1 \tag{5.33}$$

where we made explicit the dependence of the set point on the parameter r. Therefore, recalling that each agent has activity a_i, one can consider the critical value r^* such that the set point equals the threshold T_i.

Imposing condition (5.33), one can express r as a function of the activity, namely:

$$r(a_i) = \frac{1}{(m-1)\mathbb{E}[a]} \left[\frac{(1+\mu)\ln(1+Ta_i)}{m\mu} - a_i - \mathbb{E}[a] \right]. \tag{5.34}$$

This function allows us to identify, for each activity class, the value of the parameter r such that the set point of agents in that class reaches the threshold, within the mean field approximation.

We can now state the following result:

Theorem 5.2.1. *Let $\{a_i\}_{i=1}^N$ be a vector of real numbers such that $a_i \in [\varepsilon, 1]$, with $\varepsilon > 0$ arbitrarily small, and let $\langle a \rangle = \frac{1}{N}\sum_i a_i$ be its average. Let $\mu \in \mathbb{N}^+$ and $2 \leq m < T < \infty$, and consider the function:*

$$r(a) = \frac{1}{(m-1)\langle a \rangle} \left[\frac{(1+\mu)\ln(1+Ta)}{m\mu} - a - \langle a \rangle \right]. \tag{5.35}$$

Then $r(a)$ admits a maximum in the interior of the interval and is strictly concave.

Proof. To find the critical value a^*, we differentiate (5.35) and set it equal to zero:

$$\frac{dr}{da} = \frac{1}{(m-1)\langle a \rangle} \left[\left(\frac{1+\mu}{m\mu} \right) \frac{T}{1+Ta} - 1 \right] = 0 \tag{5.36}$$

Solving for a, we obtain:

$$a^* = \frac{1+\mu}{m\mu} - \frac{1}{T} \tag{5.37}$$

We now show that a^* lies in the interval $(0, 1)$. This is equivalent to requiring:

$$0 < a^* < 1 \tag{5.38}$$

We consider the two cases:

- $a^* > 0$:
  Substituting (5.37), this is equivalent to:

  $$\frac{1+\mu}{m\mu} - \frac{1}{T} > 0 \tag{5.39}$$

  which is equivalent to:

  $$\frac{T}{m} > \frac{\mu}{1+\mu} \tag{5.40}$$

  Since $T > m$, we have $\frac{T}{m} > 1$. Moreover, since $\mu \in \mathbb{N}^+$, it follows that $\frac{\mu}{1+\mu} < 1$. Hence condition (5.40) is always satisfied, and thus $a^* > 0$.

- $a^* < 1$:
  Again substituting (5.37), this is equivalent to:

  $$\frac{1+\mu}{m\mu} - \frac{1}{T} < 1 \tag{5.41}$$

  which implies:

  $$\frac{1+\mu}{m\mu} - \frac{1}{T} < 1 \Longrightarrow 1 + \mu < m\mu\left(1 + \frac{1}{T}\right) \Longrightarrow \mu\left(m + \frac{m}{T} - 1\right) > 1 \tag{5.42}$$

  Since $\mu \in \mathbb{N}^+$ and $m \geq 2$, and the left-hand side is increasing in m, we evaluate at $m = 2$:

  $$1 < \mu\left(1 + \frac{2}{T}\right) \tag{5.43}$$

  Since $T < \infty$, and taking $\mu = 1$ for the minimum, we obtain:

  $$1 < \left(1 + \frac{2}{T}\right) = 1 + k\,(T) \tag{5.44}$$

  with $k(T) > 0$. Hence $a^* < 1$.

This proves that the critical point lies in the interior of the interval.

The second derivative of (5.35) is:

$$\frac{d^2r}{da^2} = -\left[\frac{(1+\mu)T^2}{(m-1)\langle a\rangle\, m\mu(1+Ta)^2}\right] < 0 \tag{5.45}$$

since $m \geq 2$, $\mu \in \mathbb{N}^+$ and $T > 0$.

Therefore, a^* is a maximum, it lies in the interior of the interval, and the function (5.35) is strictly concave. □

To sum up, considering the specific formulation of the model and building on the discussion so far, we can distinguish two regimes:

1. *No Isolation*: for values $r < r^*$, every agent remains in the long run below the threshold T, and is therefore in a state of *Chronic Isolation*;

2. *Isolation*: for values $r > r^*$, group interactions enable a fraction of agents to persistently exceed the threshold T_i, thus allowing the emergence of *Isolation* in the long run.

5.3 Heuristic phase transition with constant threshold T

Consider a homogeneous threshold $T \in \mathbb{R}_0^+$. In order to provide an heuristic argument for the existence of a phase transition, we interpret T as a control parameter and $ChIS_\infty$ as a macroscopic quantity.

We consider the distribution of set points at time t given that the parameter of group interaction is equal to r, namely:

$$p_t(\phi \mid r) \tag{5.46}$$

We define the asymptotic fraction of agents in chronic isolation as:

$$ChIS_\infty = \lim_{t \longrightarrow \infty} \int_0^T p_t(\phi \mid r)\, d\phi \tag{5.47}$$

This quantity represents the fraction of individuals whose set point remains below the threshold T, and therefore captures the long-term level of isolation in the system.

For small values of T, assuming that the set points are bounded away from zero in the long run, we have:

$$ChIS_\infty = \lim_{t \longrightarrow \infty} \int_0^T p_t(\phi \mid r)\, d\phi = 0 \tag{5.48}$$

Hence, no chronic isolation emerges in this regime.

If, on the other hand, T is sufficiently large, since the set points are bounded from above, we obtain:

$$ChIS_\infty = \lim_{t \longrightarrow \infty} \int_0^T p_t(\phi \mid r)\, d\phi = 1 \tag{5.49}$$

In this case, all agents are in a state of chronic isolation, as the threshold T is too high to be reached even by highly active nodes.

Finally, for intermediate values of T, we have:

$$0 < ChIS_\infty < 1 \tag{5.50}$$

In this regime, both isolated and non-isolated individuals coexist, suggesting the presence of a non-trivial phase.

The parameter r still plays a role, as it can substantially alter the distribution $p_t(\phi \mid r)$. In particular, increasing r tends to shift the distribution towards

higher values of ϕ, thus reducing the mass below the threshold T and consequently decreasing $ChIS_\infty$.

Hence, we can identify the phases in terms of the *minimum relevant set points* ϕ^*, which mark the thresholds separating distinct behavioral regimes:

- *Full Chronic Isolation Phase ($ChIS_\infty = 1$):* There exists a minimum ϕ^* such that
$$\int_{\phi^*}^{T} p_t(\phi \mid r)\, d\phi = 0. \tag{5.51}$$
In this case, all agents have set points below the threshold T, meaning that the threshold is higher than any relevant set point in the system. Consequently, the entire population remains in chronic isolation, representing a saturated phase. One can interpret $T = \phi^*$ as the critical threshold beyond which the system cannot escape full isolation.

- *No Chronic phase ($ChIS_\infty = 0$):* There exists a minimum ϕ^* such that
$$\int_{0}^{\phi^*} p_t(\phi \mid r)\, d\phi > 0. \tag{5.52}$$
If $T \gg \phi^*$, no agent's set point falls below the threshold, and therefore the fraction of chronically isolated individuals vanishes. This regime corresponds to a fully active population where the threshold is too low to "capture" any agent in chronic isolation.

- *Intermediate phase ($0 < ChIS_\infty < 1$):* For thresholds satisfying $\phi^*_{\min} < T < \phi^*_{\max}$, only part of the distribution of set points lies below T, while the rest lies above. In this regime, both isolated and non-isolated agents coexist, resulting in a non-trivial phase where the system exhibits partial chronic isolation.

The interaction parameter r further shapes $p_t(\phi \mid r)$: increasing r shifts the distribution toward higher values of ϕ, reducing the fraction below T and therefore decreasing $ChIS_\infty$. This highlights the interplay between intrinsic thresholds and social interactions in determining the long-term isolation patterns.

Remark 14. *If a significant portion of the distribution is concentrated near the minimum, i.e., there exists a small interval $[\phi_{\min}, \phi_{\min} + \epsilon]$ such that*
$$\lim_{\epsilon \to 0} \int_{\phi_{\min}}^{\phi_{\min}+\epsilon} p_t(\phi \mid r)\, d\phi \gg 0, \tag{5.53}$$
then as T increases past $\phi_{\min}$, this mass enters the threshold abruptly. This causes a sudden jump in $ChIS_\infty$, indicating a first-order phase transition.

5.3.1 Homogeneous and Heterogeneous threshold

We have observed, albeit through different mechanisms, the emergence of a phase transition and the role of r in both the homogeneous and heterogeneous threshold cases. It is therefore worth examining more closely the role of r and the resulting phenomenology in the two scenarios, anchoring the discussion to a sociological interpretation.

In both cases, increasing r, consistently with the results of the $rSAD$ model, disproportionately benefits nodes with low activity. The crucial role of group interactions, moreover, is well established in sociological theory, as emphasized, for instance, in [86]. In that work, Putnam highlights the erosion of social capital and links it to detrimental outcomes such as the deterioration of public discourse and political life.

However, the role of group interactions is multifaceted. On the one hand, they act as a booster for the contacts of less active nodes. As shown earlier, however, this benefit arises primarily from received interactions. This makes such nodes dependent on the behavior of more active nodes, especially given the disassortative nature of activity-driven networks.

Despite these common elements, the phenomenology that emerges in the homogeneous and heterogeneous threshold cases is markedly different.

In the homogeneous threshold case, as the threshold increases, and given that the number of contacts-and thus the set point-is correlated with activity, the agents that fall below the threshold are predominantly those with lower activity.

By contrast, in the heterogeneous threshold case, we have seen that nodes with intermediate activity are the most prone to chronic isolation. Nodes with lower activity, instead, due to the heterogeneous threshold specification-particularly given the scaling assumptions adopted-tend to exhibit a low frequency of visits to the chronic isolation state. This admits a natural sociological interpretation: less active nodes, which require a lower level of social stimulation, are more easily satisfied with the number of interactions they receive, further amplified by group interactions. Conversely, more active nodes, which require higher levels of social stimulation, are more exposed to chronic isolation and the associated loss of motivation, as reflected in the disappearance of increased effort.

Overall, the model's phenomenology suggests a more nuanced view of isolation and chronic isolation. These patterns are not determined solely by individual social propensity, but also by the structure of the contact network and by heterogeneous social expectations. While this interpretation calls for dedicated empirical validation, the presence of threshold heterogeneity fundamentally alters not only the interpretation of the phenomenon, but also the potential policy interventions aimed at mitigating it.

5.4 Discussion and Limitations

In this chapter, we applied the framework developed in Chapter 4 to a specific contact network, namely the rSAD model introduced in Chapter 3, incorporating an adaptive activity that models the increase in effort. In line with other studies cited in the literature, we considered both the case in which the agent accounts only for contacts in the current time step and the case in which the previous time step is also taken into account, as encoded by the parameter μ. We introduced a heterogeneous threshold T_i, drawing on the microeconomic literature. As a choice for the RAF, we adopted the hyperbolic tangent function tanh.

First, we provided an approximation of the dynamics of the set points. Despite the strong assumptions introduced, the approximation was found to qualitatively capture the behavior of the set points, except in the regime where $\mu = 1$ and r is low.

We then simulated the system in its entirety, considering various observables. We observed that, although individual set points do not converge to equilibrium, the average set point $\bar{\phi}(t)$ tends in the long run to a *dynamical equilibrium*, even under different initial conditions. We showed that this phenomenon arises from the impossibility of satisfying the social needs of every individual agent, a phenomenon we termed *Social Frustration*, emerging from *Balanced Dissatisfaction*.

We then analyzed the final number of agents in Isolation, denoted by IS_∞. Simulations revealed two distinct regimes depending on the value of r, which governs the probability of group interactions. For low values of r, no agents are found in *Isolation* at the end of the simulation. However, there exists a critical value r^*, which itself depends on μ, above which $IS_\infty > 0$.

We further investigated this transition by evaluating the number of agents in *Chronic Isolation* for different values of r across the two regimes. It was observed that, as r increases, there is a marked decrease in the fraction of agents in *Chronic Isolation*.

Finally, we examined the visitation frequencies of the states *Isolation* and *Chronic Isolation*. While in the former case an inverse relationship between activity and visitation frequency is observed for values of r both above and below the threshold, the latter case reveals a more interesting phenomenon. Specifically, for values of r above the critical threshold, the visitation frequencies exhibit a non-monotonic behavior, with a peak at intermediate activity levels. This phenomenon can be interpreted in light of the results from the rSAD and SH models. In particular, nodes with intermediate activity display a form of structural fragility. Group interactions tend to benefit low-activity nodes more, while highly active nodes can form contacts due to their frequent presence in the social system. These two effects leave an intermediate region in which the benefits of group interactions are relatively weaker and cannot be compensated by activity, as is the case for highly active nodes, despite the lower threshold associated with intermediate ones.

We also considered, from a heuristic perspective, the case in which the threshold T is homogeneous, focusing on the fraction of agents in *Chronic Isolation* as the main observable. Although not rigorous, the analysis identified three distinct regimes depending on the value of T. For low values, the set point lies above the threshold, implying the absence of *Chronic Isolation*. As T increases, a growing fraction of agents falls below the threshold, leading to increasing levels of *Chronic Isolation* and a possible coexistence with *Isolation*. For high values of T, the entire population falls into *Chronic Isolation*. Since r tends to increase the value of the set point, this suggests the need for further investigation into the interplay between the parameters T and r.

The model naturally lends itself to several future research directions, some of which have already been mentioned. First, more realistic contact networks could

be considered, although this would come at the cost of reduced interpretability of the mechanisms highlighted here. Moreover, the choices regarding the RAF and the threshold could be modified to explore their impact more broadly. Finally, a more refined analytical treatment, even if approximate, would represent a powerful tool for gaining deeper insight into the dynamics of Isolation and Chronic Isolation.

Chapter 6

Future Directions

6.1 Boltzmann Reinforcement Mechanism

Since the early developments of Complex Network theory [7], it has been well established that contacts are not purely random. For instance, in the well-known *Albert-Barabási Model*, new nodes follow a *Preferential Attachment* mechanism, in contrast with random network models [2], where links are formed uniformly at random. In particular, the Albert-Barabási model belongs to the class of evolving networks: starting from an initial configuration, nodes are progressively added over time, and each new node establishes connections according to a non-uniform rule that depends on the existing structure.

One of the main limitations of the Activity-Driven model stems from the assumption that, once a node i becomes active, it selects another node j uniformly at random. As a consequence, the model does not account for memory effects. If two agents have interacted at time $t - \tau$, this information does not influence their probability of interacting again in subsequent time steps.

However, empirical evidence shows that memory plays a crucial role in shaping real temporal networks [62]. Repeated interactions, reinforcement of social ties, and persistence of relationships are all key features of social systems that are not captured by memoryless formulations.

Several extensions of activity-driven models have incorporated memory mechanisms [99]. In these approaches, when a node becomes active, it connects with a previously contacted node with probability q, and with a new node with probability $1 - q$. This mechanism can be further refined by introducing heterogeneous weights over past interactions, thereby defining a non-uniform selection among previously contacted nodes [61].

In this work, we propose an alternative approach based on stochastic optimisation techniques, in particular *Markov Chain Monte Carlo* (MCMC) methods [71]. Leveraging the properties of the Boltzmann distribution, these methods provide a flexible way to define a probability measure over the set of possible interaction partners. Unlike deterministic optimisation procedures such as *Gradient Descent*, which may become trapped in local minima, Boltzmann-based sampling allows for controlled exploration of the state space, including transitions toward higher-energy configurations [40].

Within this framework, we define a probabilistic choice mechanism in which

nodes preferentially reconnect with past contacts, while still retaining a non-zero probability of exploring new interactions. The balance between reinforcement and exploration is governed by the temperature parameter of the Boltzmann distribution.

Formally, let G_t denote the network at time t and $A(t)$ the corresponding adjacency matrices.

We define the *Boltzmann Reinforcement Mechanism* as follows: for every node i, the probability of selecting node j at time $\bar{t}$ is given by

$$p_{i|j}(\bar{t}) = \frac{e^{\beta \sum_{t=0}^{\bar{t}} a_{ij}(t)}}{\sum_{j \nsim i} e^{\beta \sum_{t=0}^{\bar{t}} a_{ij}(t)}} \tag{6.1}$$

At $t = 0$, this formulation reduces to the uniform distribution. Indeed, since the adjacency matrix is initially null, all exponents are equal to zero, yielding

$$p_{i|j}(0) = \frac{1}{N-1} \tag{6.2}$$

Thus, the mechanism is consistent with the standard activity-driven model at initialization, and can be interpreted as a natural generalization that progressively incorporates memory effects.

One of the key advantages of this formulation lies in its flexibility. Because it originates from a stochastic optimisation framework, the exponent in Eq. 6.1 can be generalized to include additional features beyond simple interaction counts. For instance, node attributes, tie strengths, or even signed interactions may be incorporated, in line with recent developments in *Signed Networks* [27].

The parameter β controls the strength of the reinforcement mechanism. For small β, the distribution approaches uniformity, corresponding to high-entropy exploration. For large β, the dynamics become increasingly concentrated on previously observed interactions, leading to low-entropy, highly reinforced contact patterns. This provides a natural way to investigate how the structure of interaction patterns affects dynamical processes on the network, such as the emergence of *Isolation* and *Chronic Isolation*.

While the above discussion applies naturally to dyadic interactions, extending this framework to group interactions is less straightforward. In the current formulation, higher-order interactions emerge from individual preferences.

Although this lies beyond the scope of the present work, a promising direction would be the introduction of a *social Hamiltonian* $H(\sigma)$ encoding non-trivial dependencies among group configurations. Such approach could provide a principled framework to study the formation and stability of social groups from a statistical physics perspective.

6.2 Other Future Directions

With regard to *rSAD*, as a generative model that isolates the *ceteris paribus* effect of higher-order interactions, it provides a natural framework to study a wide class

of dynamical processes, including opinion dynamics [91, 95] and epidemic models beyond the standard SIS framework [81]. Moreover, it enables a systematic investigation of the structural properties of the networks it generates, extending previous analyses conducted for activity-driven models [94]. Additional directions are discussed in the dedicated chapter.

The model presented in Chapter 4 can be extended along several dimensions. A more complete characterization of its properties represents a natural next step, potentially combining analytical and numerical approaches. In particular, most results currently focus on the single set-point level; a macroscopic description, building on the microscopic dynamics discussed in the *BD* section, would significantly enhance the understanding of the system. Furthermore, although the analysis focuses on *Social Homeostasis* (SH), the model structure is sufficiently general to allow applications in other domains, including finance [10] and economics within the broader framework of complex adaptive systems [30, 57].

A second line of inquiry concerns the interpretation of activity within the activity-driven framework. While activity is typically defined as the *propensity to engage in social interactions* [76], in practice it is measured through observed activations, i.e., realized participation in the network. This creates a conceptual mismatch between latent inclination and observed behavior.

This distinction becomes particularly relevant when nodes are willing to interact but fail to establish connections due to the absence of available or receptive partners. In this sense, observed activity conflates individual propensity with structural constraints, potentially leading to biased interpretations.

Within a generative framework, this suggests at least two extensions. First, one may introduce a link rejection mechanism, whereby active nodes attempt to form connections but targets may refuse. In this setting, activity represents an attempt process rather than realized connectivity, effectively decoupling initiative from outcome.

Second, activity itself may be modeled as an adaptive stochastic process. Rather than being fixed, it can evolve in response to past interaction outcomes. For example, repeated failures may decrease activity, while successful interactions may reinforce it. A natural framework for capturing such feedback is provided by self-exciting processes (SEP), in particular Hawkes processes [60], where the conditional intensity λ^* depends on past events.

Although related ideas have been explored in [106], they remain largely underdeveloped in the context of activity-driven networks. Incorporating such feedback mechanisms would allow the model to capture adaptive behavior, bringing it closer to a behavioral interpretation of social dynamics. This extension could also be naturally integrated into the SH framework, where past interactions influence both network structure and agents' internal states.

A final issue concerns validation and data availability. The SH model depends not only on contact structure but also on the benefits that interactions provide to agents, which complicates empirical validation. While recent datasets on social in-

teractions have become increasingly available, they are often limited to structured environments such as schools, workplaces, or households (see [70]).

However, the SH framework requires a more nuanced characterization of interactions, as not all contacts contribute equally to an agent's social state. This raises a fundamental question: which interactions are relevant for the social set point? Any empirical calibration must therefore rely on assumptions regarding the qualitative importance of different types of contacts.

One possible direction is to extend data collection to more heterogeneous contexts, including informal and leisure interactions. Nevertheless, contact data alone may not suffice to capture phenomena such as loneliness or chronic isolation. In this respect, studies combining objective and subjective measures are particularly informative. For example, [36] highlights the limitations of self-reported data and proposes integrating behavioral logs with structured diaries. This suggests that single-layer observations are insufficient, pointing toward the need for richer, multi-dimensional representations of social interaction. Related perspectives are also discussed in [37].

Finally, the structure of the SH model suggests potential connections with statistical learning approaches [42, 50]. In particular, the classification into EC states naturally lends itself to supervised learning methods, which could help identify the key factors driving transitions between social conditions. Such approaches could complement the theoretical framework by providing empirical insights into the mechanisms underlying social homeostasis.

Chapter 7

Summary

As stated in the introduction, the aim of this thesis was to study the dynamics of *Isolation* and *Chronic Isolation* by formulating a model based on the theory of *Social Homeostasis* within the context of a *High-Order Temporal Networks*.

In Chapter 2, we discussed some concepts from network science. We reviewed the fundamentals of graph theory, introduced the two main generative models in the literature, and included a section on power laws and dynamic processes in networks, with a particular focus on the SIS model.

Subsequently, recent developments were presented in a non-systematic manner. Firstly, *Temporal Networks* were discussed, with a presentation of the paradigmatic model, the *Activity Driven Model*. High Order Networks were then introduced, recalling the two main representations of higher-order interactions. Finally, we touched upon the field of *Adaptive Networks*.

In Chapter 3 we first defined a generative model of temporal networks that interpolates between the Activity Driven (AD) model where interactions are dyadic-and the Simplicial Activity Driven (SAD) model where interactions are simplicial. By introducing a single parameter-r- that accounts for the probability of group interactions, we showed that this interpolation has profound consequences for both the structure of the Network and the dynamics of a paradigmatic model in the field, namely the SIS model.

In particular, we showed that group interactions-ceteris paribus-increase the connectivity of the 1-skeleton, with larger gains for less active nodes, a phenomenon we renamed *Poor Get Richer*.

By contrast, in the SIS dynamics, an increase in group interactions leads to a reduction of the epidemic threshold, in agreement with the impact of superspreader events on pathogen diffusion. The results were obtained analytically and compared with numerical simulations.

Within the broader discussion on Higher-Order Interactions, the model suggests the importance of accounting for group interactions in temporal networks even when one is only interested in the pairwise structure.

In Chapter 4, we introduced a minimal framework for the study of *Isolation* and

Chronic Isolation, grounded in the theory of *Social Homeostasis*, which we refer to as the *SH model*. This framework can be interpreted as an adaptive process driven by the realization of random variables.

The analysis of the model allowed us to distinguish the nature of these two phenomena. *Isolation* emerges as a dynamical condition that arises only above a certain threshold of optimal sociality, when the agent's adaptive process fails to restore a state of homeostasis. In contrast, *Chronic Isolation* is identified as a structural deficiency of contacts that drives the optimal level of sociality below the threshold required for *Isolation* to occur.

The model was then mapped, in a specific case, onto a Markov chain. This allows one to leverage the well-established theory of such mathematical objects in order to gain deeper insight into the adaptive dynamics associated with a random variable representing contacts weighted by their benefit.

By combining the results of Chapters 3 and 4, in Chapter 5 we simulated a specific instance of the *SH model* on the *rSAD* network, with the aim of understanding how group interactions affect the dynamics of *Isolation* and *Chronic Isolation*.

The simulation results highlighted several key aspects. First, we observed a convergence of the average set point, which was linked to a microscopic mechanism whereby it is not possible to simultaneously satisfy the social expectations of all agents in the system.

Second, the system exhibits a phase transition as the group interaction parameter r varies, distinguishing a *No Isolation* phase from an *Isolation* phase, closely intertwined with *Chronic Isolation*. Further simulations, interpreted in light of the results from the rSAD and SH models, revealed-under heterogeneous thresholds-a structural fragility affecting nodes with intermediate activity. These nodes are unable to compensate for the reduced benefits of group interactions-which disproportionately favor less active nodes-through their intrinsic activity. This highlights the role of group interactions in shaping *Isolation* and the heterogeneous effects that emerge when node activity is taken into account.

We concluded with a heuristic discussion on the relationship between *Chronic Isolation* and the threshold T in the case where it is homogeneous across agents. In this setting as well, group interactions play a crucial role in determining the observed regimes.

Finally, the last chapter discusses several future research directions building on the results obtained in this work.

Bibliography

[1] Dillon C. Adam et al. "Clustering and superspreading potential of SARS-CoV-2 infections in Hong Kong". In: *Nature Medicine* 26.11 (Nov. 2020), pp. 1714–1719. ISSN: 1546-170X. DOI: 10.1038/s41591-020-1092-0. URL: https://www.nature.com/articles/s41591-020-1092-0.

[2] Réka Albert and Albert-Ĺaszló Barabási. "Statistical mechanics of complex networks". In: *ArXiv* cond-mat/0106096 (2001).

[3] Elsa Andres et al. *Competition between simple and complex contagion on temporal networks*. 2024. arXiv: 2410.22115 [physics.soc-ph]. URL: https://arxiv.org/abs/2410.22115.

[4] Robert Axelrod. "The Dissemination of Culture". In: *Journal of Conflict Resolution* 41 (1997), pp. 203–226.

[5] Per Bak and Kim Sneppen. "Punctuated equilibrium and criticality in a simple model of evolution". In: *Phys. Rev. Lett.* 71 (24 Dec. 1993), pp. 4083–4086. DOI: 10.1103/PhysRevLett.71.4083. URL: https://link.aps.org/doi/10.1103/PhysRevLett.71.4083.

[6] Per Bak, Chao Tang, and Kurt Wiesenfeld. "Self-organized criticality: An explanation of the 1/f noise". In: *Phys. Rev. Lett.* 59 (4 July 1987), pp. 381–384. DOI: 10.1103/PhysRevLett.59.381. URL: https://link.aps.org/doi/10.1103/PhysRevLett.59.381.

[7] Albert-Ĺaszló Barabási and Réka Albert. "Emergence of scaling in random networks". In: *Science* 286 5439 (1999), pp. 509–12.

[8] Albert-László Barabási, Réka Albert, and Hawoong Jeong. "Mean-field theory for scale-free random networks". In: *Physica A: Statistical Mechanics and its Applications* 272.1–2 (Oct. 1999), pp. 173–187. ISSN: 0378-4371. DOI: 10.1016/s0378-4371(99)00291-5. URL: http://dx.doi.org/10.1016/S0378-4371(99)00291-5.

[9] Albert-László Barabási and Márton Pósfai. *Network science*. Cambridge: Cambridge University Press, 2016. ISBN: 9781107076266 1107076269. URL: http://barabasi.com/networksciencebook/.

[10] Marco Bardoscia et al. "The physics of financial networks". In: *Nature Reviews Physics* 3.7 (June 2021), pp. 490–507. ISSN: 2522-5820. DOI: 10.1038/s42254-021-00322-5. URL: http://dx.doi.org/10.1038/s42254-021-00322-5.

[11] Alain Barrat, Marc Barthlemy, and Alessandro Vespignani. "Dynamical Processes on Complex Networks". In: 2008.

[12] Federico Battiston et al. "Networks beyond pairwise interactions: structure and dynamics". In: *ArXiv* abs/2006.01764 (2020).

[13] Federico Battiston et al. “The physics of higher-order interactions in complex systems”. In: *Nature Physics* 17 (2021), pp. 1093–1098.

[14] Fabian Baumann et al. “Emergence of Polarized Ideological Opinions in Multidimensional Topic Spaces”. In: *Physical Review X* 11.1 (2021). ISSN: 2160-3308. DOI: 10.1103/physrevx.11.011012. URL: http://dx.doi.org/10.1103/PhysRevX.11.011012.

[15] Rico Berner et al. *Adaptive Dynamical Networks*. 2023. arXiv: 2304.05652 [nlin.AO]. URL: https://arxiv.org/abs/2304.05652.

[16] Ginestra Bianconi. *Higher-Order Networks: An Introduction to Simplicial Complexes*. Cambridge University Press, 2021. ISBN: 9781108770996. DOI: 10.1017/9781108770996.

[17] Christian Bick et al. “What Are Higher-Order Networks?” In: *SIAM Review* 65.3 (Aug. 2023), pp. 686–731. ISSN: 1095-7200. DOI: 10.1137/21m1414024. URL: http://dx.doi.org/10.1137/21M1414024.

[18] S. Boccaletti et al. “Complex networks: Structure and dynamics”. In: *Physics Reports* 424.4 (2006), pp. 175–308. ISSN: 0370-1573. DOI: https://doi.org/10.1016/j.physrep.2005.10.009. URL: https://www.sciencedirect.com/science/article/pii/S037015730500462X.

[19] Nino Boccara. *Modeling Complex Systems*. 2nd. Graduate Texts in Physics. Springer, 2010. ISBN: 978-1-4419-6561-5. DOI: 10.1007/978-1-4419-6562-2.

[20] Béla Bollobás. *Random graphs*. 2nd ed. Cambridge studies in advanced mathematics 73. Cambridge University Press, 2001. ISBN: 0-521-80920-7.

[21] F. Brauer, C. Castillo-Chavez, and Z. Feng. *Mathematical Models in Epidemiology*. New York, NY: Springer, 2019.

[22] Fred Brauer and Carlos Castillo-Chavez. *Mathematical Models in Population Biology and Epidemiology*. First Edition. Springer, 2001. ISBN: 978-1-4757-3516-1.

[23] Ronald L Breiger and Philippa E Pattison. “Cumulated social roles: The duality of persons and their algebras”. In: *Social Networks* 8.3 (1986), pp. 215–256. ISSN: 0378-8733. DOI: https://doi.org/10.1016/0378-8733(86)90006-7. URL: https://www.sciencedirect.com/science/article/pii/0378873386900067.

[24] G. Caldarelli et al. “Scale-Free Networks from Varying Vertex Intrinsic Fitness”. In: *Phys. Rev. Lett.* 89 (25 Dec. 2002), p. 258702. DOI: 10.1103/PhysRevLett.89.258702. URL: https://link.aps.org/doi/10.1103/PhysRevLett.89.258702.

[25] J. M. Carlson and John Doyle. “Highly optimized tolerance: A mechanism for power laws in designed systems”. In: *Physical Review E* 60.2 (Aug. 1999), pp. 1412–1427. ISSN: 1095-3787. DOI: 10.1103/physreve.60.1412. URL: http://dx.doi.org/10.1103/PhysRevE.60.1412.

[26] Bing Chen and Adnan Om. Abuassba. “Compartmental Models with Application to Pharmacokinetics”. In: *Procedia Computer Science* 187 (2021), pp. 60–70.

[27] Fernando Diaz-Diaz et al. *Signed Networks: theory, methods, and applications*. 2026. arXiv: 2511.17247 [physics.soc-ph]. URL: https://arxiv.org/abs/2511.17247.

[28] P.S. Dodds and D.J. Watts. “A generalized model of social and biological contagion”. In: *Journal of Theoretical Biology* 232.4 (Feb. 2005), pp. 587–604. ISSN: 0022-5193. DOI: 10.1016/j.jtbi.2004.09.006. URL: http://dx.doi.org/10.1016/j.jtbi.2004.09.006.

[29] Sergey N. Dorogovtsev and José F. F. Mendes. “The Nature of Complex Networks”. In: 2022.

[30] Giovanni Dosi and Andrea Roventini. *More is Different ... and Complex! The Case for Agent-Based Macroeconomics*. LEM Papers Series 2019/01. Laboratory of Economics and Management (LEM), Sant’Anna School of Advanced Studies, Pisa, Italy, Jan. 2019. DOI: None. URL: https://ideas.repec.org/p/ssa/lemwps/2019-01.html.

[31] Shiv Ram Dubey, Satish Kumar Singh, and Bidyut Baran Chaudhuri. “Activation functions in deep learning: A comprehensive survey and benchmark”. In: *Neurocomputing* 503 (2022), pp. 92–108. ISSN: 0925-2312. DOI: https://doi.org/10.1016/j.neucom.2022.06.111. URL: https://www.sciencedirect.com/science/article/pii/S0925231222008426.

[32] Paul Erdos and Alfred Renyi. “On the evolution of random graphs”. In: *Publ. Math. Inst. Hungary. Acad. Sci.* 5 (1960), pp. 17–61.

[33] P. Erdös and A. Rényi. “On Random Graphs I”. In: *Publicationes Mathematicae Debrecen* 6 (1959), p. 290.

[34] E. N. Gilbert. “Random Graphs”. In: *Annals of Mathematical Statistics* 30.4 (1959), pp. 1141–1144.

[35] M. Girvan and M. E. J. Newman. “Community structure in social and biological networks”. In: *Proceedings of the National Academy of Sciences* 99.12 (June 2002), pp. 7821–7826. ISSN: 1091-6490. DOI: 10.1073/pnas.122653799. URL: http://dx.doi.org/10.1073/pnas.122653799.

[36] Fausto Giunchiglia et al. “Mobile social media usage and academic performance”. In: *Computers in Human Behavior* 82 (May 2018), pp. 177–185. ISSN: 0747-5632. DOI: 10.1016/j.chb.2017.12.041. URL: http://dx.doi.org/10.1016/j.chb.2017.12.041.

[37] Miguel A. González-Casado, Andreia Sofia Teixeira, and Angel Sánchez. “Evidence of equilibrium dynamics in human social networks evolving in time”. In: *Communications Physics* 8.1 (June 2025). ISSN: 2399-3650. DOI: 10.1038/s42005-025-02156-4. URL: http://dx.doi.org/10.1038/s42005-025-02156-4.

[38] Geoffrey Grimmett and David Stirzaker. *Probability and Random Processes*. 4th. Oxford University Press, 2020.

[39] Douglas Guilbeault, Joshua Becker, and Damon Centola. *Complex Contagions: A Decade in Review*. 2017. arXiv: 1710.07606 [cs.SI]. URL: https://arxiv.org/abs/1710.07606.

[40] Olle Häggström. *Finite Markov Chains and Algorithmic Applications*. London Mathematical Society Student Texts. Cambridge University Press, 2002.

[41] Zhihao Han et al. “Probabilistic activity driven model of temporal simplicial networks and its application on higher-order dynamics”. In: *Chaos: An Interdisciplinary Journal of Nonlinear Science* 34.2 (Feb. 2024), p. 023137. DOI: 10.1063/5.0188424. URL: https://doi.org/10.1063/5.0188424.

[42] Trevor Hastie, Robert Tibshirani, and Jerome Friedman. *The Elements of Statistical Learning: Data Mining, Inference and Prediction*. 2nd. 2009.

[43] Allen Hatcher. *Algebraic Topology*. Cambridge University Press, 2002. URL: https://pi.math.cornell.edu/~hatcher/AT/AT.pdf.

[44] Herbert W. Hethcote. "The Mathematics of Infectious Diseases". In: *SIAM Review* 42.4 (2000), pp. 599–653. DOI: 10.1137/S0036144500371907.

[45] Petter Holme. "Modern temporal network theory: a colloquium". In: *The European Physical Journal B* 88.9 (Sept. 2015). ISSN: 1434-6036. DOI: 10.1140/epjb/e2015-60657-4. URL: http://dx.doi.org/10.1140/epjb/e2015-60657-4.

[46] Petter Holme and Fredrik Liljeros. "Mechanistic models in computational social science". In: *ArXiv* abs/1507.00477 (2015).

[47] Petter Holme and Jari Saramäki. "Temporal networks". In: *Physics Reports* 519.3 (Oct. 2012), pp. 97–125. ISSN: 0370-1573. DOI: 10.1016/j.physrep.2012.03.001. URL: http://dx.doi.org/10.1016/j.physrep.2012.03.001.

[48] Julianne Holt-Lunstad and Timothy B. Smith. "Loneliness and social isolation as risk factors for CVD: implications for evidence-based patient care and scientific inquiry". In: *Heart* 102 (2016), pp. 987–989.

[49] Iacopo Iacopini et al. "Simplicial models of social contagion". In: *Nature Communications* 10 (2018).

[50] Gareth James et al. *An Introduction to Statistical Learning: with Applications in R*. Springer, 2013. URL: https://faculty.marshall.usc.edu/gareth-james/ISL/.

[51] David Easley Jon Kleinberg. *Networks, Crowds, and Markets ; Reasoning about a Highly Connected World*. [S.l.]: Cambridge University Press, 2010. ISBN: 9780521195331 0521195330. URL: http://www.worldcat.org/search?qt=worldcat_org_all&q=9780521195331.

[52] Sune Lehmann Jørgensen. "The Structure of Complex Networks". Ph.D. Thesis. Copenhagen, Denmark: University of Copenhagen, 2007.

[53] NG Van Kampen. *Stochastic processes in physics and chemistry*. North Holland, 2007.

[54] Fariba Karimi and Petter Holme. "Threshold model of cascades in empirical temporal networks". In: *Physica A: Statistical Mechanics and its Applications* 392.16 (Aug. 2013), pp. 3476–3483. ISSN: 0378-4371. DOI: 10.1016/j.physa.2013.03.050. URL: http://dx.doi.org/10.1016/j.physa.2013.03.050.

[55] Matt J. Keeling and Pejman Rohani. *Modeling Infectious Diseases in Humans and Animals*. 1st ed. Princeton, N.J.: Princeton University Press, Oct. 2007. ISBN: 9780691116174.

[56] WO Kermack and AG McKendrick. "A contribution to the mathematical theory of epidemics". In: *Proc. R. Soc. Lond. Ser. Math. Phys. Eng. Sci.* 115.772 (1927), pp. 700–721.

[57] Alan P. Kirman. "Whom or What Does the Representative Individual Represent?" In: *Journal of Economic Perspectives* 6.2 (June 1992), pp. 117–136. DOI: 10.1257/jep.6.2.117. URL: https://www.aeaweb.org/articles?id=10.1257/jep.6.2.117.

[58] P. L. Krapivsky, S. Redner, and F. Leyvraz. "Connectivity of Growing Random Networks". In: *Physical Review Letters* 85.21 (Nov. 2000), pp. 4629–4632. ISSN: 1079-7114. DOI: 10.1103/physrevlett.85.4629. URL: http://dx.doi.org/10.1103/PhysRevLett.85.4629.

[59] Jisca S. Kuiper et al. "Social relationships and risk of dementia: A systematic review and meta-analysis of longitudinal cohort studies". In: *Ageing Research Reviews* 22 (2015), pp. 39–57.

[60] Patrick J. Laub, Thomas Taimre, and Philip K. Pollett. *Hawkes Processes*. 2015. arXiv: 1507.02822 [math.PR]. URL: https://arxiv.org/abs/1507.02822.

[61] Guillaume Laurent, Jari Saramäki, and Márton Karsai. "From calls to communities: a model for time-varying social networks". In: *The European Physical Journal B* 88.11 (Nov. 2015). ISSN: 1434-6036. DOI: 10.1140/epjb/e2015-60481-x. URL: http://dx.doi.org/10.1140/epjb/e2015-60481-x.

[62] Didier Le Bail, Mathieu Génois, and Alain Barrat. "Modeling framework unifying contact and social networks". In: *Physical Review E* 107.2 (Feb. 2023). ISSN: 2470-0053. DOI: 10.1103/physreve.107.024301. URL: http://dx.doi.org/10.1103/PhysRevE.107.024301.

[63] Christopher R. Lee, Alon Chen, and Kay M. Tye. "The neural circuitry of social homeostasis: Consequences of acute versus chronic social isolation". In: *Cell* 184.6 (2021), pp. 1500–1516. ISSN: 0092-8674. DOI: https://doi.org/10.1016/j.cell.2021.02.028. URL: https://www.sciencedirect.com/science/article/pii/S0092867421001781.

[64] Michael Y. Li. *An Introduction to Mathematical Modeling of Infectious Diseases*. Vol. 2. Mathematics of Planet Earth. Cham, Switzerland: Springer, 2018. ISBN: 978-3-030-17852-4. DOI: 10.1007/978-3-030-17852-4.

[65] James O. Lloyd-Smith et al. "Superspreading and the effect of individual variation on disease emergence". In: *Nature* 438.7066 (Nov. 2005), pp. 355–359. ISSN: 1476-4687. DOI: 10.1038/nature04153.

[66] Christian Maes. *What is nonequilibrium?* 2026. arXiv: 2601.16716 [cond-mat.stat-mech]. URL: https://arxiv.org/abs/2601.16716.

[67] Marco Mancastroppa et al. "Burstiness in activity-driven networks and the epidemic threshold". In: *Journal of Statistical Mechanics: Theory and Experiment* 2019.5 (May 2019), p. 053502. DOI: 10.1088/1742-5468/ab16c4. URL: https://doi.org/10.1088/1742-5468/ab16c4.

[68] Marco Mancastroppa et al. "Preserving system activity while controlling epidemic spreading in adaptive temporal networks". In: *ArXiv* abs/2402.09076 (2024).

[69] Benoit Mandelbrot. "A note on a class of skew distribution functions: Analysis and critique of a paper by H. A. Simon". In: *Information and Control* 2.1 (1959), pp. 90–99. ISSN: 0019-9958. DOI: https://doi.org/10.1016/S0019-9958(59)90098-1. URL: https://www.sciencedirect.com/science/article/pii/S0019995859900981.

[70] Adriana Manna et al. *Generalized contact matrices for epidemic modeling*. 2023. arXiv: 2306.17250 [physics.soc-ph]. URL: https://arxiv.org/abs/2306.17250.

[71] Enzo Marinari. *Optimized Monte Carlo Methods*. 1996. arXiv: cond-mat/9612010 [cond-mat.dis-nn]. URL: https://arxiv.org/abs/cond-mat/9612010.

[72] Andreu Mas-Colell, Michael D. Whinston, and Jerry R. Green. *Microeconomic Theory*. New York: Oxford University Press, 1995.

[73] Gillian A Matthews and Kay M Tye. "Neural mechanisms of social homeostasis". In: *Annals of the New York Academy of Sciences* 1457.1 (2019), pp. 5–25.

[74] John M. McNamara and Alasdair I. Houston. "Integrating function and mechanism." In: *Trends in ecology & evolution* 24 12 (2009), pp. 670–5.

[75] Antoine Moinet, Michele Starnini, and Romualdo Pastor-Satorras. "Burstiness and Aging in Social Temporal Networks". In: *Phys. Rev. Lett.* 114 (10 Mar. 2015), p. 108701. DOI: 10.1103/PhysRevLett.114.108701. URL: https://link.aps.org/doi/10.1103/PhysRevLett.114.108701.

[76] Matthieu Nadini et al. *Epidemic spreading in modular time-varying networks*. 2017. arXiv: 1710.01355 [physics.soc-ph]. URL: https://arxiv.org/abs/1710.01355.

[77] Mark E. J. Newman. "Networks: An Introduction". In: 2010.

[78] MEJ Newman. "Power laws, Pareto distributions and Zipf's law". In: *Contemporary Physics* 46.5 (Sept. 2005), pp. 323–351. ISSN: 1366-5812. DOI: 10.1080/00107510500052444. URL: http://dx.doi.org/10.1080/00107510500052444.

[79] Andrzej Nowak, Jacek Szamrej, and Bibb Latané. "From private attitude to public opinion: A dynamic theory of social impact." In: *Psychological Review* 97 (1990), pp. 362–376.

[80] Romualdo Pastor-Satorras and Alessandro Vespignani. "Epidemic Spreading in Scale-Free Networks". In: *Phys. Rev. Lett.* 86 (14 Apr. 2001), pp. 3200–3203. DOI: 10.1103/PhysRevLett.86.3200. URL: https://link.aps.org/doi/10.1103/PhysRevLett.86.3200.

[81] Romualdo Pastor-Satorras et al. "Epidemic processes in complex networks". In: *Reviews of Modern Physics* 87.3 (Aug. 2015), pp. 925–979. ISSN: 1539-0756. DOI: 10.1103/revmodphys.87.925. URL: http://dx.doi.org/10.1103/RevModPhys.87.925.

[82] N. Perra et al. "Activity driven modeling of time varying networks". In: *Scientific Reports* 2.1 (June 2012). ISSN: 2045-2322. DOI: 10.1038/srep00469. URL: http://dx.doi.org/10.1038/srep00469.

[83] Giovanni Petri and Alain Barrat. "Simplicial Activity Driven Model." In: *Physical review letters* 121 22 (2018), p. 228301.

[84] Mason A. Porter and James P. Gleeson. "Dynamical Systems on Networks: A Tutorial". In: *ArXiv* abs/1403.7663 (2014).

[85] Iacopo Pozzana, Kaiyuan Sun, and Nicola Perra. "Epidemic spreading on activity-driven networks with attractiveness". In: *Physical Review. E* 96 (2017).

[86] Robert D. Putnam. *Bowling Alone: The Collapse and Revival of American Community*. New York: Simon & Schuster, 2000. DOI: 10.1145/358916.361990.

[87] Linda E. Reichl. *A Modern Course in Statistical Physics*. 3rd. New York: Wiley, 2009.

[88] Sebastian Ruder. "An overview of gradient descent optimization algorithms". In: *ArXiv* abs/1609.04747 (2016).

[89] P. Sapiezynski et al. "Interaction data from the Copenhagen Networks Study". en. In: *Scientific Data* 6.1 (Dec. 2019), p. 315. ISSN: 2052-4463. DOI: 10.1038/s41597-019-0325-x. URL: https://doi.org/10.1038/s41597-019-0325-x.

[90] Thomas C. Schelling. "Dynamic models of segregation". In: *Journal of Mathematical Sociology* 1 (1971), pp. 143–186.

[91] Mohammad Shirzadi, Emilio Cruciani, and Ahad N. Zehmakan. *Opinion Dynamics: A Comprehensive Overview*. 2025. arXiv: 2511.00401 [cs.SI]. URL: https://arxiv.org/abs/2511.00401.

[92] Karl Sigmund. "Introduction to Evolutionary Game Theory". In: 2010.

[93] Herbert A. Simon. "On a Class of Skew Distribution Functions". en. In: *Biometrika* 42.3-4 (Dec. 1955), pp. 425–440. DOI: 10.1093/biomet/42.3-4.425. URL: https://doi.org/10.1093/biomet/42.3-4.425.

[94] Michele Starnini and Romualdo Pastor-Satorras. "Topological properties of a time-integrated activity-driven network". In: *Physical Review E* 87.6 (June 2013). ISSN: 1550-2376. DOI: 10.1103/physreve.87.062807. URL: http://dx.doi.org/10.1103/PhysRevE.87.062807.

[95] Michele Starnini et al. *Opinion dynamics: Statistical physics and beyond*. 2025. arXiv: 2507.11521 [physics.soc-ph]. URL: https://arxiv.org/abs/2507.11521.

[96] Lewi Stone, Daniel Simberloff, and Yael Artzy-Randrup. "Network motifs and their origins". In: *PLOS Computational Biology* 15.4 (Apr. 2019), pp. 1–7. DOI: 10.1371/journal.pcbi.1006749. URL: https://doi.org/10.1371/journal.pcbi.1006749.

[97] Steven H. Strogatz. *Nonlinear Dynamics and Chaos: With Applications to Physics, Biology, Chemistry and Engineering*. Westview Press, 2000.

[98] Harry Owen Taylor et al. "The state of loneliness and social isolation research: current knowledge and future directions". In: *BMC Public Health* 23 (2023).

[99] Enrico Ubaldi et al. "Asymptotic theory of time-varying social networks with heterogeneous activity and tie allocation". In: *Scientific Reports* 6 (2015).

[100] Enrico Ubaldi et al. "Burstiness and tie activation strategies in time-varying social networks". In: *Scientific Reports* 7 (2017), p. 46225. DOI: 10.1038/srep46225. arXiv: 1607.08910. URL: https://www.nature.com/articles/srep46225.

[101] Nicole K Valtorta et al. "Loneliness and social isolation as risk factors for coronary heart disease and stroke: systematic review and meta-analysis of longitudinal observational studies". In: *Heart* 102 (2016), pp. 1009–1016.

[102] Duncan J. Watts. "A simple model of global cascades on random networks". In: *Proceedings of the National Academy of Sciences of the United States of America* 99 (2002), pp. 5766–5771.

[103] Duncan J. Watts and Steven H. Strogatz. “Collective dynamics of ‘small-world’ networks”. In: *Nature* 393.6684 (1998), pp. 440–442. DOI: 10.1038/30918.

[104] Thomas Witelski and Mark Bowen. *Methods of Mathematical Modelling: Continuous Systems and Differential Equations*. Springer Undergraduate Mathematics Series. Springer, 2015. ISBN: 978-3-319-23041-2.

[105] Wayne W Zachary. “An Information Flow Model for Conflict and Fission in Small Groups”. In: *Journal of anthropological research* (1977), pp. 452–473. URL: http://www.jstor.org/stable/3629752.

[106] Lorenzo Zino, Alessandro Rizzo, and Maurizio Porfiri. “Modeling Memory Effects in Activity-Driven Networks”. In: *SIAM Journal on Applied Dynamical Systems* 17.4 (2018), pp. 2830–2854. DOI: 10.1137/18M1171485. eprint: https://doi.org/10.1137/18M1171485. URL: https://doi.org/10.1137/18M1171485.